

## INFORMATION TO USERS

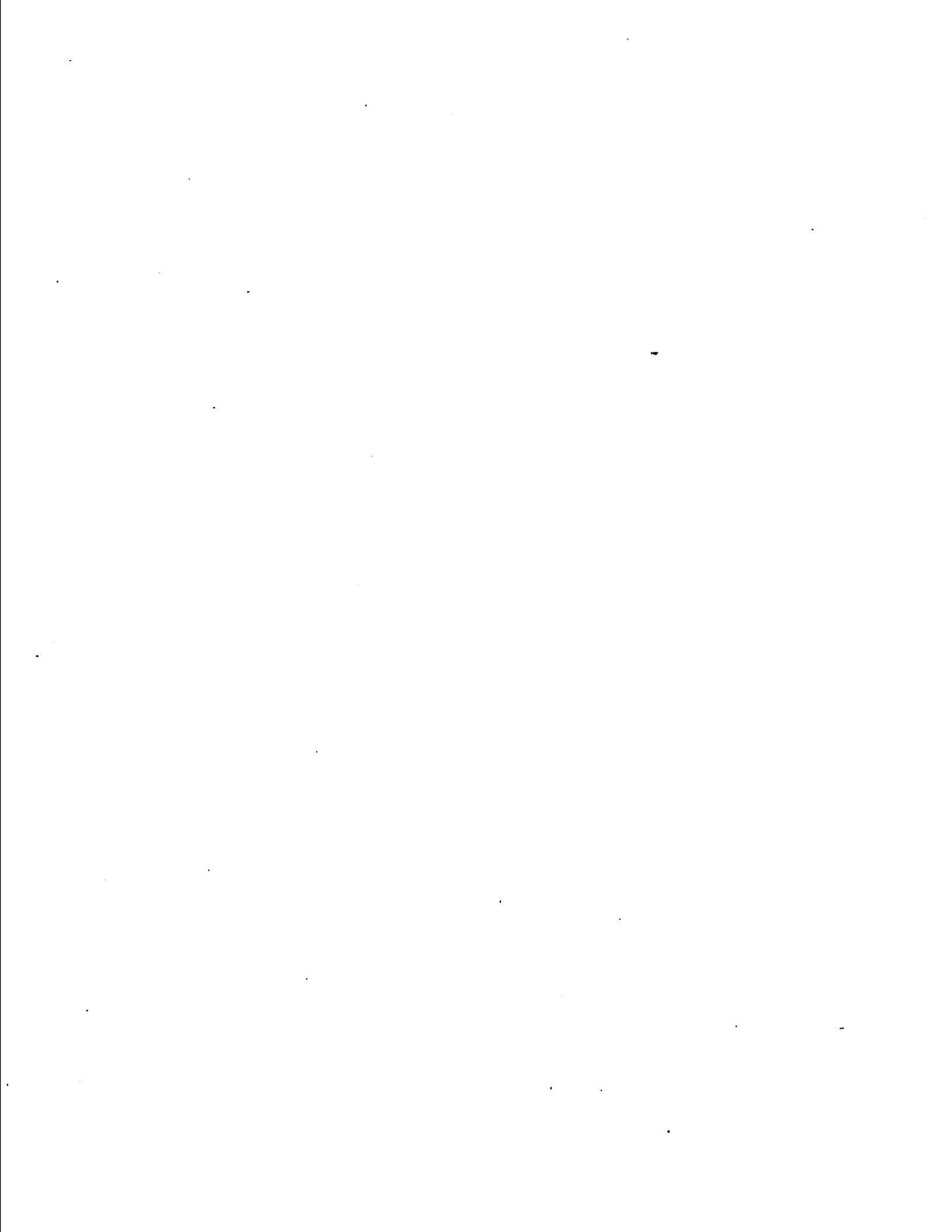
This reproduction was made from a copy of a document sent to us for microfilming. While the most advanced technology has been used to photograph and reproduce this document, the quality of the reproduction is heavily dependent upon the quality of the material submitted.

The following explanation of techniques is provided to help clarify markings or notations which may appear on this reproduction.

1. The sign or "target" for pages apparently lacking from the document photographed is "Missing Page(s)". If it was possible to obtain the missing page(s) or section, they are spliced into the film along with adjacent pages. This may have necessitated cutting through an image and duplicating adjacent pages to assure complete continuity.
2. When an image on the film is obliterated with a round black mark, it is an indication of either blurred copy because of movement during exposure, duplicate copy, or copyrighted materials that should not have been filmed. For blurred pages, a good image of the page can be found in the adjacent frame. If copyrighted materials were deleted, a target note will appear listing the pages in the adjacent frame.
3. When a map, drawing or chart, etc., is part of the material being photographed, a definite method of "sectioning" the material has been followed. It is customary to begin filming at the upper left hand corner of a large sheet and to continue from left to right in equal sections with small overlaps. If necessary, sectioning is continued again—beginning below the first row and continuing on until complete.
4. For illustrations that cannot be satisfactorily reproduced by xerographic means, photographic prints can be purchased at additional cost and inserted into your xerographic copy. These prints are available upon request from the Dissertations Customer Services Department.
5. Some pages in any document may have indistinct print. In all cases the best available copy has been filmed.

**University  
Microfilms  
International**

300 N. Zeeb Road  
Ann Arbor, MI 48106



1329852

**Alameddine, Fadel Fouad**

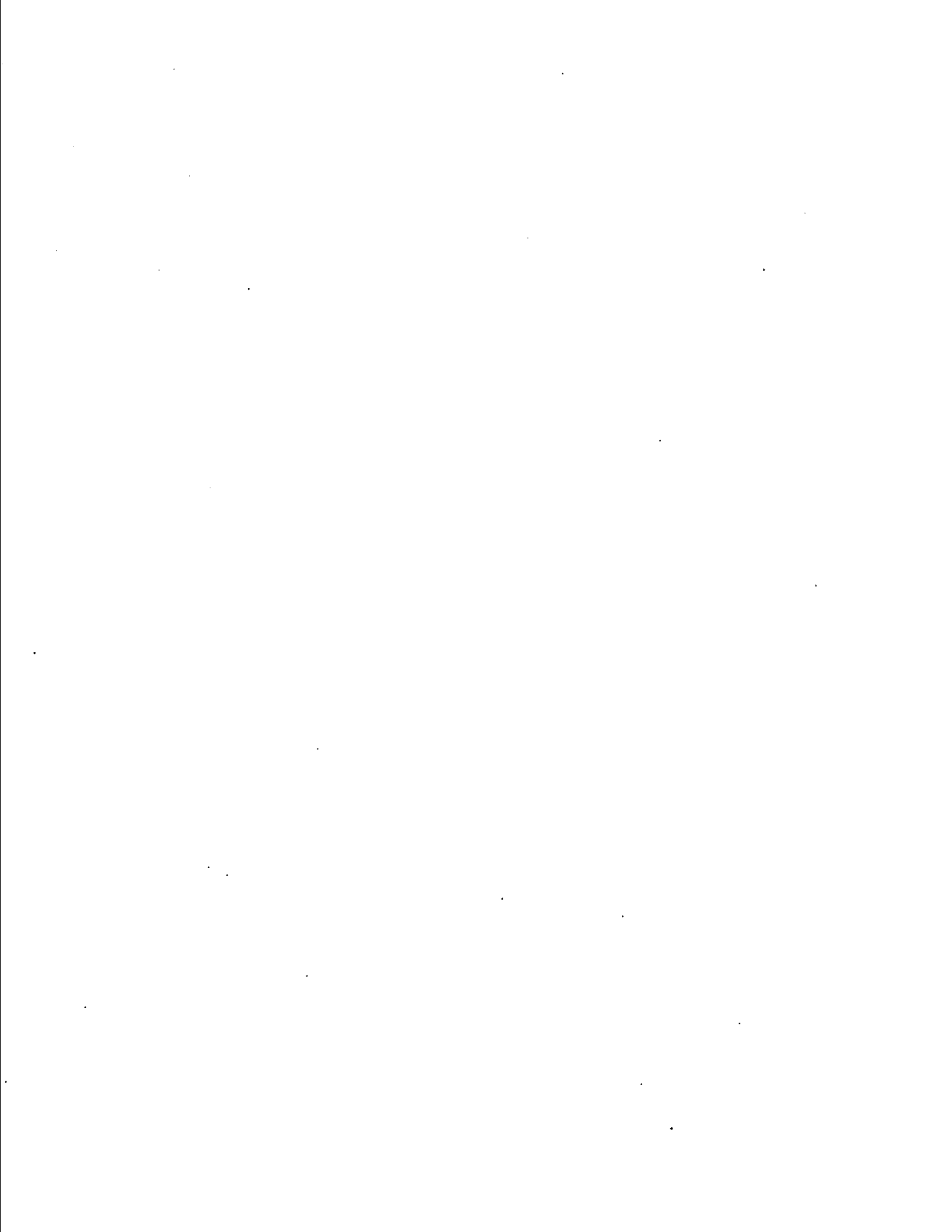
**FLEXURAL STIFFNESS OF CIRCULAR REINFORCED CONCRETE COLUMNS**

*The University of Arizona*

**M.S. 1986**

**University  
Microfilms**

**International** 300 N. Zeeb Road, Ann Arbor, MI 48106



**PLEASE NOTE:**

In all cases this material has been filmed in the best possible way from the available copy. Problems encountered with this document have been identified here with a check mark .

1. Glossy photographs or pages \_\_\_\_\_
2. Colored illustrations, paper or print \_\_\_\_\_
3. Photographs with dark background \_\_\_\_\_
4. Illustrations are poor copy \_\_\_\_\_
5. Pages with black marks, not original copy
6. Print shows through as there is text on both sides of page \_\_\_\_\_
7. Indistinct, broken or small print on several pages
8. Print exceeds margin requirements \_\_\_\_\_
9. Tightly bound copy with print lost in spine \_\_\_\_\_
10. Computer printout pages with indistinct print \_\_\_\_\_
11. Page(s) \_\_\_\_\_ lacking when material received, and not available from school or author.
12. Page(s) \_\_\_\_\_ seem to be missing in numbering only as text follows.
13. Two pages numbered \_\_\_\_\_. Text follows.
14. Curling and wrinkled pages \_\_\_\_\_
15. Dissertation contains pages with print at a slant, filmed as received \_\_\_\_\_
16. Other \_\_\_\_\_  
\_\_\_\_\_  
\_\_\_\_\_

University  
Microfilms  
International



**FLEXURAL STIFFNESS OF CIRCULAR  
REINFORCED CONCRETE COLUMNS**

by

Fadel Alameddine

---

A Thesis Submitted to the Faculty of the  
DEPARTMENT OF CIVIL ENGINEERING AND ENGINEERING MECHANICS

In Partial Fulfillment of the Requirements  
For the Degree of

MASTER OF SCIENCE  
WITH A MAJOR IN CIVIL ENGINEERING

In the Graduate College

THE UNIVERSITY OF ARIZONA

1 9 8 6

STATEMENT BY AUTHOR

This thesis has been submitted in partial fulfillment of requirements for an advanced degree at The University of Arizona and is deposited in the University Library to be made available to borrowers under rules of the Library.

Brief quotations from this thesis are allowable without special permission, provided that accurate acknowledgment of source is made. Requests for permission for extended quotation from or reproduction of this manuscript in whole or in part may be granted by the head of the major department or the Dean of the Graduate College when in his or her judgment the proposed use of the material is in the interests of scholarship. In all other instances, however, permission must be obtained from the author.

SIGNED: Fradel Alameddine

APPROVAL BY THESIS DIRECTOR

This thesis has been approved on the date shown below:

M. R. Ehsani

M. R. EHSANI

Assistant Professor of Civil Engineering and Engineering Mechanics

DEC. 8-1986

Date

This thesis is dedicated to my mother.  
Special thanks to Dr. Khoulousi Chaarani  
and Mr. Loutfi Kabbara for their  
support and encouragement.

## ACKNOWLEDGMENTS

I would like to express my sincere appreciation to Dr. M. R. Ehsani for careful guidance, generous time, and constructive criticism he gave throughout this study. I am thankful to Dr. R. Bjorhovde and to Dr. P. D. Kiouisis for reviewing the manuscript of this thesis.

I give special thanks to fellow graduate student Cesar Vallenilla for his helpful suggestions.

## TABLE OF CONTENTS

	Page
LIST OF ILLUSTRATIONS.....	vii
LIST OF TABLES.....	xi
NOTATION.....	xii
ABSTRACT.....	xiv
1. INTRODUCTION.....	1
2. LITERATURE REVIEW.....	4
2.1 Slender Column Behavior.....	4
2.2 ACI Code Estimation of the EI Value...	8
2.3 A Reexamination of the ACI EI Value...	14
2.4 Moment Magnifier Method.....	24
2.5 Proposed EI Values.....	29
3. SCOPE AND OBJECTIVES.....	33
4. ANALYTICAL STUDY.....	36
4.1 Computer Program.....	36
4.2 Parametric Study.....	43
4.3 Accuracy of the Proposed EI Values to the Computer Solution.....	49
4.4 Variables Affecting EI Value.....	57
5. DERIVATION OF EI EXPRESSION.....	68
5.1 Development of the General Design Equations for EI.....	68
5.2 Development of the Minimum EI Expression.....	85
6. CONCLUSION AND RECOMMENDATIONS.....	90
APPENDIX A: FLOWCHART AND COMPUTER LISTING OF PROGRAM CIR_COL.....	93

TABLE OF CONTENTS--Continued

	Page
APPENDIX B: DESIGN EXAMPLE.....	103
LITERATURE CITED.....	115

## LIST OF ILLUSTRATIONS

Figure		Page
2.1	Eccentrically loaded slender column.....	5
2.2	Interaction diagram for a reinforced concrete column illustrating short and long column P-M behavior up to failure.....	5
2.3	Construction of slender column interaction diagrams.....	7
2.4	Comparison of the ACI mode equations for EI with EI values for moment-curvature diagrams...	11
2.5	Rectangular column cross-section with two faces of steel.....	13
2.6	Cross-section shapes investigated in the analysis.....	16
2.7	Effect of steel ratio $\rho_t$ and reinforcement lever arm, $\gamma$ , on EI for tied columns with bars in two faces, $e/h = 0.1$ and $l/h = 20$ .....	18
2.8	Effect of steel ratio $\rho_t$ and reinforcement lever arm, $\gamma$ , on EI for tied columns with bars in two faces, $e/h = .25$ and $l/h = 20$ .....	18
2.9	Effect of steel ratio on EI for tied columns with bars in two faces, $e/h = 0.1$ and $l/h = 20$ .....	19
2.10	Effect of steel ratio on EI for tied columns with bars in four faces, $e/h = 0.1$ and $l/h = 20$ .....	19
2.11	Effect of $\gamma$ and $e/h$ for tied columns with bars in two faces, $\rho_t = 0.04$ and $l/h = 20$ .....	20
2.12	Column bending in single curvature.....	26
2.13	Representation of column behavior.....	28

LIST OF ILLUSTRATIONS--Continued

Figure		Page
4.1	Elastic perfectly plastic approximation for the steel stress-strain curve.....	38
4.2	Stress-strain curve for concrete using Hognestad's model.....	38
4.3	Reinforced concrete cracked section when flexural strength is reached.....	41
4.4	Cracked section showing variables used to compute the effective moment of inertia.....	42
4.5	Circular column cross-section.....	47
4.6	Transformed circular cross-section.....	48
4.7	Axial load-moment curvature relationship for a typical circular column.....	50
4.8	Variation of moment of inertia with different axial loads for a column with 1% reinforcement.....	51
4.9	Variation of moment of inertia with different axial loads for a column with 3% reinforcement.....	52
4.10	Variation of moment of inertia with different axial loads for a column with 5% reinforcement.....	53
4.11	Variation of moment of inertia with different axial loads for a column with 7% reinforcement.....	54
4.12	Effect of steel ratio $\rho$ on $I/I_t$ .....	58
4.13	Effect of steel reinforcement yield stress on the ratio $I/I_t$ with respect to axial load for $\rho = 0.03$ .....	60
4.14	Effect of steel reinforcement yield stress on the ratio $I/I_t$ with respect to axial load for $\rho = 0.05$ .....	61

LIST OF ILLUSTRATIONS--Continued

Figure		Page
4.15	Effect of concrete strength $f'_c$ on the ratio $I/I_t$ .....	62
4.16	Effect of $\gamma$ ratio on $I/I_t$ .....	65
4.17	Effect of diameter dimension in $I/I_t$ .....	66
5.1	Improved solution vs approximate solution for different steel ratios with $f'_c = 4$ ksi, $f_y = 60$ ksi and $h = 24$ in.....	74
5.2	Improved solution vs approximate solution for different steel ratios with $f'_c = 4$ ksi, $f_y = 50$ ksi and $h = 24$ in.....	76
5.3	Improved solution vs approximate solution for different steel ratios with $f'_c = 5$ ksi, $f_y = 50$ ksi and $h = 24$ in.....	77
5.4	Improved solution vs approximate solution for different steel ratios with $f'_c = 5$ ksi, $f_y = 60$ ksi and $h = 24$ in.....	78
5.5	Improved solution vs approximate solution for different steel ratios with $f'_c = 4$ ksi, $f_y = 70$ ksi and $h = 24$ in.....	79
5.6	Improved solution vs approximate solution for different steel ratios with $f'_c = 4$ ksi, $f_y = 60$ ksi and $h = 42$ in.....	80
5.7	Improved solution vs approximate solution for different steel ratios with $f'_c = 6$ ksi, $f_y = 50$ ksi and $h = 42$ in.....	81
5.8	Improved solution vs approximate solution for different steel ratios with $f'_c = 5$ ksi, $f_y = 50$ ksi and $h = 42$ in.....	82
5.9	Improved solution vs approximate solution for different steel ratios with $f'_c = 3$ ksi, $f_y = 60$ ksi and $h = 42$ in.....	83

LIST OF ILLUSTRATIONS--Continued

Figure		Page
5.10	Improved solution vs approximate solution for different steel ratios with $f'_c = 4$ ksi, $f_y = 50$ ksi and $h = 42$ in.....	84
5.11	Variation of the ratio $I/I_c$ with respect to $\rho$ using the Minimum EI expression as opposed to MacGregor and ACI equations.....	89

## LIST OF TABLES

Table		Page
2.1	Minimum values of $\rho_t$ making $EI_2$ govern over $EI_1$ .....	15
4.1	Typical values for different column diameters..	45
5.1	Coefficients for third-degree polynomial.....	72
5.2	Coefficients for second-degree polynomial.....	72
5.3	Coefficients for $C_c$ .....	73
5.4	Coefficients for $C_d$ .....	73
5.5	Coefficients for $C_y$ .....	74
5.6	Comparison of governing ACI values for EI with values derived from computer solution.....	87

## NOTATION

$A_c$	= concrete area of the column cross-section
$A_s$	= total area of longitudinal reinforcement
$C_m$	= equivalent column correction factor
$E_c$	= modulus of elasticity of concrete
$E_s$	= modulus of elasticity of steel
$EI$	= flexural stiffness of compression member
$EI_R$	= reduced stiffness to account for sustained load effects
$I_g$	= column gross moment of inertia
$I_s$	= moment of inertia of reinforcement
$I_t$	= transformed moment of inertia
$K$	= effective length factor
$M$	= moment applied on column
$M_o$	= moment from a first-order structural analysis
$M_u$	= ultimate column moment capacity
$P$	= column load
$P_o$	= ultimate column capacity
$P_c$	= critical load
$b$	= width of rectangular section
$e$	= eccentricity of axial column load measure to centroid of section

- $f'_c$  = compressive strength of concrete determined by the 28-day cylinder test
- $f''_c$  = compressive strength of concrete in columns
- $f_y$  = yield strength of reinforcing steel
- $h$  = diameter of the column
- $l_u$  = buckling length of column
- $n$  = modulus ratio
- $r$  = radius of gyration of a column
- $\Delta$  = column deflection
- $\beta_d$  = ratio of maximum design dead load moment to maximum total load moment
- $\beta_p$  = ratio of design dead load to design total load
- $\gamma$  = ratio of distance between centroids of outermost bars in section to overall depth of section
- $\rho$  = total reinforcement ratio

## ABSTRACT

The 1983 ACI Building Code presents a moment-magnifier method for analyzing the effects of slenderness on the strength of columns. This design procedure is strongly affected by the flexural stiffness,  $EI$ , used in the calculation of the column buckling load. In many cases, the  $EI$  values given in the ACI Code are too conservative.

An improved solution for the flexural stiffness,  $EI$ , of a circular cross section was derived in terms of the material properties and the applied axial load. In addition, a simpler minimum  $EI$  expression was developed which is only in terms of the reinforcement ratio.

Both solutions give values for  $EI$  that are less conservative to use than the ACI Code. The advantage of the use of these expressions is shown in a design example.

## CHAPTER 1

### INTRODUCTION

Columns are structural members which carry pure axial compressive loads or a combination of axial load and bending. There are two types of columns: short columns and long columns. A short column is one for which the design is governed only by strength requirements of the materials and the cross-sectional dimensions. A long column, also referred to as a slender column, is one for which the design for ultimate load at a given eccentricity involves slenderness effects that tend to produce additional moments because of lateral deflections. Thus, the failure of these columns is governed by buckling.

In lieu of an exact method that takes into account the effects of axial loads, fixed end moments, the variation of moment of inertia on member stiffness, the secondary moments created by additional lateral deflections and the duration of loads or creep influence, the ACI Building Code (ACI, 1983) presents a moment-magnifier method to account for the effects of slenderness on the strength of these compression members. This design procedure is strongly influenced by the choice of a stiffness parameter  $EI$ , used for the calculation of the critical load,  $P_c$ , defined as

$$P_c = \frac{\pi^2 EI}{(Kl_u)^2} \quad (1.1)$$

where

$EI$  = flexural stiffness of compression member

$K$  = effective length factor computed according to section 10.11.2.1 of the ACI code.

$l_u$  = unsupported length of a compression member taken as the clear distance between members providing lateral support

The ACI Building Code proposes two approximations for the value of the stiffness parameter  $EI$ . Excluding the creep factor  $\beta_d$ , the two equations take the following forms:

$$EI = 0.2E_c I_g + E_s I_{se} \quad (1.2)$$

or conservatively,

$$EI = 0.4E_c I_g \quad (1.3)$$

where

$E_c$  = modulus of elasticity of concrete

$E_s$  = modulus of elasticity of reinforcing steel

$I_g$  = moment of inertia of the gross concrete section about centroidal axis, neglecting the contribution of the reinforcing steel

$I_{se}$  = moment of inertia of the reinforcing steel about the centroidal axis of the member cross-section

For practical use, most engineers choose Eq. (1.3) because it is conservative and easier to compute. In many cases, the designer limited to certain required outside dimensions of the column is forced to increase the strength of the column by providing more steel reinforcement. The problem created by such a solution involves difficulties in the placing of reinforcing steel while satisfying the code requirements for clear distance between vertical reinforcement as given in Chapter 7.6 of the ACI Building Code (ACI 318R, 1983). Often the solution to this problem is inherent in the designer's computation of column strength based on a very conservative value of EI.

This report presents a less conservative solution to approximate the value of EI for a circular column, taking into account the magnitude of the applied axial load on the column. It is still important to note that a reduction of these values is mandatory in light of the column end conditions and additional moments computed in a second-order analysis.

## CHAPTER 2

### LITERATURE REVIEW

#### 2.1 Slender Column Behavior

A slender column is defined as a column whose strength is reduced by lateral deflections causing additional moments. The additional deflection  $\Delta$  is shown in Fig. 2.1 for a column bending in single curvature caused by load  $P$  initially applied with equal eccentricity  $e$  at each end. The bending deformation of the column creates an additional eccentricity  $\Delta$ , therefore the maximum bending moment increases to  $P(e + \Delta)$ . The significance of second-order moments introduced depends on the type of loading and the column end conditions.

As opposed to a slender column, a short column is defined as one in which the strength is not reduced by the additional moments because the eccentricity  $\Delta$  is generally negligible. Figure 2.2 illustrates the axial load-moment behavior for slender and short columns up to failure. For a short column, the intersection of the P-M line with the interaction diagram represents a material failure of the section. This type of failure characterizes short column behavior.

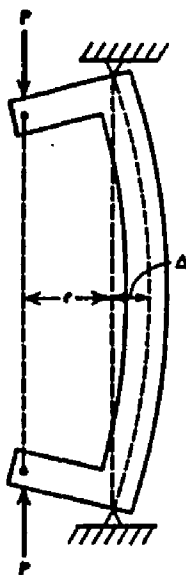


Fig. 2.1. Eccentrically loaded slender column (3).

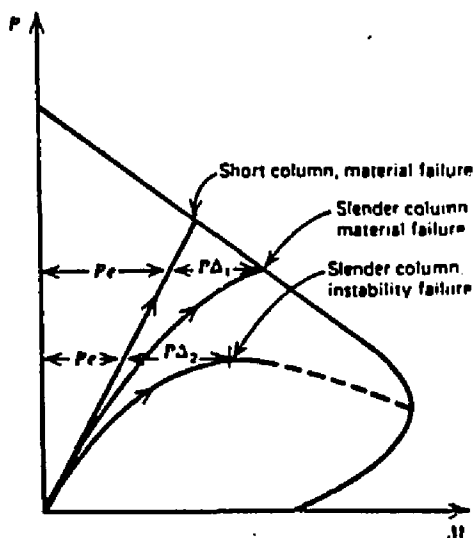


Fig. 2.2. Interaction diagram for a reinforced concrete column illustrating short and long column P-M behavior up to failure (3).

Two types of slender column behavior may occur. First, a column may still be stable when lateral deflections are introduced, but having reached the interaction line a material failure occurred. Second, the column may become unstable before reaching the interaction line. The first type of slender column failure is common in frames braced against sway, while the second type presents an instability failure which mainly occurs in unbraced columns.

The effects of slenderness on column strength for particular loading and end conditions can be shown by the use of slender column interaction diagrams (Park and Paulay, 1975). The construction of such a diagram is illustrated in Fig. 2.3. The slender column has an unsupported length to section thickness ratio of  $l_u/h = 30$ . Failure of the column occurs at point B for a given load and includes the contribution of the second-order moment introduced by lateral deflections. The same load at a primary moment,  $P_e$ , is given by the point A. The point A is determined for a range of  $e/h$  and  $l_u/h$  values and a family of curves in Fig. 2.3b may be traced, giving the load  $P$  and primary moment  $P_e$  which cause failure of the column. Such diagrams indicate the reduction in strength due to slenderness for various loading cases.

Many variables affect the strength of slender columns. These variables include the type of curvature

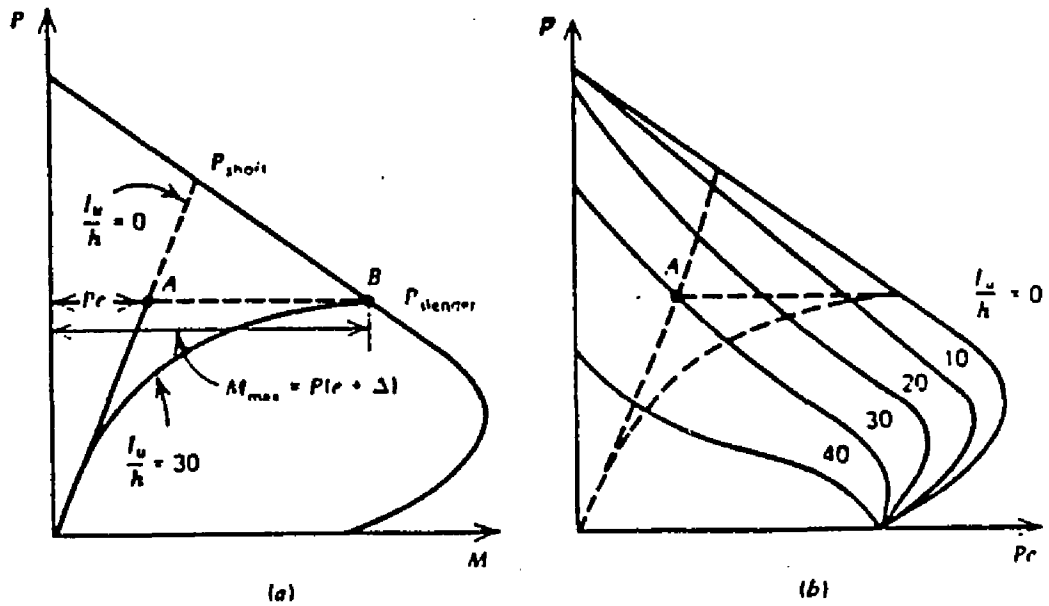


Fig. 2.3. Construction of slender column interaction diagrams (3). -- (a) Slender column behavior; and (b) Slender column interaction diagrams.

(Breen and Ferguson, 1964), the degree of rotational end restraint, the degree of lateral restraint, the ratio of unsupported height to section thickness  $l_u/h$ , and many others (Pfrang and Siess, 1964). The discussion of the effects of these variables goes beyond the scope of this report.

The variable studied in this investigation is the flexural stiffness of columns,  $EI$ , which depends on the following:

1. The content of steel reinforcement and the strength of the concrete.
2. The magnitude and type of axial load applied on the column.
3. The degree of cracking which varies along the column length.
4. The degree of nonlinearity of the concrete stress-strain curve and the type of tensile or compressive reinforcement (MacGregor et al., 1970).
5. The creep of concrete occurring when load is sustained, which tends to reduce the strength of the column (Drysdale and Huggins, 1971).

## 2.2 ACI Code Estimation of the EI Value

The moment-magnifier procedure used in the ACI code was originally derived for a particular type of column bending in symmetrical single curvature without any

transverse loads between its ends (Furlong and Ferguson, 1966). Other loading patterns do not strongly influence the EI expression for hinged columns bending in single curvature.

The maximum moment for a column in an elastic frame bending in symmetrical single curvature,  $M_u$ , can be calculated for design purposes to be (MacGregor et al., 1970):

$$M_u = \frac{P_o e}{1 - \frac{P_o}{P_c}} \quad (2.1)$$

where

$$P_c = \frac{\pi^2 EI}{lu^2} \text{ in the single curvature case}$$

$P_o$  = column axial load capacity

The other terms were previously defined. In order to obtain EI values including the effects of cracking, sets of data presenting the value of  $P_o$ ,  $M_u$ ,  $e$ ,  $l$  were collected from previous tests and investigations, and the value of EI was found to be (MacGregor et al., 1970):

$$EI = \frac{P_o M_u}{M_u - e P_c} \cdot \frac{l^2}{\pi^2} \quad (2.2)$$

The EI values computed from the columns analyzed were then used to evaluate a simplified EI equation containing the most significant variables.

Equations (10-10) and (10-11) in the ACI Building Code (ACI 318R, 1983) are used in the Moment-Magnifier procedure:

$$EI = \frac{E_c I_g / 5 + E_s I_s}{1 + \beta_d} \quad (\text{ACI Eq. 10-10}) \quad (2.3)$$

or conservatively,

$$EI = \frac{E_c I_g / 2.5}{1 + \beta_d} \quad (\text{ACI Eq. 10-11}) \quad (2.4)$$

where

$\beta_d$  = absolute value of ratio of maximum factored dead load moment to maximum factored total load moment, always positive.

This factor reflects the reduction of the strength for a column under sustained load. This decrease in the column capacity is due to the additional deflection induced over time.

The latter equation is used when  $\rho_t$ , defined as the total steel reinforcement ratio, is small (0.01 or up to 0.02 for small columns) and especially for columns that nearly qualify as short columns (Ferguson, 1978). This equation greatly underestimates EI when the value of  $\rho_t$  is large, leading to an overdesign of the column. With either Eq. (2.3) or (2.4), the scatter is broad, as shown in Fig. 2.4.

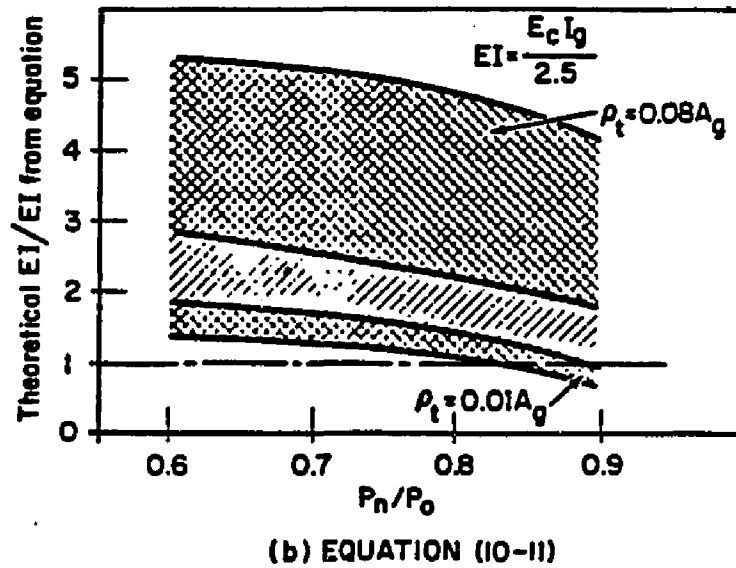
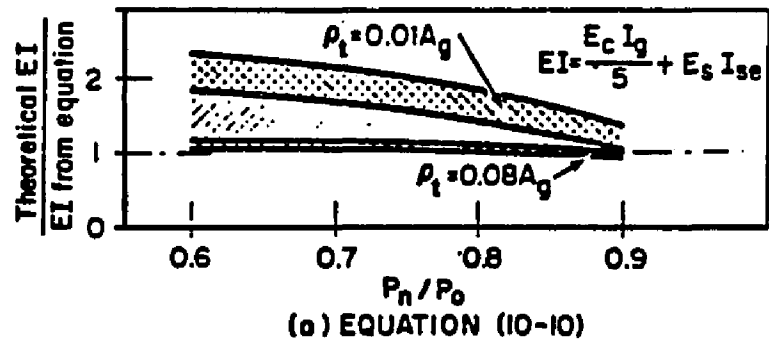


Fig. 2.4 Comparison of the ACI code equations for EI with EI values for moment-curvature diagrams (9).

It is also important to notice that the ratio (Theoretical EI) / (EI from ACI equation) is strongly dependent on the ratio  $P/P_o$  (ACI Commentary, 1983) and also depends on  $\rho_t$ . This shows the need for a better approximation of EI, which would include the effect of the applied axial load.

Concerning the two ACI equations, it is advantageous to calculate the larger EI, either from Eq. (2.3) referred to as  $EI_2$  or Eq. (2.4), referred to as  $EI_1$ , which would give the smaller multiplier  $\delta$  to be used in the Moment-Magnifier method. However, since both values are conservative, it is in the designer's interest to know the particular  $\rho_t$  that makes Eq. (2.3) the larger. To establish this result, the ratio  $EI_2/EI_1$  is set as unity, taking the example of a rectangular column with two faces of steel, as shown in Fig. 2.5.

$$1 = \left( \frac{E_c I_g / 5 + E_s I_s}{1 + \beta_d} \right) / \left( \frac{E_c I_g / 2.5}{1 + \beta_d} \right) \quad (2.5)$$

which simplifies to

$$1 = \frac{bh^3/60 + (E_s/E_c)\rho_t bh(\gamma h)^2/4}{bh^3/30} \quad (2.6)$$

or

$$1 = .5 + 7.5(E_s/E_c)\rho_t^2 \quad (2.7)$$

By letting the modular ratio  $n = E_s/E_c$ , the resulting equation is:

$$\text{Total reinforcement} = A'_s + A_s$$

$$\text{Area of concrete} = bh$$

$$\rho_t = \frac{A_s + A'_s}{bh}$$

$$\gamma = \frac{d - d'}{h}$$

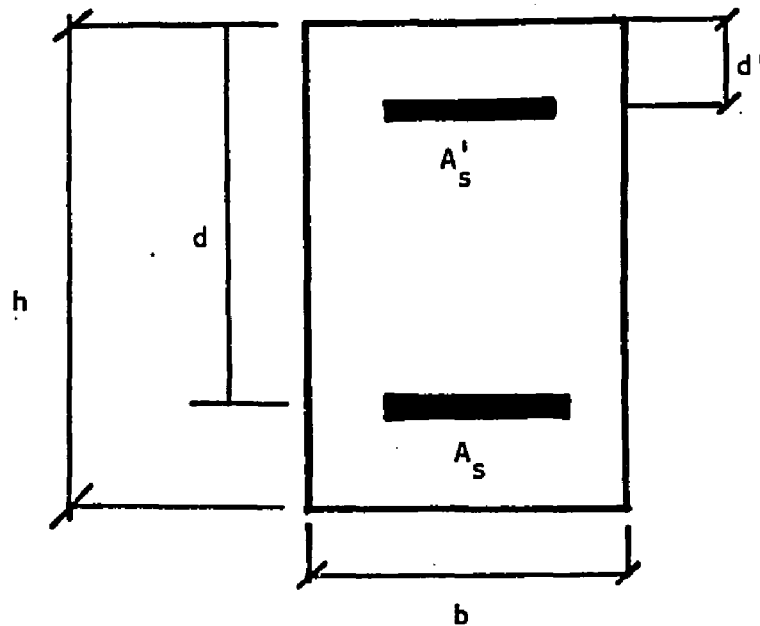


Fig. 2.5 Rectangular column cross-section with two faces of steel.

$$.5 = 7.5n\rho_t^2 \quad (2.8)$$

Based on  $EI_2/EI_1 = 1$ , this equation indicates that  $EI_2$  is larger than  $EI_1$  when  $\rho_t$  exceeds  $1/15n^2$ ; that is, when the value of  $\rho_t$  exceeds the limits shown in Table 2.1.

### 2.3. A Reexamination of the ACI EI Value

MacGregor, Oelhafeon and Hage (MacGregor et al., 1975) suggest a reexamination of the EI value for slender columns, as presented in the 1971 ACI Code. Those ACI equations 10.7 and 10.8 are the same as previously referred to as Eq. (2.3) and Eq. (2.4). An expression for EI was derived using the same assumptions as the ACI Code for a column bending in uniform single curvature. The three principal groups of columns studied included the following:

1. Eighty-one tied columns with bars in 2 faces (Shape A in Fig. 2.6) and possible combinations of the following variables:

$$\gamma = 0.6, 0.75, \text{ and } 0.9$$

$$e/h = 0.1, 0.25, \text{ and } 0.40$$

$$l_u/h = 10, 20, \text{ and } 40$$

$$\rho_t = 0.008, 0.040, \text{ and } 0.064$$

$$f'_c = 4 \text{ ksi}$$

$$f_y = 60 \text{ ksi}$$

Table 2.1. Minimum values of  $\rho_t$  making  $EI_2$  govern over  $EI_1$ .

$f'_n c$	3 Ksi 1	4 Ksi 8	5 Ksi 7
$\rho_t$	$1/(135 \gamma^2)$	$1/(120 \gamma^2)$	$1/(105 \gamma^2)$
$\gamma = .6$	.0205	.0231	.0264
.7	.0151	.0170	.0194
.8	.0115	.0130	.0149
.9	.0091	.0103	.0117

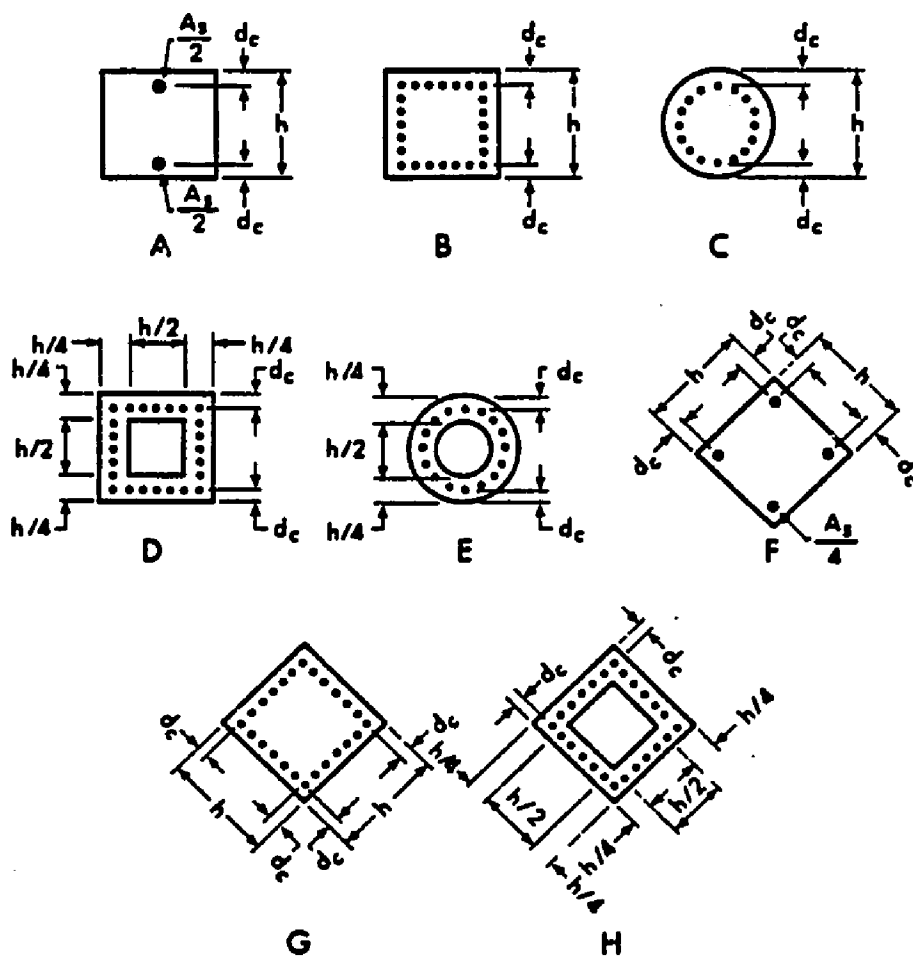


Fig. 2.6 Cross-section shapes investigated in the analysis (10).

2. Eighty-one tied columns with bars in 4 faces (Shape B in Fig. 2.6) and possible combinations of the variable given above.
3. Sixty-four other columns with the remaining cross-section shapes shown in Fig. 2.6.

The variables affecting  $EI/E_c I_g$  were grouped depending on the cross-section shape and arrangement of the steel reinforcement that characterize the three groups given above.

1.  $E_s I_s / E_c I_g$ ,  $e/h$ ,  $l_u/h$ .
2.  $\rho_t$ ,  $\gamma$ ,  $e/h$ .
3.  $\rho_t \gamma^2$ ,  $e/h$  and  $l_u/h$

The terms in each group are listed in order of decreasing significance.

As shown in Figs. 2.7 through 2.10, for columns with bars in two and four faces, the value of  $EI/E_c I_g$  tends to increase as the total steel ratio  $\rho_t$ , and the lever arm of the reinforcement,  $\gamma$ , increase. Although no figures were included to support this, it was concluded that for circular columns, a reasonable variation of  $\gamma$  does not affect the value of  $EI/E_c I_g$  (MacGregor et al., 1975). As discussed later, a similar observation was made for the circular columns which were analyzed for this study. Figure 2.11 shows the effect of  $\gamma$  and  $e/h$  on  $EI$  for tied columns with

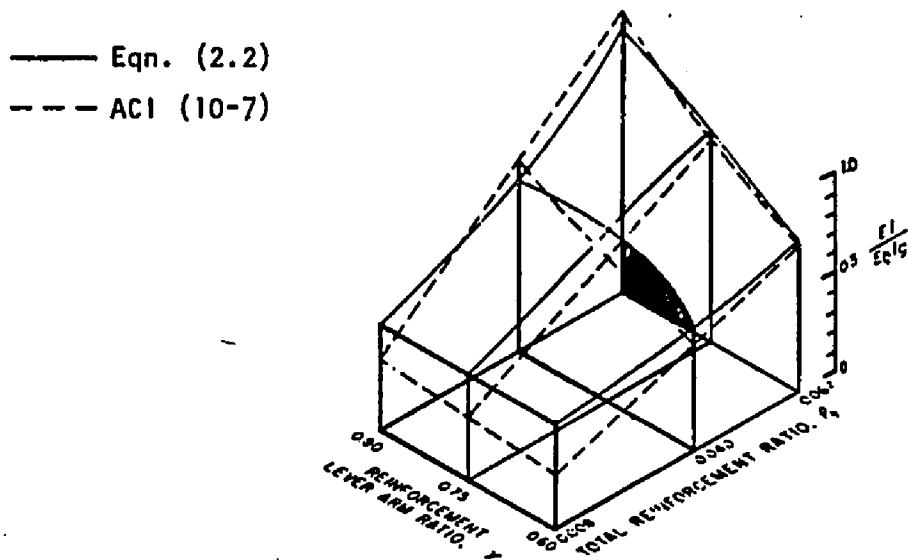


Fig. 2.7 Effect of steel ratio  $\rho_t$  and reinforcement lever arm,  $\gamma$ , on EI for tied columns with bars in two faces,  $e/h = 0.1$  and  $1/h = 20$  (10).

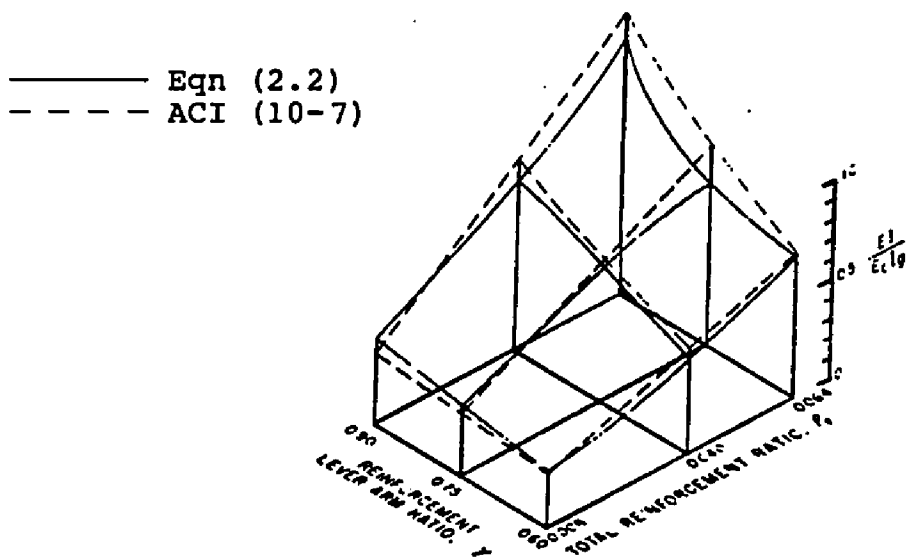


Fig. 2.8 Effect of steel ratio  $\rho_t$  and reinforcement lever arm,  $\gamma$ , on EI for tied columns with bars in two faces,  $e/h = .25$  and  $1/h = 20$  (10).

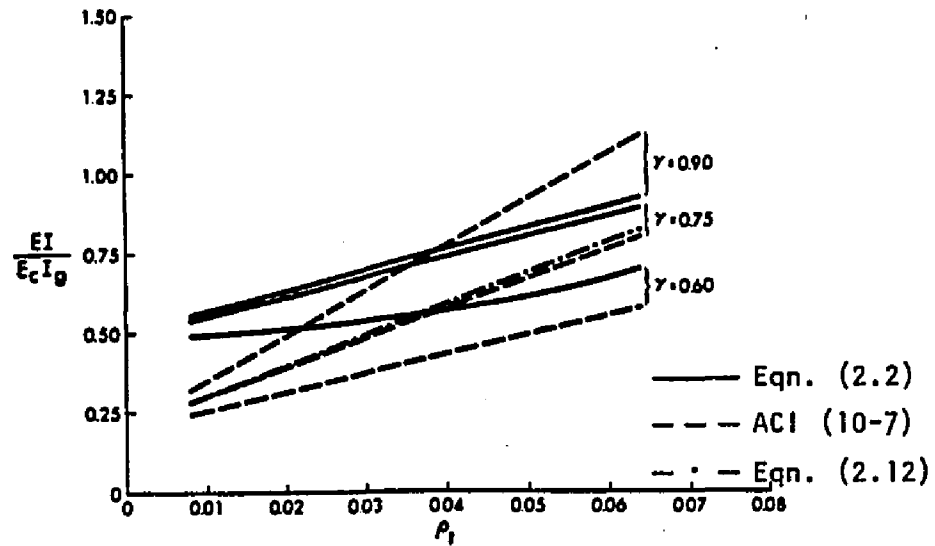


Fig. 2.9 Effect of steel ratio on EI for tied columns with bars in two faces,  $e/h = 0.1$  and  $l/h = 20$  (10).

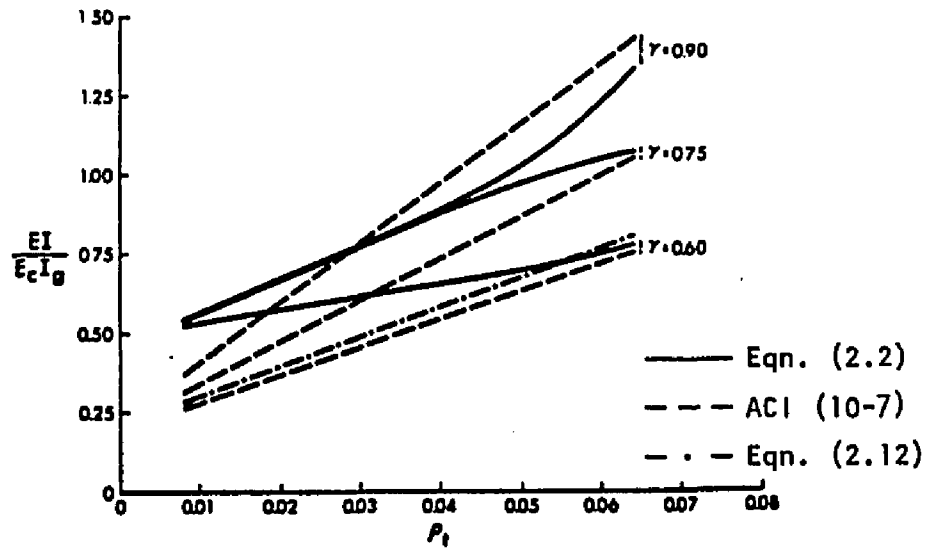


Fig. 2.10 Effect of steel ratio on EI for tied columns with bars in four faces,  $e/h = 0.1$  and  $l/h = 20$  (10).

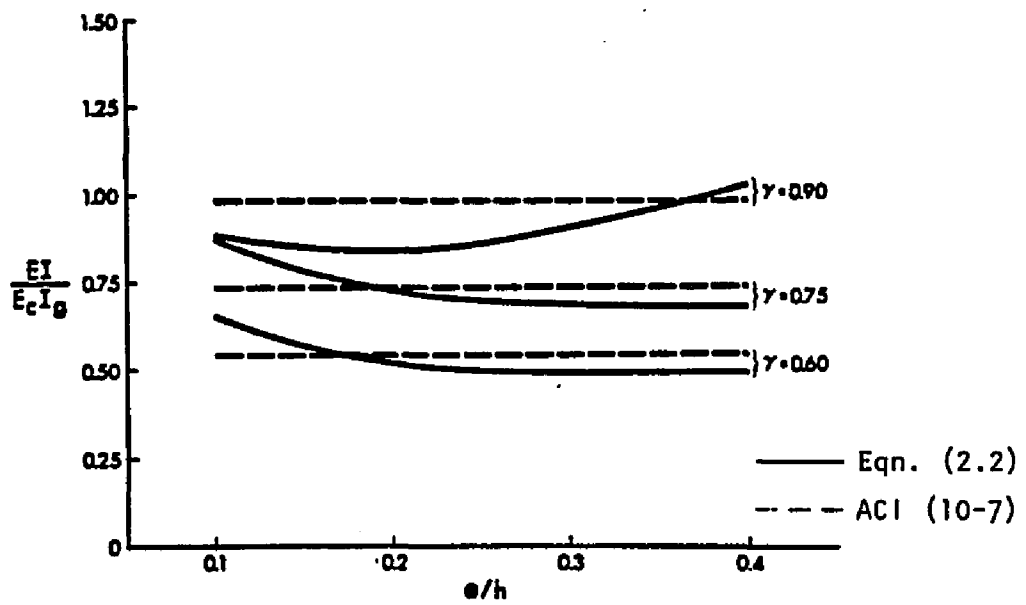


Fig. 2.11 Effect of  $\gamma$  and  $e/h$  for tied columns with bars in two faces,  $\rho_t = 0.04$  and  $l/h = 20$  (10).

bars in two faces. For small eccentricities, yielding of the compression reinforcement is generally responsible for the failure of the columns. In this case, an increase in the stiffness of the cross-section due to an increase in the value of  $\gamma$  is offset by an earlier yielding of the compression steel which causes failure.

Simplification of the results, and elimination of certain variables led to the following two equations that gave the best fit for the various groupings of variables considered.

$$\frac{EI}{E_c I_g} = (0.190 + .773 E_s I_s / E_c I_g + .0072 l_u / h - .346 e / h) \quad (2.9)$$

and then

$$\frac{EI}{E_c I_g} = (-.381 + 1.082 \frac{E_s}{E_c} \rho_t + .888\gamma - .0064 \frac{l_u}{h} - .458 \frac{e}{h}) \quad (2.10)$$

The terms in these equations are arranged in order decreasing significance. The use of term  $l_u/h$ ,  $e/h$ , and  $\gamma$  was considered impractical because the design problem would involve many iterations; the simplification of these two equations led to the following:

$$EI = 0.271 E_c I_g + 0.773 E_s I_s \quad (2.11)$$

and

$$EI = E_c I_g (.317 + 1.09 \frac{E_s}{E_c} \rho_t) \quad (2.12)$$

The coefficient 0.773 for  $E_s I_s$  indicates that the effect of reinforcement is much less than suggested by the ACI Code in Equation (10-10). Therefore, it is shown that the ACI Code overestimates the effect of reinforcement and that the coefficient is highly dependent on the magnitude and type of loading.

Further simplifications led to Eqs. (2.13) and (2.14) being recommended to replace the ACI Eqns. (10-7) and (10-8), respectively, as follows:

$$EI = \frac{E_c I_g}{5\alpha} + E_s I_s \quad (2.13)$$

or with smaller coefficient of variation as:

$$EI = \frac{E_c I_g}{5\alpha} + 1.2\rho_t E_s I_g \quad (2.14)$$

where  $\alpha = .75 + 1.8\beta_p$  but no less than 1.0, and  $\beta_p$  is defined as the ratio of the design sustained load to the total design load. This is different from the ACI definition in which the ratio of moment is used.

The two main reasons for this proposed change are:

1. In many cases, the original ACI definition seems to be impractical. One such case is where the design of the column is controlled by the required minimum eccentricity. An illustrative example would be the case of a column in the lower floor of a building. In such a case, the design of the column is governed

by the minimum eccentricity because of small applied moments and large axial forces. This results in an underestimation of the creep factor in the presence of large axial loads.

A second error is introduced when the signs of the moment at the two ends of the column are different, such as when the moments are caused by lateral loads. If wind moments control the design of a certain column for one direction of the wind, the column end moments have the same sign and are therefore added to obtain the total moment. For the wind blowing in the opposite direction, however, the moments are subtracted from each other, leading to an underestimation of the total moment (Goyal and Jackson, 1971).

2. No complete study has been made for columns loaded with sustained loads other than that of the rapidly applied load. The reduction in stiffness due to creep is generally offset by hydration effects and the stress transfer from concrete to steel over a short time period. The deflection increase caused by creep, tending to reduce the stiffness, is more pronounced over a longer time period following the hydration phase.

#### 2.4 Moment Magnifier Method

Different methods for designing slender columns have been developed. These include the moment magnifier method, the complementary moment method, and the long column reduction factor method. The last two methods are considered to be variations of the Moment Magnifier method adopted by the ACI Code for approximate evaluation of slenderness effects (Winter and Nilson, 1979). This design method involves an elastic frame analysis to compute the design forces and moments which are then modified for each individual column to account for slenderness effects. The idealization of the structure as a plane frame of linear elements is considered to be adequate for first-order approximation of moments and deflections. The moment curvature relationships can be used to provide accurate value of deflections and secondary moments. The analysis must consider the influence of the axial load on the rotational stiffness of the member and the possibility of having a maximum moment occurring at sections other than the ends of the member.

Because of the complexity of the problem, the proposed extensive analysis should show some accuracy comparable with the approximate design presented in Section 10.11 of the ACI Code (MacGregor et al., 1970). This more conservative design procedure uses the Moment Magnification

as the main tool for the design of compression members. In this method, the maximum moment in an elastic beam-column bending in single curvature is given by

$$M_{\max} = M_o + \frac{P\Delta_o}{1 - (P/P_c)} \quad (2.15)$$

where  $M_o$  and  $\Delta_o$  are the first-order moment and deflection, respectively,  $P$  is the column axial load, and  $P_c$  is the buckling load of the column. The evaluation of  $M_{\max}$  can be approximated (Johnston, 1976) by

$$M_{\max} = \frac{M_o}{1 - (P/P_c)} \quad (2.16)$$

This approximation is reasonably accurate for a column bending in symmetric single curvature because in this case the maximum moment and maximum deflection occur at the same point, as shown in Fig. 2.12.

In the more usual case where the end moments are not equal, the maximum moment may be estimated using an "equivalent uniform moment"  $C_m M_o$ . In this case, the expression for the maximum moment becomes:

$$M_{\max} = \frac{C_m M_o}{1 - (P/P_c)} \geq M_o \quad (2.17)$$

where  $C_m$  is the ratio of the equivalent uniform end moment to the numerically larger end moment. Values of  $C_m$  for several common design cases are presented in reference by the column research council (Johnston, 1976).

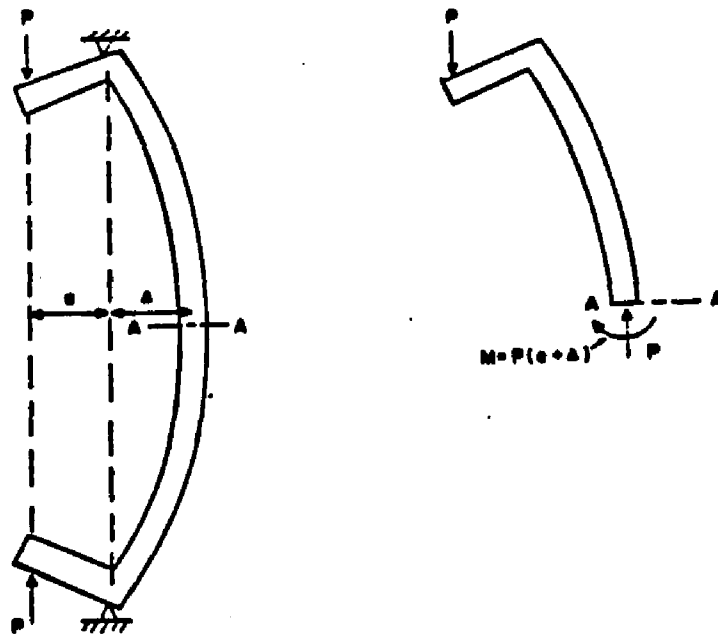


Fig. 2.12 Column bending in single curvature (2).

For reinforced concrete columns, the design can be based on the axial load  $P$  from a first-order analysis and the moment  $M_{\max}$  computed from the above equations. This design procedure closely approximates the actual case shown in Fig. 2.13 in which the most highly stressed section, section A-A, is loaded with an axial load  $P$  and a moment,  $Pe + P\Delta$ , equivalent to  $M_{\max}$ . Figure 2.13 shows the way in which this behavior is represented in the moment magnifier method. The column is designed for the axial load  $P$  and a magnified moment shown as F.M. Thus, the "moment magnifier-based load-moment path shown by the solid line in Fig. 2.13 closely approximates the test results and intersects the interaction curve at approximately the same combination of load and moment as the test.

By letting  $M_{\max} = \delta M_o$ , the moment magnifier factor  $\delta$  can be expressed in the form:

$$\delta = \frac{1}{1 - (P/\phi P_c)} \quad (2.19)$$

The strength reduction factor  $\phi$  is then introduced to give

$$\delta = \frac{1}{1 - (P/\phi P_c)} \quad (2.20)$$

The moment magnifier procedure, as first derived, assumes columns with pinned ends, single curvature, and no sidesway. Therefore, each column design should be modified

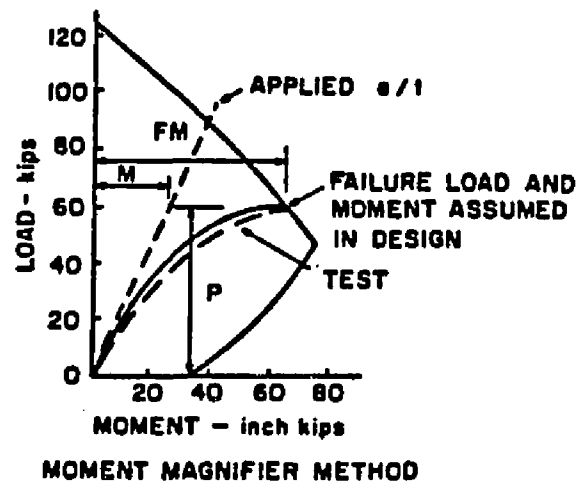


Fig. 2.13 Representation of column behavior.

by an effective length factor  $K$  to correct it to an equivalent pinned end column with single curvature. The value of  $K$  is used to determine the buckling load  $P_c = \pi^2 EI / (Kl_u)^2$  defined previously.

### 2.5 Proposed EI Values

Several investigators have presented values for  $EI$  to use in calculating the critical load of concrete columns.

For the design of columns in bridges (Bureau of Public Roads, 1966), the value  $EI$  is given as:

$$EI = E_c I_t \left[ 1.6 \frac{P}{P_o} \left( 1 - \frac{P}{P_o} \right) \right] \quad (2.21)$$

where

$E_c$  = modulus of elasticity of concrete

$I_t$  = transformed moment of inertia of the column  
cross section

$P$  = factored design column load

$P_o$  = capacity of column section in pure  
compression

This estimation tends to take into account the loading magnitude as well as the effect of concrete and steel reinforcement on the stiffness of columns, without taking into consideration the strength of the concrete or the grade of steel which influences the  $EI$  value. It is shown later that this estimation of  $EI$  is not accurate

enough and in most cases does not lead to a better result than the ACI approximations.

In his investigation, Parme expresses the critical load as  $P_{cr} = \frac{EI}{h^2}$  multiplied by a coefficient, where the value of the coefficient is dependent on the end restraint (Parme, 1966). For columns free to displace laterally, the ratio for first-order moment over the moment capacity at failure,  $M/M_u$ , is tabulated with respect to gamma,  $q = \rho_t f_y / f'_c$  and  $P/P_o$  which is the factored axial load on the column over the axial load capacity in pure compression. For columns not free to displace laterally, a different procedure is offered. The buckling load of the column for the specified end restraint is found. This, however, requires the determination of the EI value. Parme presents a table of EI values for tied columns with bars in two faces (Parme, 1966). For columns failing in compression, this table gives values of EI ranging from 0.167 to 1.625 times  $1000 f'_c I_g$  where

$$I_g = \frac{bh^3}{12} \quad (2.22)$$

In this table, EI is given as a function of  $q = \rho_t f_y / f'_c$ ,  $P/P_o$ , and the ratio  $g$  of the distance between the reinforcement to the column thickness.

Spang proposed that for columns with 4 percent steel:

$$EI = 1000 f'_c I_g \quad (2.23)$$

and for other steel percentages (Spang, 1966)

$$EI = \frac{E_c I_g}{4.1} + \frac{E_s I_s}{1.0} \quad (2.24)$$

The AASHTO specifications require that first-order loads and moments be computed on the basis of elastic analysis. Realistic moment-curvature relationships should be used to provide accurate values of deflections and moments (Lawrie and Heins, 1984). AASHTO offers no guidance as to what stiffness assumptions are considered reasonable and consistent, but the commentary on the Ontario Bridge Code suggests that reasonable results can be obtained if EI values are assumed to be:

$$EI = E_c I_g (0.2 + 1.2 \rho_t E_s / E_c) \quad (2.25)$$

for design of piers and:

$$EI = 0.5 E_c I_g \quad (2.26)$$

for superstructure stiffness.

The ACI Building Code Commentary also states that is is satisfactory to use Eqn. (2.25) in computing the column stiffness and Eq. (2.26) when evaluating the beam stiffness.

After reviewing the different approximations for EI value, it becomes clear that because of the complexity of the problem and the large number of variables that are

involved, it is very difficult to develop a general expression giving an accurate value for the EI. However, better results can be derived from moment curvature relationships as shown later in this report.

## CHAPTER 3

### SCOPE AND OBJECTIVES

Comparison of EI values as suggested by different investigators shows that there is considerable scatter in the values obtained when various column sections are considered or different loadings are applied. Therefore, a unique expression for EI cannot be derived analytically without considering solutions for different cross-sections and end restraints. The purpose of this investigation is to derive an expression for EI to evaluate a first-order approximation for the stiffness of circular columns.

The derivation of the EI equation for circular columns presented in this paper involved the following steps:

1. Develop a computer program to establish moment curvature relationships and calculate the effective moment of inertia for cracked sections corresponding to incremental loadings.
2. Determine the most significant variables that influence the value of the stiffness parameter EI. The variables studied are:

h = diameter of the circular column, referred to  
as DIA on the computer plots

$f'_c$  = concrete compressive strength

$f_y$  = yield strength of the reinforcing steel

$\gamma$  = ratio of the distance between centroids of outermost bars in the section to the overall diameter of the section, referred to as GAMMA on the computer plots

$\rho$  = steel ratio, referred to as RHO on the computer plots

$P/P_o$  = ratio of factored design load to ultimate load carrying capacity of the column in pure compression

3. Generate plots of axial load vs. stiffness for various column cross-sections to investigate the effect of the variables mentioned in step 2.
4. Select the significant variables that contribute the most in varying the EI value.
5. Develop expressions for the EI values based on the properties of the cross-sections.
6. Simplify the results obtained to eliminate variables which had little influence on the effective moment of inertia or were difficult to assess in a first-order approximation.
7. Compare the EI equations proposed by various investigators to the results of the computer solution to show the scatter in estimating the EI values.

8. Establish, if possible, that the EI expression derived in this report gives a better first-order approximation for circular columns since it represents more accurately the moment curvature relationships and is applicable for various cases encountered in different design problems.

## CHAPTER 4

### ANALYTICAL STUDY

#### 4.1 Computer Program

A computer program was developed to analyze a circular cross-section subjected to axial load and bending, calculate the effective moment of inertia and plot it vs. the axial load. These two parameters are then normalized with respect to the transformed moment of inertia,  $I_t$ , and the ultimate axial load capacity of the circular column in pure compression,  $P_o$ , respectively. An incremental iterative technique is used to solve for EI by assuming a certain depth of the neutral axis and then computing the corresponding curvature, the applied force, and the applied moment on the column.

This program is based on two assumptions related to the stress-strain curves idealizing the behavior of concrete and steel. The steel is assumed to be behaving as an elastic perfectly plastic material, as shown in Fig. 4.1. This is the stress-strain curve for steel assumed by the ACI code (ACI, 1983). The stress-strain curve approximation for concrete is the Hognestad (Hognestad, 1951) second-degree parabola, given by (see Fig. 4.2)

$$f_c = f''_c \left[ \frac{2e_c}{e_o} - \left( \frac{e_c}{e_o} \right)^2 \right] \quad (4.1)$$

where

$f''_c$  = the maximum compressive stress reached in the concrete of a flexural member; the value of  $f''_c$  is assumed to be equal to  $f'_c$  for analysis purposes of this study

$e_o$  = the strain at the maximum stress assumed to be equal to 0.002 in this study

The strain at crushing of concrete is assumed to be 0.003, and the steel modulus of elasticity is taken as 29,000 ksi.

The program includes the following steps:

1. Input data which include the column diameter, the radius to longitudinal bars, the number of bars, the cross-sectional area of a rebar, the value of  $f'_c$ , the value of  $f_y$ , the crushing strain of concrete, the Young's modulus of steel, the unit weight of concrete, and the lateral and rotational shift of the rebar reference axis.
2. Calculate the x and y coordinates of each bar with respect to the reference axis.
3. Calculate the maximum compressive capacity of the column using the expression

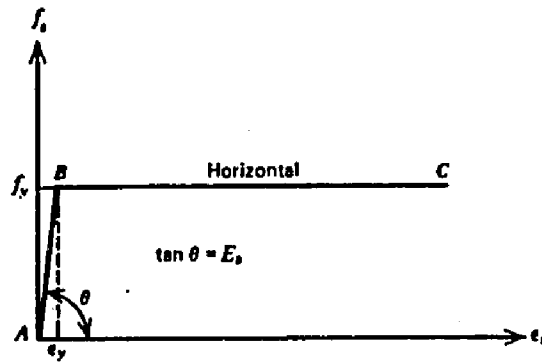


Fig. 4.1. Elastic perfectly plastic approximation for the steel stress-strain curve.

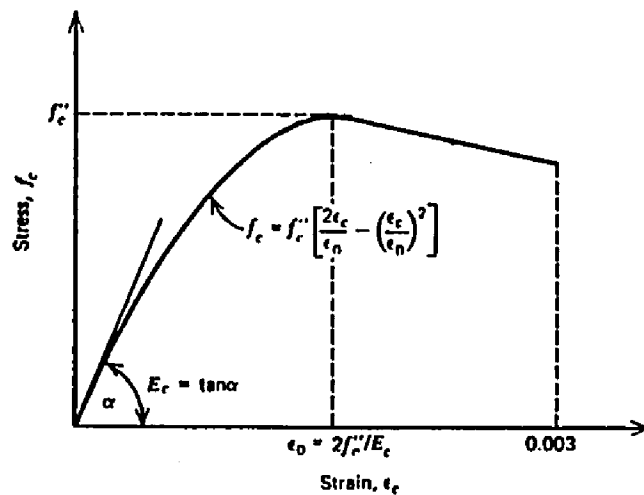


Fig. 4.2. Stress-strain curve for concrete using Hognestad's model.

$$P_o = .85f'_c A_c + A_s f_y \quad (4.2)$$

4. Develop data points for moment curvature diagram. The cross-section of a column subjected to uniaxial bending and compression is divided into a number of concrete and steel slices parallel to the neutral axis. By assuming an arbitrary depth to the neutral axis and using the maximum compressive strain of 0.003 for the extreme compression fiber of concrete, the strain at all points throughout the depth of the column cross-section can be calculated. From the strains, the concrete compressive forces  $C_i$  and the steel compressive and the tensile forces  $C_s$  and  $T_s$  for different layers may be computed from the stress-strain relationships of each material.

The load  $P$  and the moment  $M$  associated with the assumed location of neutral axis are given by:

$$P = \sum_{i=1}^i C_i + \sum_{i=1}^i (C_{si} - A_{si} f_{ci}) - \sum_{i=1}^i T_{si} \quad (4.3)$$

and

$$M = \sum_{i=1}^i C_i Y_{ci} + \sum_{i=1}^i (C_s - A_{si} f_{ci}) Y_{si} + \sum_{i=1}^i T_{si} Y_{si} \quad (4.4)$$

where the index  $i$  refers to the number of the slice,  $y_{ci}$  is the lever arm to the centroid of the concrete slice and  $y_{si}$  the lever arm to the steel centroid. In the procedure described above, the influence of the tensile capacity of concrete was ignored. The stress-strain diagram illustrating this procedure is shown in Fig. 4.3.

5. Incrementing the position of the neutral axis, new sets of axial loads and moments are computed and the complete moment curvature relationship is obtained.
6. At each increment the effective moment of inertia is computed for a cracked section as shown in Fig. 4.4 and then normalized with respect to  $I_t$ . Considering the following variables:

$A$  = area of cracked section of concrete

$r$  = radius of circular column

$Y_c$  = vertical distance to centroid of cracked section of concrete

$Y_a$  = vertical distance to centroid of cracked section including steel

$$A = r^2 (\alpha - \sin\alpha\cos\alpha)$$

$$\Delta = \frac{\sin^3\alpha \cos\alpha}{\alpha - \sin\alpha\cos\alpha}$$

$$Y_c = \frac{2r}{3} \frac{\sin^3\alpha}{\alpha - \sin\alpha\cos\alpha}$$

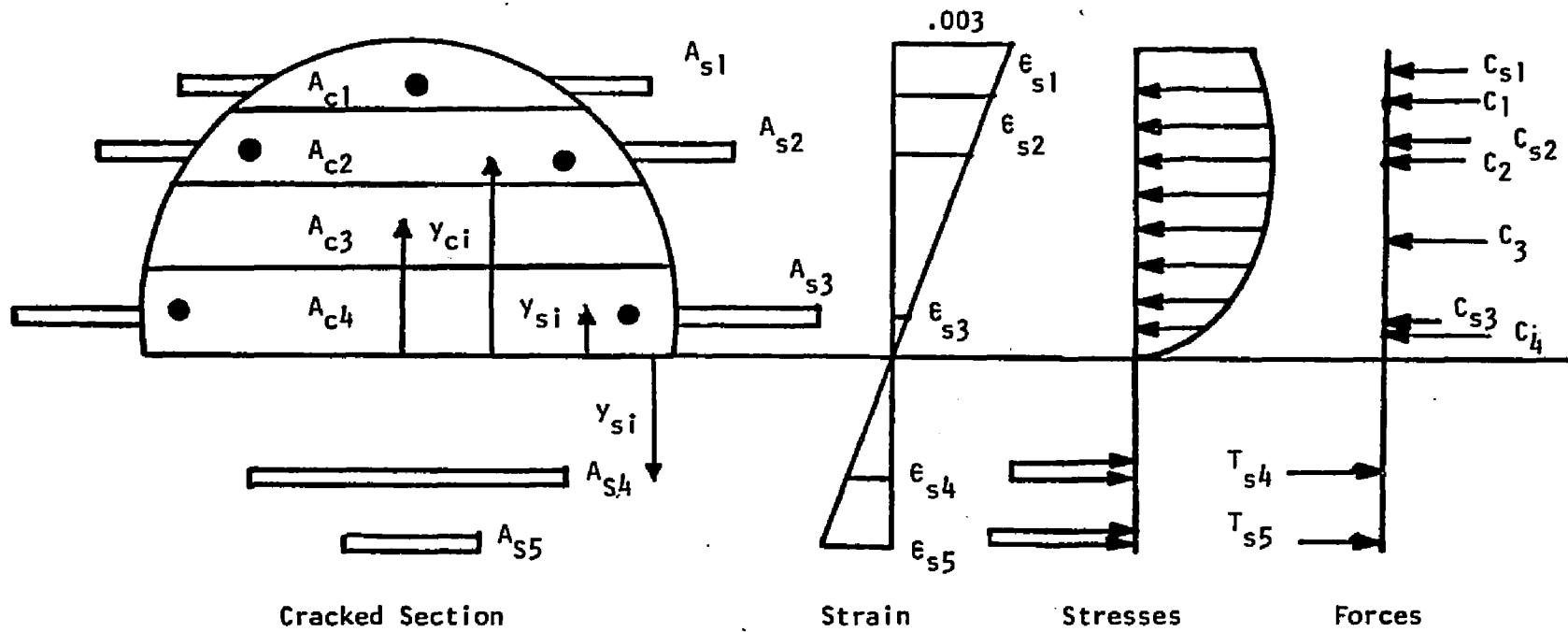


Fig. 4.3. Reinforced concrete cracked section when flexural strength is reached.

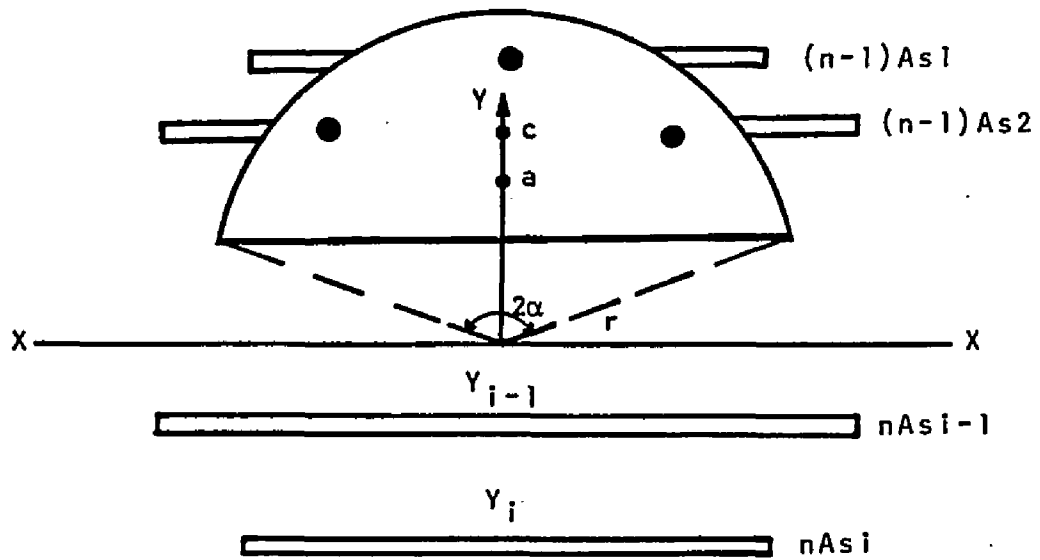


Fig. 4.4. Cracked section showing variables used to compute the effective moment of inertia.

$$I_{xx} = \frac{Ar^2}{4} (1 + 2\Delta)$$

The effective moment of inertia can be calculated given

$$I_{eff} = I_{xx} + (Y_c - Y_a)^2 A + (n - 1) \sum_{i=1}^m Y_i^2 A_i$$

7. The graphics part of the program plots the stored data for various variables for a specific circular cross-section in the form of  $I/I_t$  vs.  $(1 - P/P_o)$ .

The values of moments and loads for the interaction diagram are compared to design charts and excellent agreement is found.

A complete listing of the program and the corresponding flowchart are given in Appendix A of this report.

#### 4.2 Parametric Study

Earlier studies of the behavior of slender columns (MacGregor et al., 1975) suggest that the following five variables have the most effect on the strength and stiffness of such columns: slenderness ratio  $l/h$ ; shape of cross-section and reinforcement position; reinforcement ratio  $\rho_t$ ; ratio of the distance between the outer reinforcement layers and the overall thickness,  $\gamma$ , and eccentricity,  $e/h$ . The use of the term  $e/h$  in a first-order approximation was considered impractical because this term tends to zero for a

small eccentricity and large  $h$ . The term  $l/h$  is also eliminated to simplify a first-order approximation of  $EI$  value.

The principal variables selected in this study for circular columns include the following. The diameters of 12, 18, 24, 30, 42, and 50 in. were considered to cover a wide range of practical cross-sections. The ratio  $\gamma$  was varied for different diameters as given in Table 4.1. The ratio  $\gamma$  was chosen to satisfy the ACI clear cover requirements. As given in Section 7.7 of the ACI Code, the minimum cover for spiral ties must be 1.5 in. Certain codes require larger covers, especially for circular piles which are permanently exposed to earth. This, combined with the different diameters of longitudinal reinforcing steel, led to the typical values of  $\gamma$  which are given in Table 4.1. The values for  $f'_c$  were taken as 3, 4, 5, and 6 ksi. The values of  $f_y$  ranged from 40 ksi to 70 ksi by an increment of 10.

The ACI 318-83 Building Code requires the area of the longitudinal reinforcement for compression members to be between 1% and 8% of the gross area of the cross-section. Therefore, the reinforcing steel ratios were selected as  $\rho = 0.01, 0.03, 0.05, \text{ and } 0.07$ .

A parametric study was performed for different combinations of the variables that have been chosen in order to determine the effect of each variable and its significance

Table 4.1. Typical  $\gamma$  values for different column diameters.

h (in)	$\gamma$
12	0.60, 0.65
18	0.70, 0.75
24	0.80
30	0.80, 0.85
42	0.85, 0.90
50	0.85, 0.90

in the overall stiffness calculations. Thus, a total of 192 columns was analyzed by the computer program to detect a general pattern of the effective moment of inertia vs. the load applied on the column as a function of the above variables.

Figure 4.5 illustrates a cross-section of the circular column studied in this report. Considering the following parameters:

$$A_C = \text{gross area of concrete} = \pi h^2/4$$

$$A_S = \text{total reinforcement} = \sum A_b$$

$d'$  = distance from the centroid of longitudinal reinforcement to the outside concrete cover

$h$  = diameter of the circular column

The variables  $\rho$ (RHO) and  $\gamma$ (GAMMA) can be calculated given

$$\rho = A_S/A_C$$

$$\gamma = \frac{h - 2d'}{h}$$

Figure 4.6 shows a transformed circular cross-section. Considering the following parameters:

$A_b$  = cross-sectional area of longitudinal bar

$E_C$  = modulus of elasticity of concrete

$E_S$  = modulus of elasticity of steel

$m$  = number of longitudinal bars

$$n = E_S/E_C$$

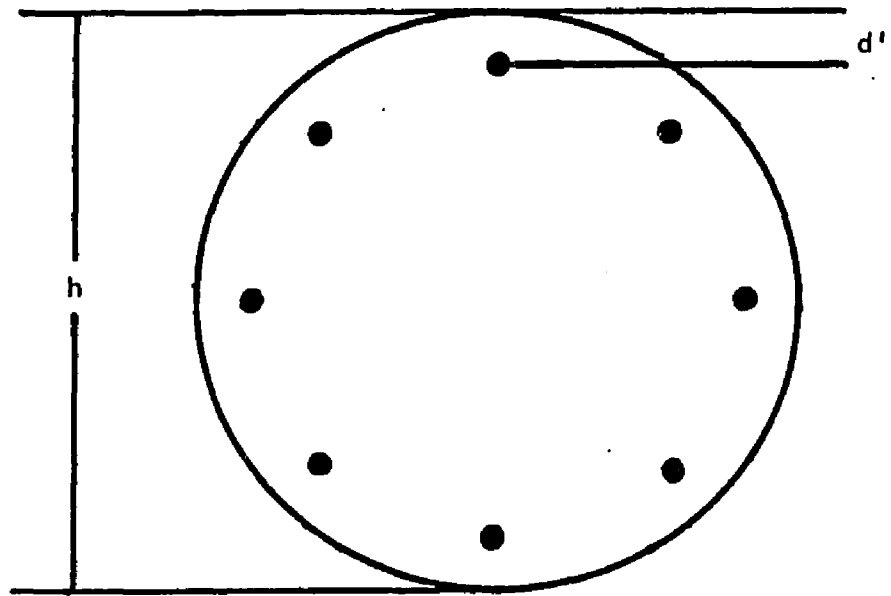


Fig. 4.5. Circular column cross-section.

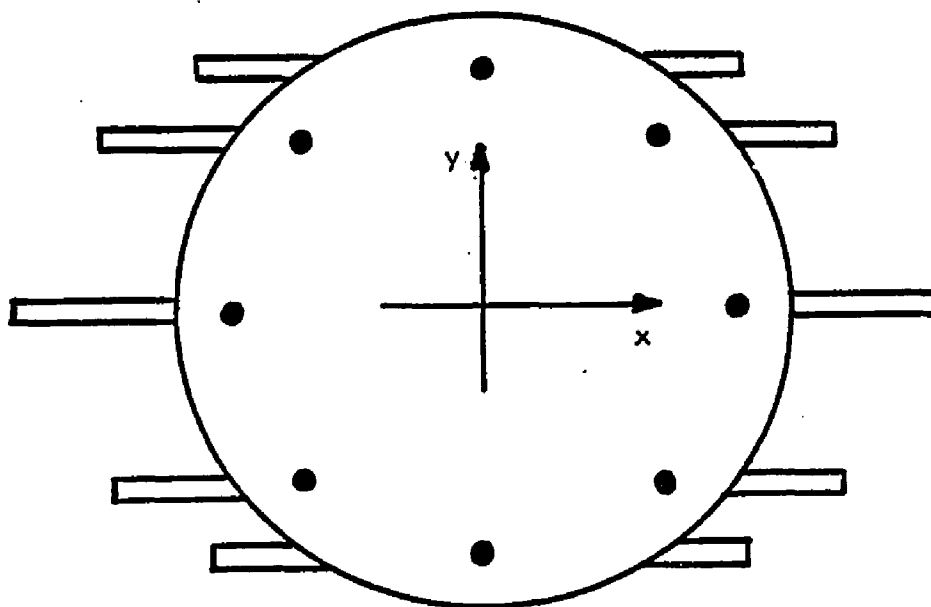


Fig. 4.6. Transformed circular cross-section.

$h$  = diameter of circular column

$Y_i$  = y-coordinate to  $i$ th bar

The transformed moment of inertia can be computed given:

$$I_t = \frac{\pi h^4}{64} + (n - 1) \sum_{i=1}^m A_b Y_i^2$$

#### 4.3 Comparison of the Proposed EI Values to the Computer Solution

The improved EI values computed using the computer program previously described were compared to the two ACI Eqs. (10-10) and (10-11), the equation proposed by Heins as  $EI = 1.6E_c I_t \frac{P}{P_o} (1 - P/P_o)$ , and the equation presented by MacGregor as  $EI = E_c I_g (0.2 + 1.2\rho_t E_s/E_c)$ .

The calculated moments of inertia were normalized with respect to the transformed moment of inertia while the loading on the column derived from moment-curvature diagram as in Fig. 4.7 was normalized with respect to the ultimate column compressive capacity,  $P_o$ .

The comparison was carried for various combinations of the variables mentioned in Chapter 4.3. For the sake of brevity, comparison of the different methods only for a 24" diameter column with  $f'_c = 4000$  psi and  $f_y = 60$  ksi are presented in detail. These results are shown in Figs. 4.8 through 4.11. The value of  $\gamma$  (GAMMA) was selected as 0.8 and the reinforcement ratio varied between 1% and 7%. It is

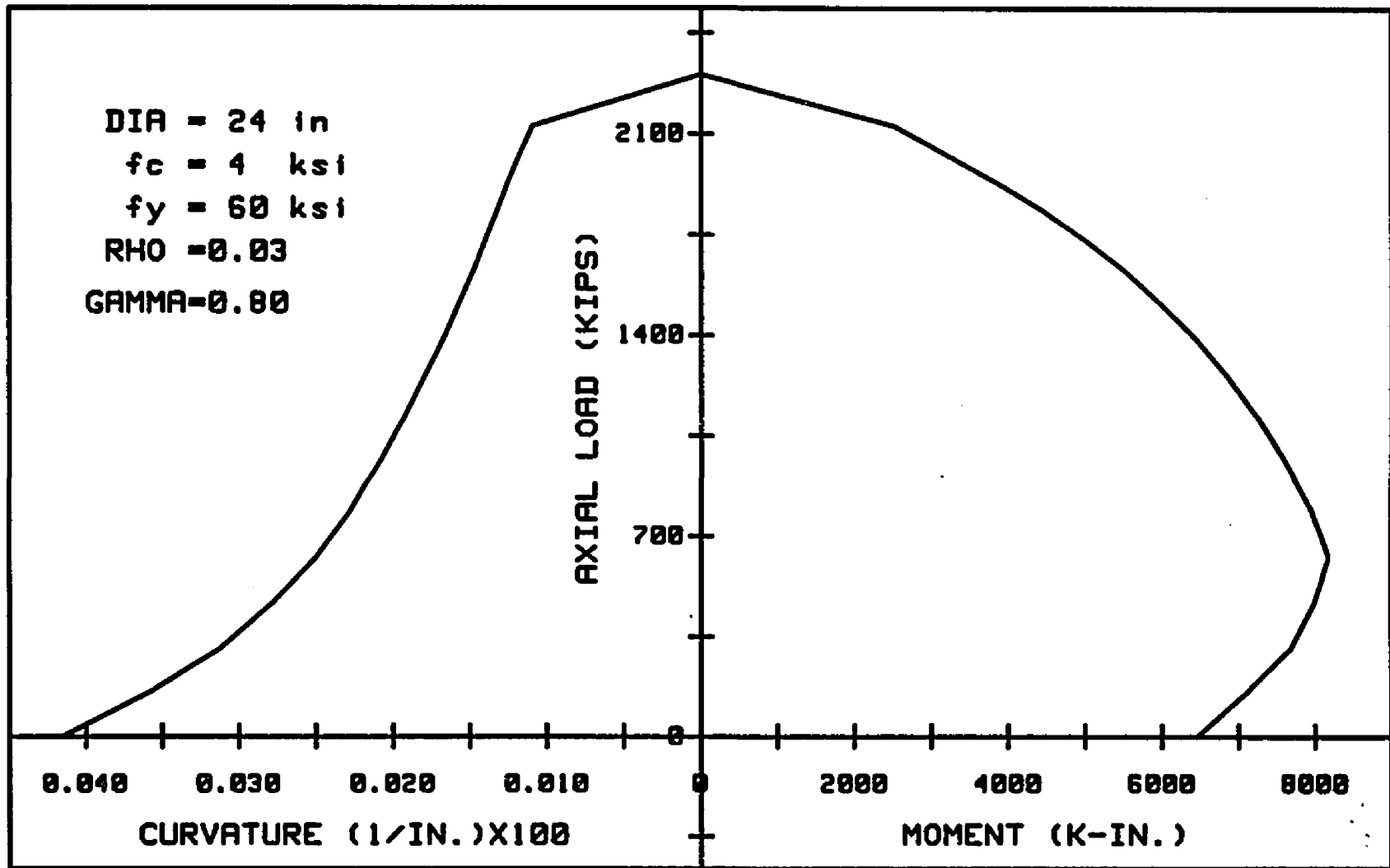


Fig. 4.7. Axial load-moment-curvature relationship for a typical circular column.

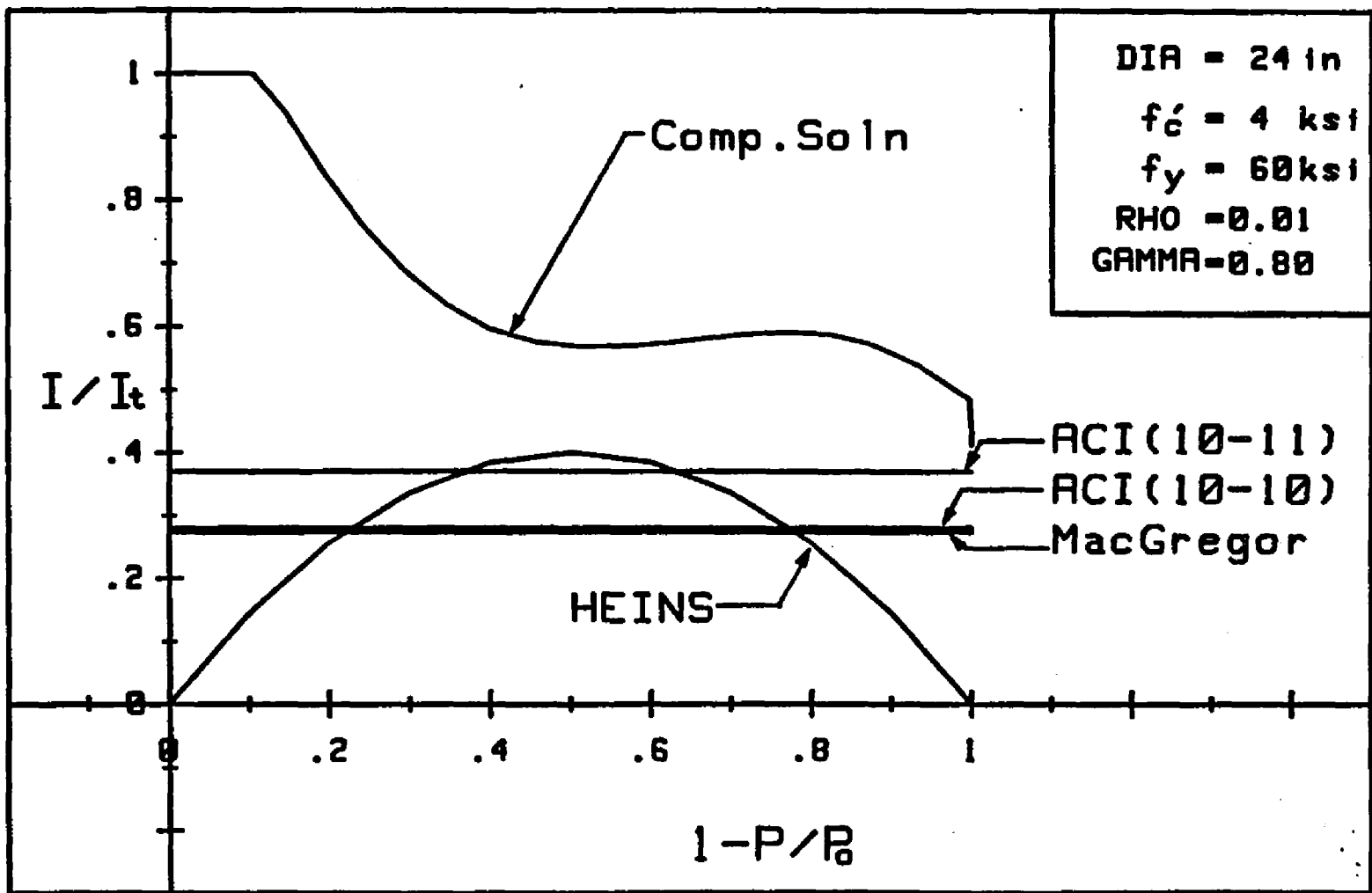


Fig. 4.8. Variation of moment of inertia with different axial loads for a column with 1% reinforcement.

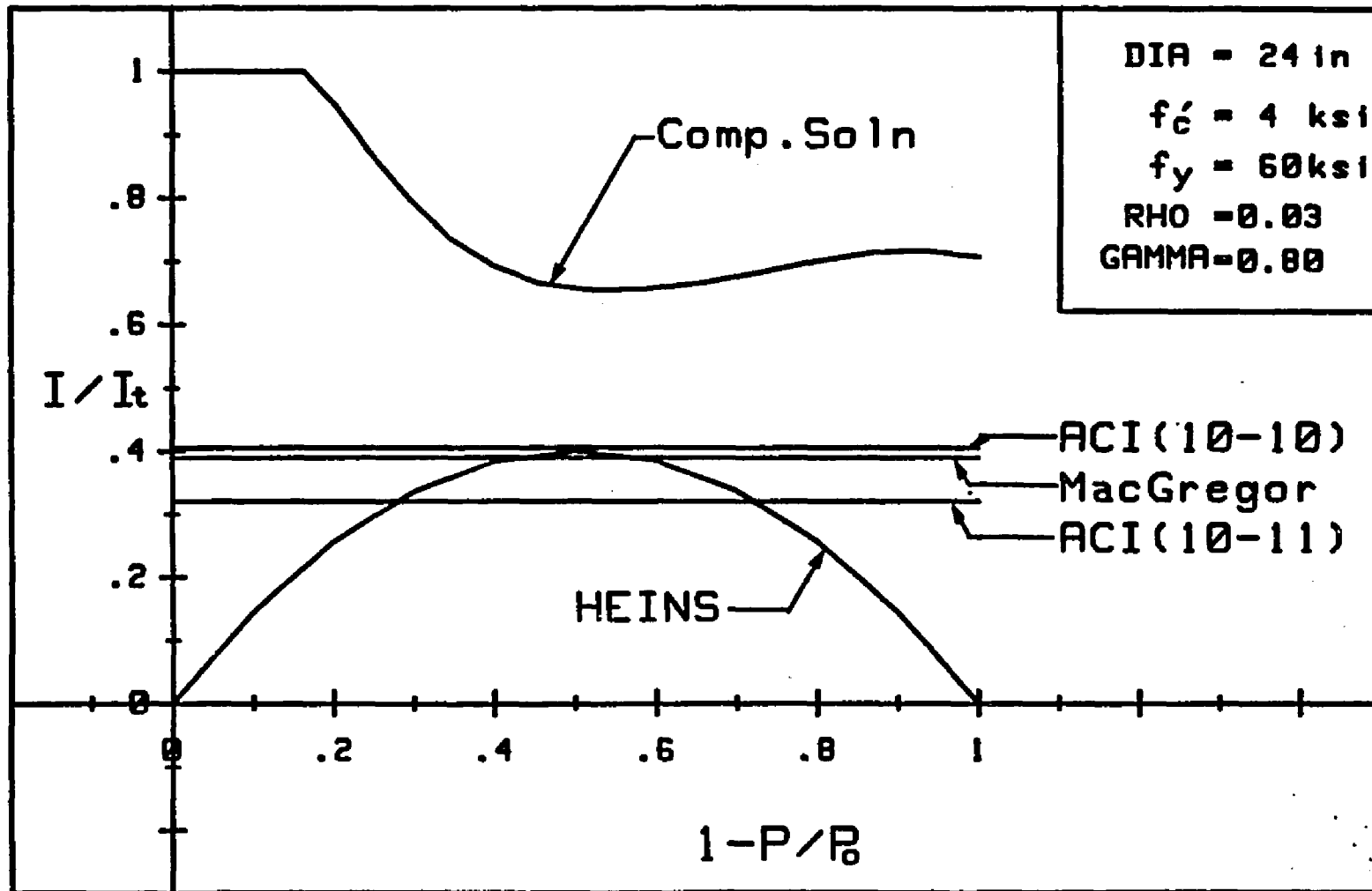


Fig. 4.9. Variation of moment of inertia with different axial loads for a column with 3% reinforcement.

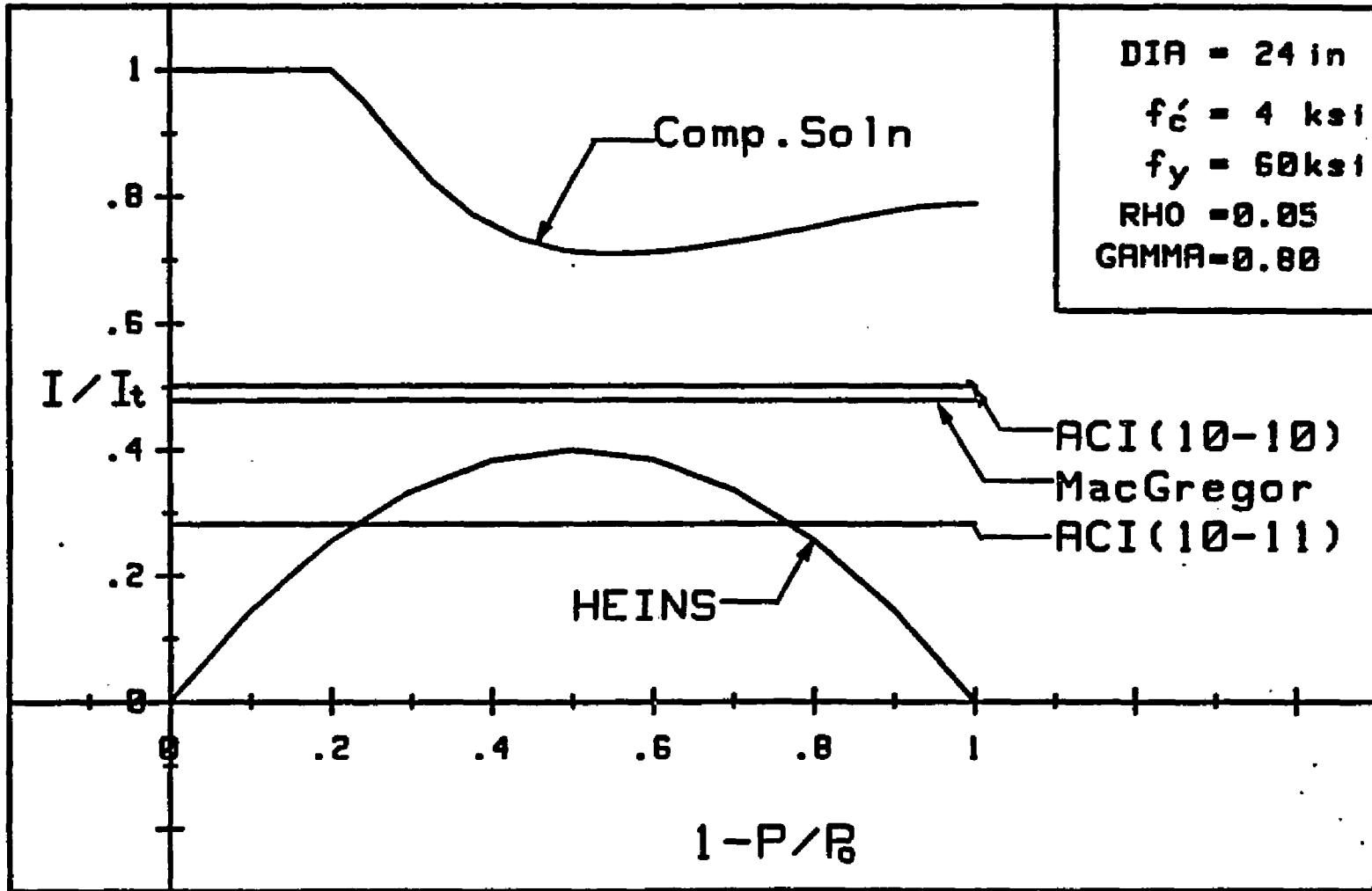


Fig. 4.10. Variation of moment of inertia with different axial loads for a column with 5% reinforcement. 53

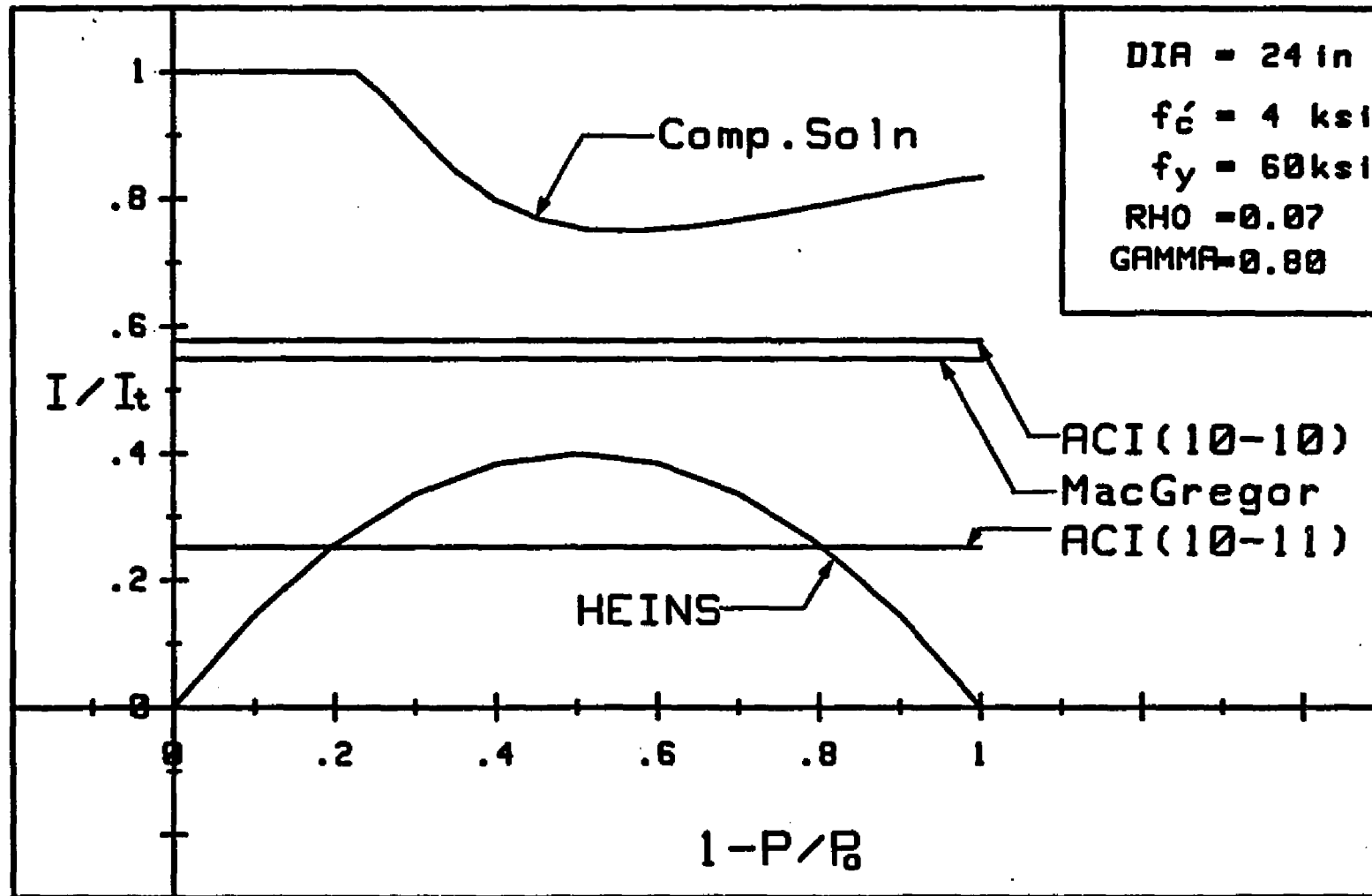


Fig. 4.11. Variation of moment of inertia with different axial loads for a column with 7% reinforcement.

noted that similar observations as those given below were made for all different columns investigated.

1. With the exception of the equation given by Heins, the other three equations ignore the effect of the axial load, which strongly influences the value of the effective moment of inertia. It is shown in Figures 4.8 through 4.11 that for high values of  $P/P_0$ , the value of  $I_{\text{effective}}$  tends to increase. This is due to the fact that at large axial loads the depth to the neutral axis is also large, resulting in a larger value for the effective moment of inertia of the uncracked section of the column.
2. All four equations tend to underestimate the value of EI as compared to the improved computer solution. This difference is as high as 20% of the transformed moment of inertia when the column is subjected to the maximum moment at balanced condition. Figures 4.8 through 4.11 illustrate this difference that appears between the inflection point of the exact computer solution and the least conservative curve of the equations involved in that comparison.
3. It is shown from the comparison of Figures 4.8 through 4.11 that for a low reinforcement percentage, such as 1%, the ACI Eq. (10-11) is less conservative than the ACI Eq. (10-10). For high

reinforcement percentage, i.e., 3% to 7%, the ACI Eq. (10-10) is less conservative than the ACI Eq. (10-11) and tends to better approximate the lowest value of  $I_{\text{effective}}$  given by the improved computer solution.

4. MacGregor's solution tends to approach ACI Eq. (10-10). However, this approximation is more conservative than ACI Eq. (10-10).
5. While taking into consideration the effect of the applied axial loads on the column, Heins' equation does not seem to represent the true variation of  $I_{\text{effective}}$  with respect to various ratios of  $P/P_0$ . It only tends to converge to the other three equations for values of  $P/P_0$  ranging between 0.3 and 0.7. This equation tends to zero for very large or small axial loads. This violates the fact that for  $P/P_0 = 1$  the column would be subjected to pure compression and the value of the effective moment of inertia would be equal to the transformed moment of inertia.
6. As shown in Figs. 4.8 through 4.11, there is considerable scatter in the EI values obtained using the existing methods when various column properties are considered. The need for a new estimation of

the EI value is obvious, considering the multiplicity of these equations that do not converge to an accurate appropriate value for EI given a cross-section and specific properties.

#### 4.4 Variables Affecting EI Value

The effects of the previously mentioned variables on the improved EI values obtained by the computer analysis were studied using a variance, covariance, and a linear regression analysis. Considering a circular column with 24" diameter,  $f'_c$  value of 4 ksi,  $f_y$  value of 60 ksi, and steel ratio  $\rho$  of 0.01. The different parameters are varied with respect to this set of data in order to obtain the effects of each variable. The steel ratio  $\rho$  is found to be the main parameter affecting the value of  $I_{\text{effective}}$ . The polynomial coefficients are derived with respect to  $\rho$ . Once the polynomial is derived, the effects of  $f_y$ ,  $f'_c$ ,  $h$ , and  $\gamma$  are included as influence factors. As shown in Fig. 4.12, for a typical circular column the value of  $I/I_t$  tends to increase as the total steel ratio,  $\rho$ , increases. This increase seems to be decreasing with increasing  $\rho$ . The various curves corresponding to different reinforcement percentages are shifting almost parallel to each other.

At large values of  $P/P_o$ , the depth of the neutral axis is greater and the effective moment of inertia is calculated for a larger uncracked portion of the circular

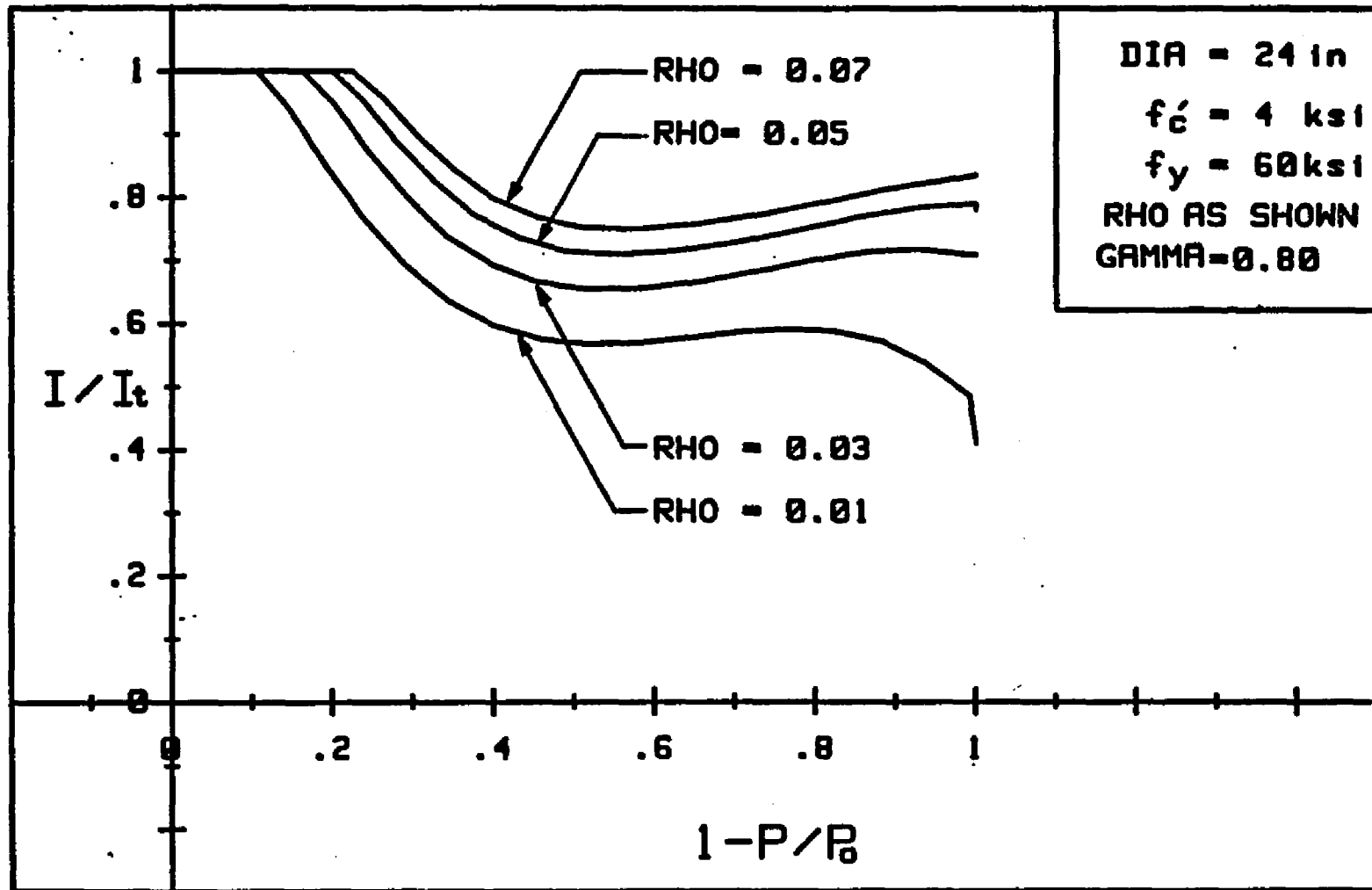


Fig. 4.12. Effect of steel ratio  $\rho$  on  $I/I_t$ .

column. This results in a smaller increase of the ratio  $I/I_t$  for high values of  $P/P_o$  than for small values of  $P/P_o$ .

The effect of  $f_y$ , the yield stress for the steel reinforcement, is shown in Figs. 4.13 and 4.14. This effect is more pronounced in Fig. 4.14 for  $\rho$  equal to 0.05 than in Fig. 4.13 for  $\rho$  equal to 0.03. These figures indicate that  $I/I_t$  values tend to increase with increasing  $f_y$  for large  $P/P_o$  while staying the same for small values of  $P/P_o$ . This is due to the fact that for large  $P/P_o$ , the depth of neutral axis tends to be large and an increase in the yield stress creates a larger tension value. This means a larger concrete area is needed to create a compressive force for equilibrium to the tensile force. The larger effective area of concrete results in a higher value of the effective moment of inertia for large  $P/P_o$  values. In the case of low values of  $P/P_o$ , the contribution of steel area in computing the effective moment of inertia is very high since the depth of the neutral axis is low. An increase in the tensile stress would result in a slight increase of the depth of neutral axis which does not affect the value of  $I_{\text{effective}}$  significantly. Therefore, the value of  $I_{\text{effective}}$  is almost the same for different steel yield stresses at low  $P/P_o$  values.

The effect of varying  $f'_c$  is very small, as shown in Fig. 4.15. By increasing the value of  $f'_c$ , the ultimate

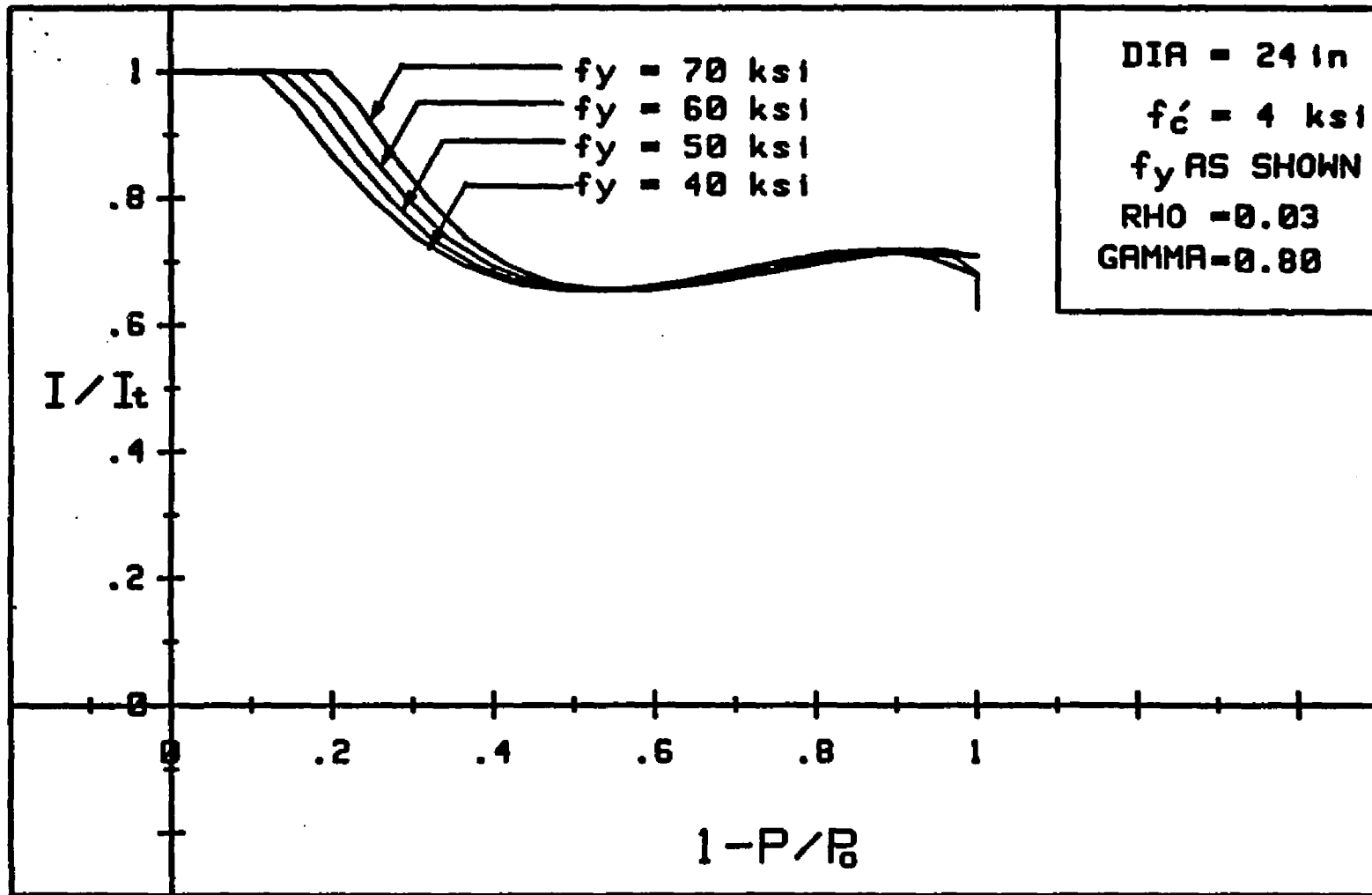


Fig. 4.13. Effect of steel reinforcement yield stress on the ratio  $I/I_t$  with respect to axial load for  $\rho = 0.03$ . 90

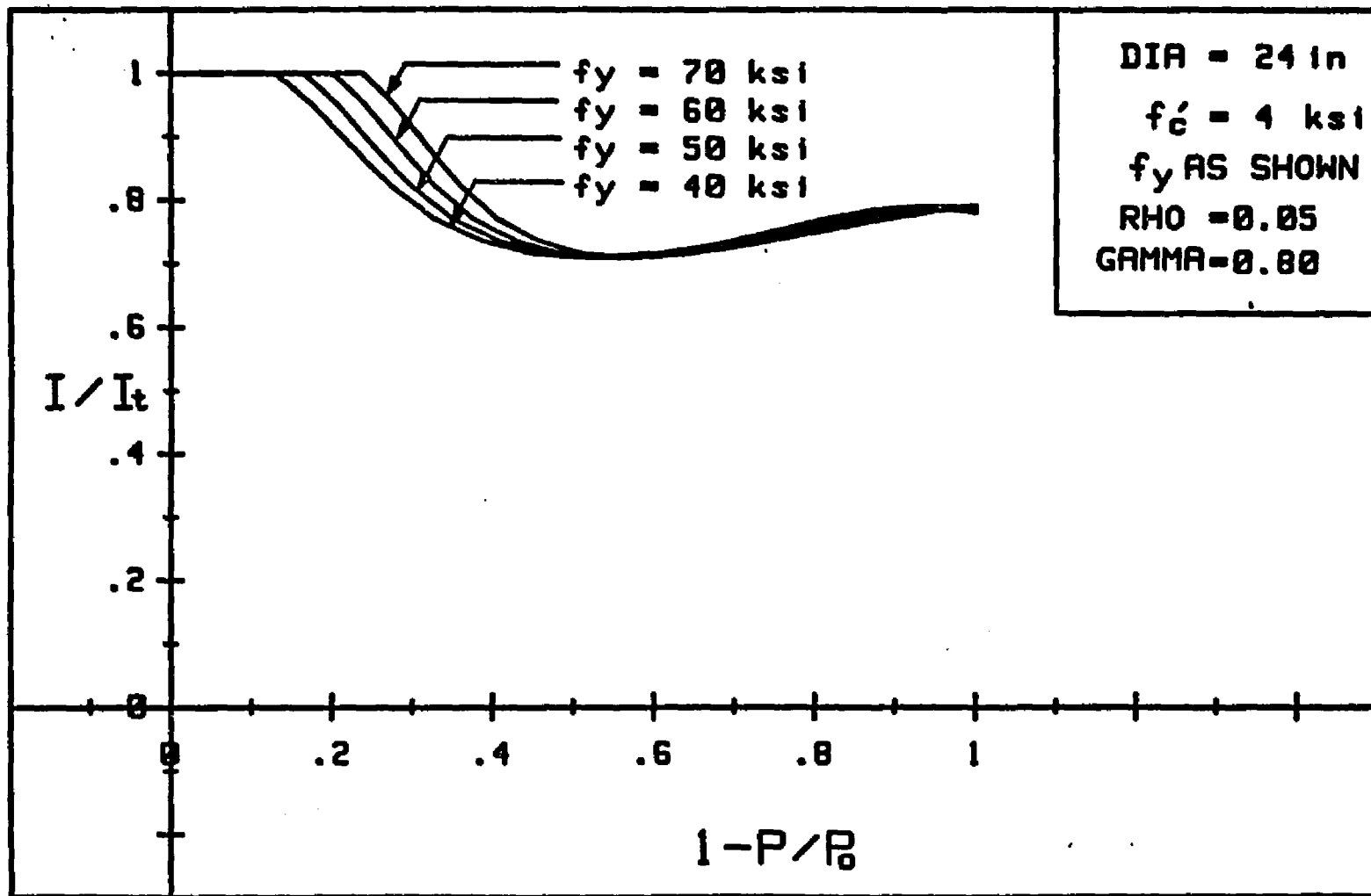


Fig. 4.14. Effect of steel reinforcement yield stress on the ratio  $I/I_t$  with respect to axial load for  $\rho = 0.05$ .

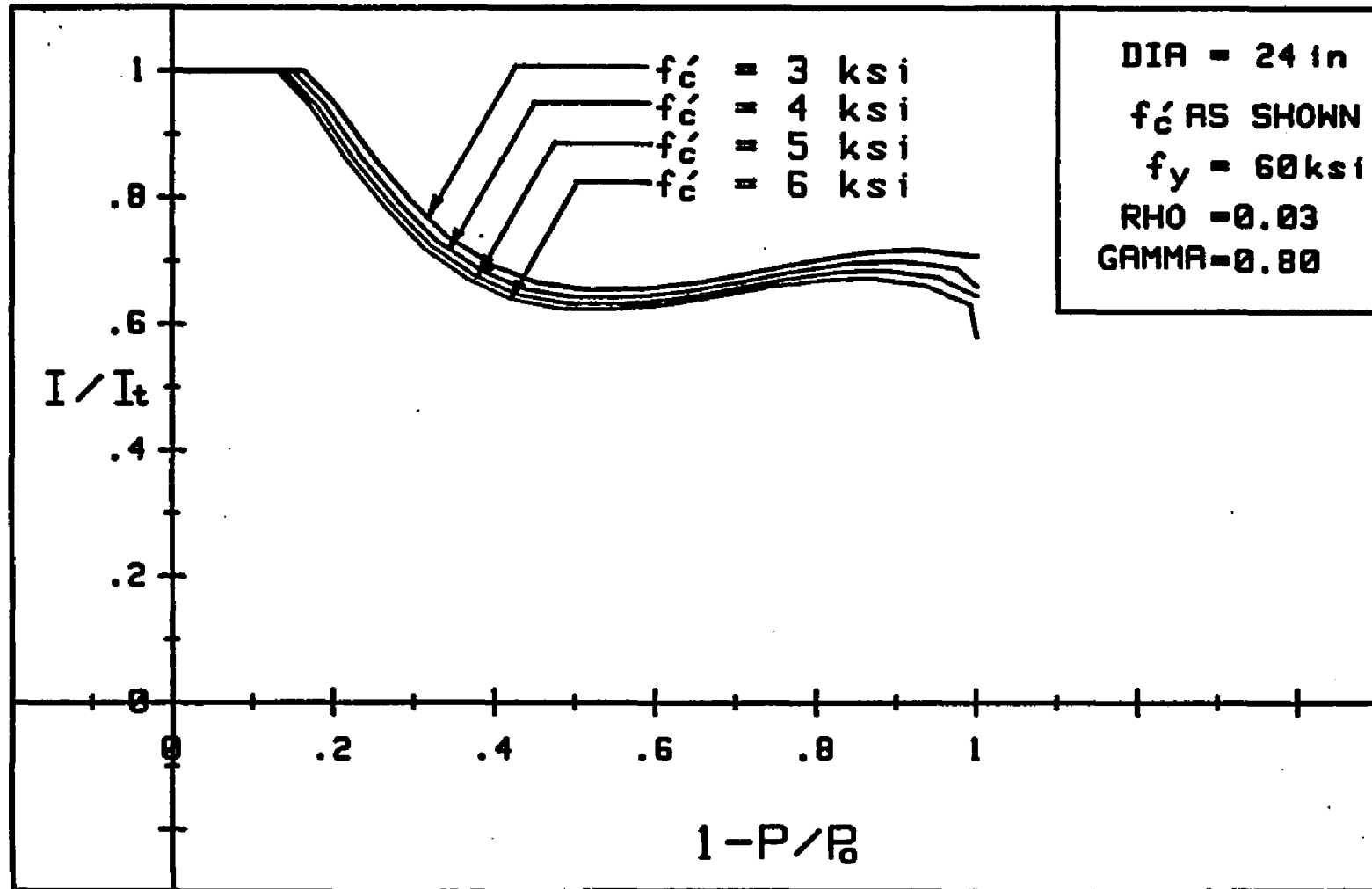


Fig. 4.15. Effect of concrete strength  $f'_c$  on the ratio  $I/I_t$ .

capacity of the column increases. This would result in a lower value of  $P/P_o$ , giving a decrease in the depth of the neutral axis. Here, the smaller effective area of concrete leads to a lower value of the effective moment of inertia. Also, it is important to note that the decrease in the value of the modulus ratio due to an increase of  $f'_c$  would equally affect the value of  $I_{\text{effective}}$  and  $I_{\text{transformed}}$ . It can be seen in Fig. 4.15 that the curves are shifting upward parallel to each other with decreasing  $f'_c$ .

The last two variables, namely  $\gamma$  and  $h$ , were found to be interrelated and dependent on each other. The choice of  $\gamma$  is highly dependent on the designer. It is difficult to consider  $\gamma$  as a variable when deriving an expression for EI value. The underlying assumption here is that in order to achieve the most economical cross-section, minimum allowable cover concrete is used. Depending on the diameters of the spiral tie and the longitudinal steel, the distance from the outer face of the column to the centroid of the longitudinal steel is between 2.5 in. to 3.5 in. including a 1.5 in. clear cover. This dimension remains almost the same regardless of the diameter of the column.

As discussed earlier, the only exception to this is when local codes or permanent exposure to adverse environments requires slightly larger cover concrete. In such

cases the value of  $\gamma$  may be closer to the smaller values listed in Table 4.1.

Consequently, a typical gamma value for a 12 in. diameter column is 0.6, while that for a 36 in. diameter column is approximately 0.85. Therefore, while an increase in  $\gamma$  would result in an increase of the moment arm used in computing the effective moment of inertia, the practical implications of this variation are questionable. Figure 4.16 shows that  $I/I_t$  tends to increase with increasing  $\gamma$ . The values 0.6 and 0.9 are considered impractical for a 24 in. diameter column. The optimum  $\gamma$  for such a column is between 0.7 and 0.8, depending on the required concrete cover and the diameter of the reinforcing steel. This indicates that a very slight variation in the value of EI can occur due to a practical and realistic change in  $\gamma$ . This trend is unique for circular columns and does not hold for other cross-sections. Based on the assumption of required concrete cover, if we consider a column with a 24 in. diameter, and another with a 48 in. diameter, the ratio  $I/I_t$  tends to increase with increasing diameter. This is due to the fact that an increase in the diameter from 24 in. to 48 in. is more than sufficient for the additional cover requirement, resulting in a relative increase of the moment arm of bars for the 48 in. diameter column, thus a higher value of EI as shown in Fig. 4.17. Because of the

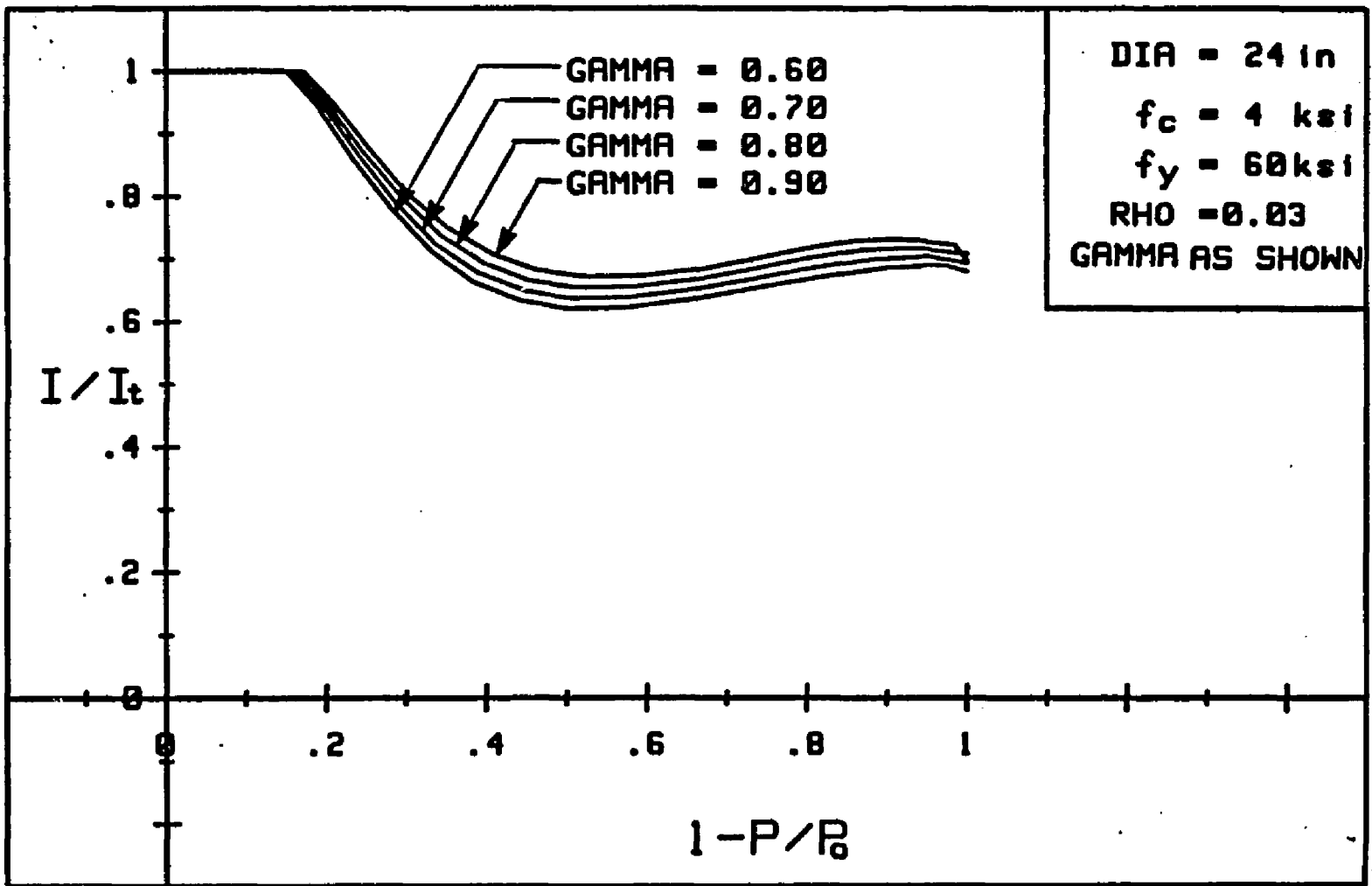


Fig. 4.16. Effect of  $\gamma$  ratio on  $I/I_t$ .

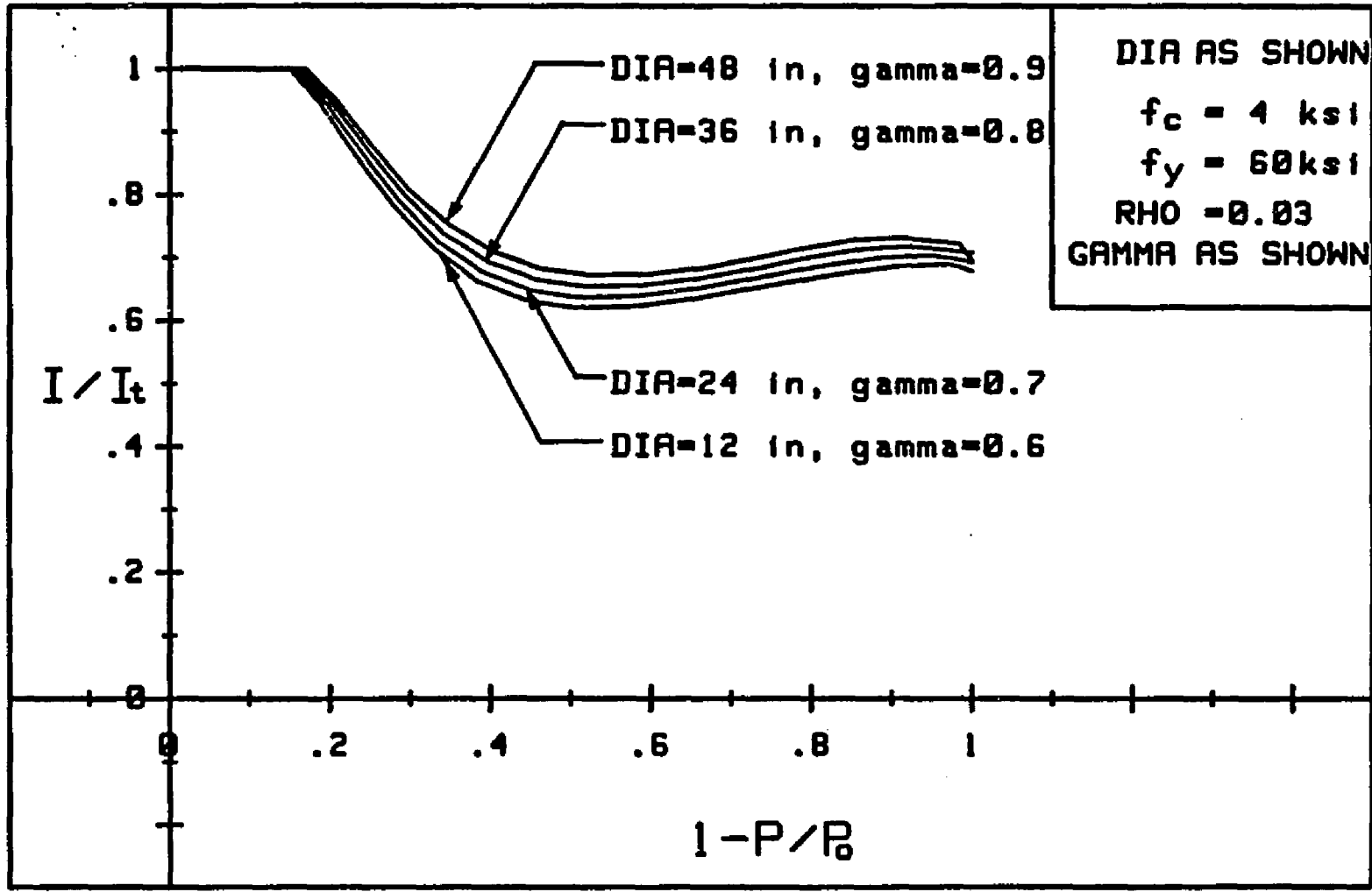


Fig. 4.17. Effect of diameter dimension on  $I/I_t$ .

complexity in distinguishing between the interrelated effects of gamma and diameter on the resulting EI value, and based on the assumption of the required concrete cover ranging from 2.5 in. to 3.5 in., only the diameter was included as a variable in the EI expression. In addition, the effects of  $\rho$ ,  $f'_c$ , and  $f_y$  are included in the derivation of a general expression for estimating the stiffness of a circular cross-section.

## CHAPTER 5

### DERIVATION OF EI EXPRESSION

#### 5.1 Development of the General Design Equations for EI

The development of an expression for EI value was based on a minimum error analysis, and a variance analysis (18, 19). Intuitively, the variation of  $I/I_t$  with respect to  $(1 - P/P_0)$  was noted to be a third-degree polynomial because of the presence of two inflection points that appear in the variation of  $I/I_t$  for different values of RHO. The coefficients for the third-degree polynomial were obtained from the following error expression:

$$E = \sum W_i (f(x_i) - y_i)^2$$

where

$w_i$  = significance weight factor for each data point

$i$  considered to be equal to 1 for all points

$f(x_i)$  = third-degree polynomial function of  $x_i =$   
 $(1 - P/P_0)_i$

$y_i$  = ratio  $I/I_t$  correspondent to  $x_i$

$i$  = number of data points considered to be 4 for a  
third-degree polynomial

$$f(x) = a_0 + a_1x + a_2x^2 + a_3x^3$$

The error expression was to be minimized by taking the derivative of  $E$  with respect to each coefficient ( $a_0, a_1, a_2, a_3$ ) to be equal to zero, and solving for the coefficients at different values of  $\rho$ . Many sets of data points were considered in order to find the best fitting curves that cover all values of  $\rho$  ranging from 0.01 to 0.07. These coefficients were then expressed as functions of  $\rho$ . Later, it was found that for values of  $1 - P/P_0$  less than .5, the expression for  $EI$  can be simplified to a second-degree polynomial which would make it easier to evaluate. The effects of various parameters  $f_y, f'_c$ , and diameter dimensions were then introduced in terms of additional coefficients to the whole polynomial. The influence of  $f'_c$  is found to be linear due to the vertical parallel shift of  $I/I_t$  variation shown in Fig. 4.15 and discussed previously.

The effect of  $f_y$  is shown in Fig. 4.14. It can be seen that up to point of  $P/P_0 = 0.5$  the moment of inertia is assumed to depend linearly on  $P/P_0$ . Beyond that point, the influence of  $f_y$  on the moment of inertia can be considered negligible.

The exponential form of the diameter effect is due to the vanishing increase of  $I/I_t$  with increasing diameter dimensions. After performing this analysis on the 192 cross-sections analyzed by the computer, the following two

equations gave the best correlation for the various groupings of variables consider. Let

$$J = \rho \times 100$$

$$X = 1 - P/P_0$$

For values of X greater than 0.5 and excluding the creep coefficient

$$\frac{EI}{E_c I_t} = C_c \times C_d (a_0 + a_1 X + a_2 X^2 + a_3 X^3)$$

where

$$a_0 = 1 + .01 (67/J - 25/J^2 - 1.06)$$

$$a_1 = -3.84 \frac{\sqrt[3]{J + 1.0}}{(0.67J + 0.34)}$$

$$a_2 = 7.42 \frac{\sqrt[3]{J + 1.0}}{J + 0.14}$$

$$a_3 = -3.46 \frac{\sqrt[4]{J + 1.6}}{J}$$

$$C_c = -1.85 \times 10^{-5} f'_c + 1.072 \quad (f'_c \text{ given in psi})$$

$$C_d = (1 + .05(1 - e^{-.134(\text{dia}-12)}))$$

For values of X less than or equal to 0.5 and excluding the creep coefficient:

$$\frac{EI}{E_c I_t} = C_c \times C_d \times C_y (b_0 + b_1 X + b_2 X^2)$$

where

$$b_0 = 3.4 \rho + 1.25$$

$$b_1 = 3 \rho - 3.09$$

$$b_2 = -6.7 \rho + 3.21$$

$$C_y = (7.5 - 15X)f_y \times 10^{-3} + 0.9X + .55$$

( $f_y$  given in ksi)

These coefficients can be computed in advance and a linear interpolation is considered to be appropriate for practical use. The values for the  $a_i$  and  $b_i$  coefficients are presented in Tables 5.1 and 5.2. The values of  $C_c$ ,  $C_d$ ,  $C_y$  are shown in Tables 5.3 through 5.5.

It is important to include the creep effect by reducing the flexural stiffness to  $EI_R = EI/(1 + \beta_d)$ . This value of  $EI_R$  is then used in a moment magnifier equation to compute magnified moments for the design of the column. The ACI Code defines the creep coefficient as the ratio of moment due to dead loads over the total moment due to live and dead loads. Other investigators have suggested that the creep coefficient should be taken as the ratio of the sustained axial load to the required ultimate axial load for which the column must be designed.

Excluding the creep coefficient, proposed formulas for the EI value were compared to the improved computer solution obtained for the 192 corss-sections. Different groupings including various values of  $f'_c$ ,  $f_y$ , and diameters were plotted for  $\rho$  ranging between 0.01 and 0.07, as shown in Figs 5.1 through 5.10.

The mathematical model appears to fit the computer solution with an error of less than 5%. The mathematical

Table 5.1. Coefficients for third-degree polynomial.

$\rho$	$a_0$	$a_1$	$a_2$	$a_3$
0.01	1.41	-4.79	8.20	-4.39
0.02	1.26	-3.29	5.00	-2.38
0.03	1.18	-2.59	3.75	-1.69
0.04	1.14	-2.17	3.06	-1.33
0.05	1.11	-1.89	2.62	-1.11
0.06	1.09	-1.68	2.31	-0.96
0.07	1.08	-1.52	2.08	-0.85

Table 5.2. Coefficients for second-degree polynomial.

$\rho$	$b_0$	$b_1$	$b_2$
0.01	1.284	-3.06	3.143
0.02	1.318	-3.03	3.076
0.03	1.352	-3.00	3.009
0.04	1.386	-2.97	2.942
0.05	1.420	-2.94	2.875
0.06	1.454	-2.91	2.808
0.07	1.488	-2.88	2.741

Table 5.3. Coefficients for  $C_c$ .

$f'_c$ (psi)	3000	4000	5000	6000
$C_c$	1.02	1.00	0.98	0.96

Table 5.4. Coefficients for  $C_d$ .

$h$ (in)	12	18	24	30	36	42	48
$C_d$	1.0	1.03	1.04	1.046	1.048	1.05	1.05

Table 5.5. Coefficients for  $C_y$ .

$P/P_o$	Reinforced Steel Yield Stress, $f_y$	
	40 Ksi	60 Ksi
0.5	1.0	1.0
0.6	0.97	1.0
0.7	0.94	1.0
0.8	0.91	1.0
0.9	0.88	1.0
1.0	0.85	1.0

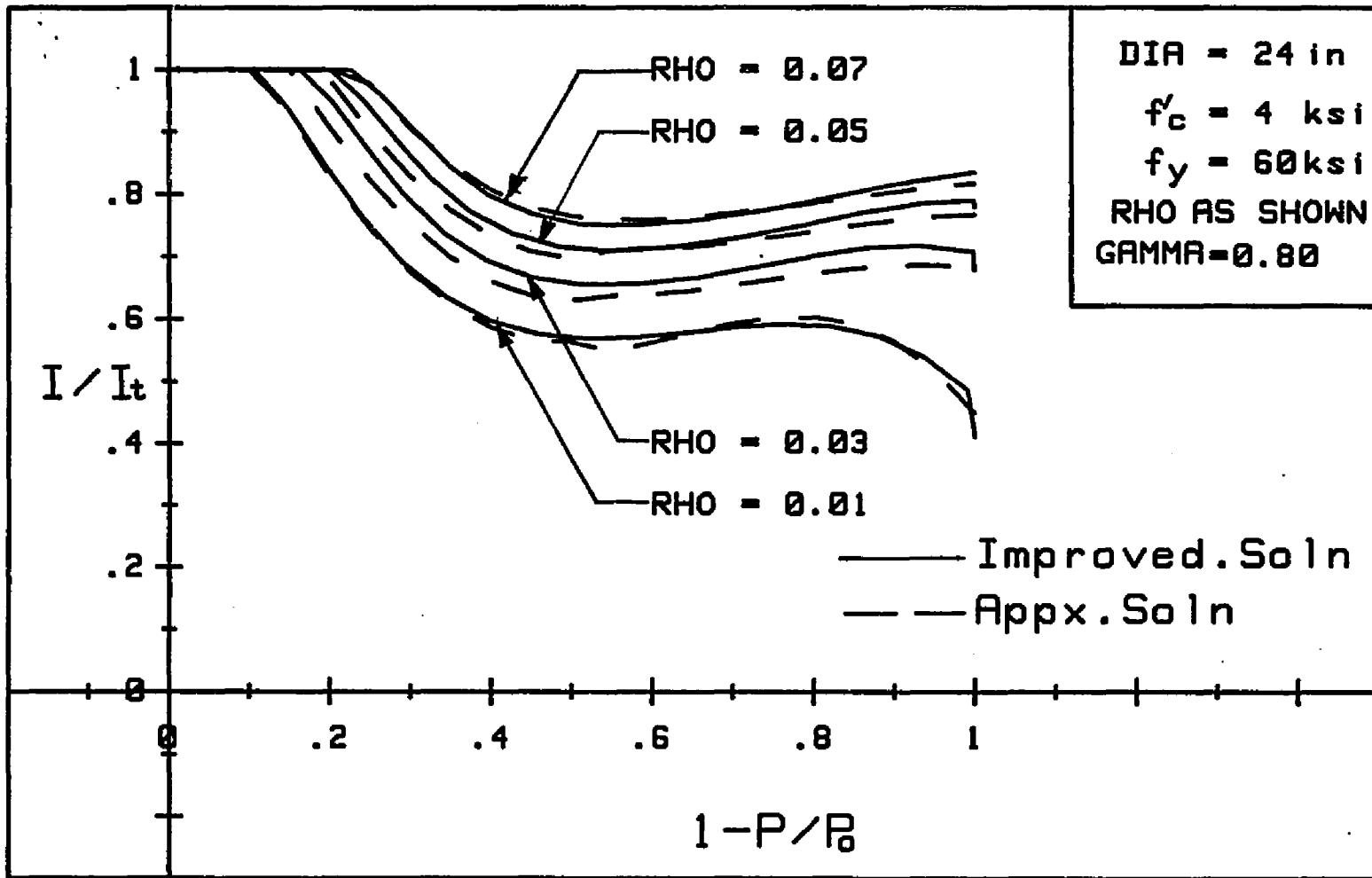


Fig. 5.1. Improved solution vs approximate solution for different steel ratios with  $f'_c = 4$  ksi,  $f_y = 60$  ksi and  $h = 24$  in.

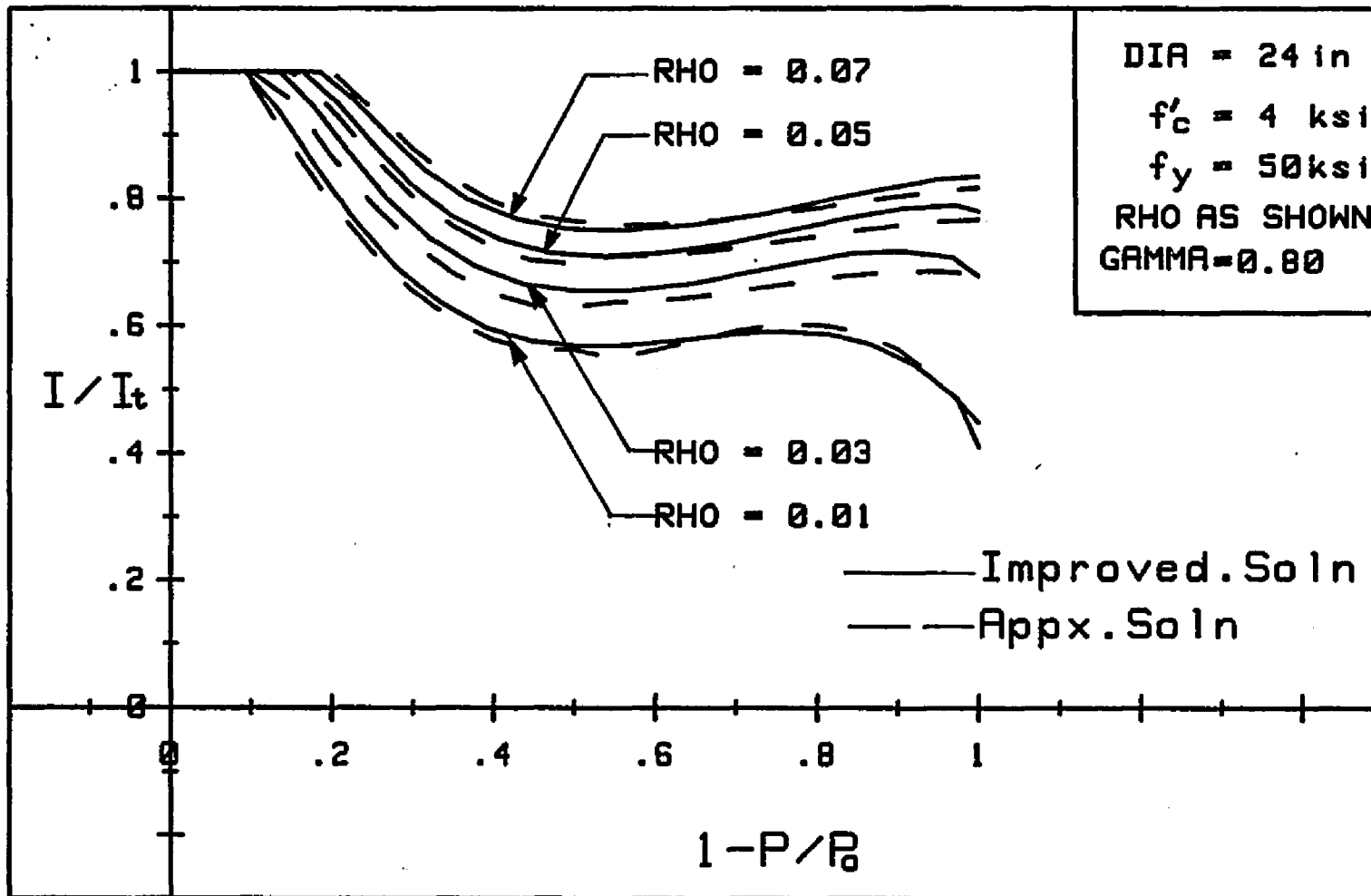


Fig. 5.2. Improved solution vs approximate solution for different steel ratios with  $f'_c = 4$  ksi,  $f_y = 50$  ksi and  $h = 24$  in.

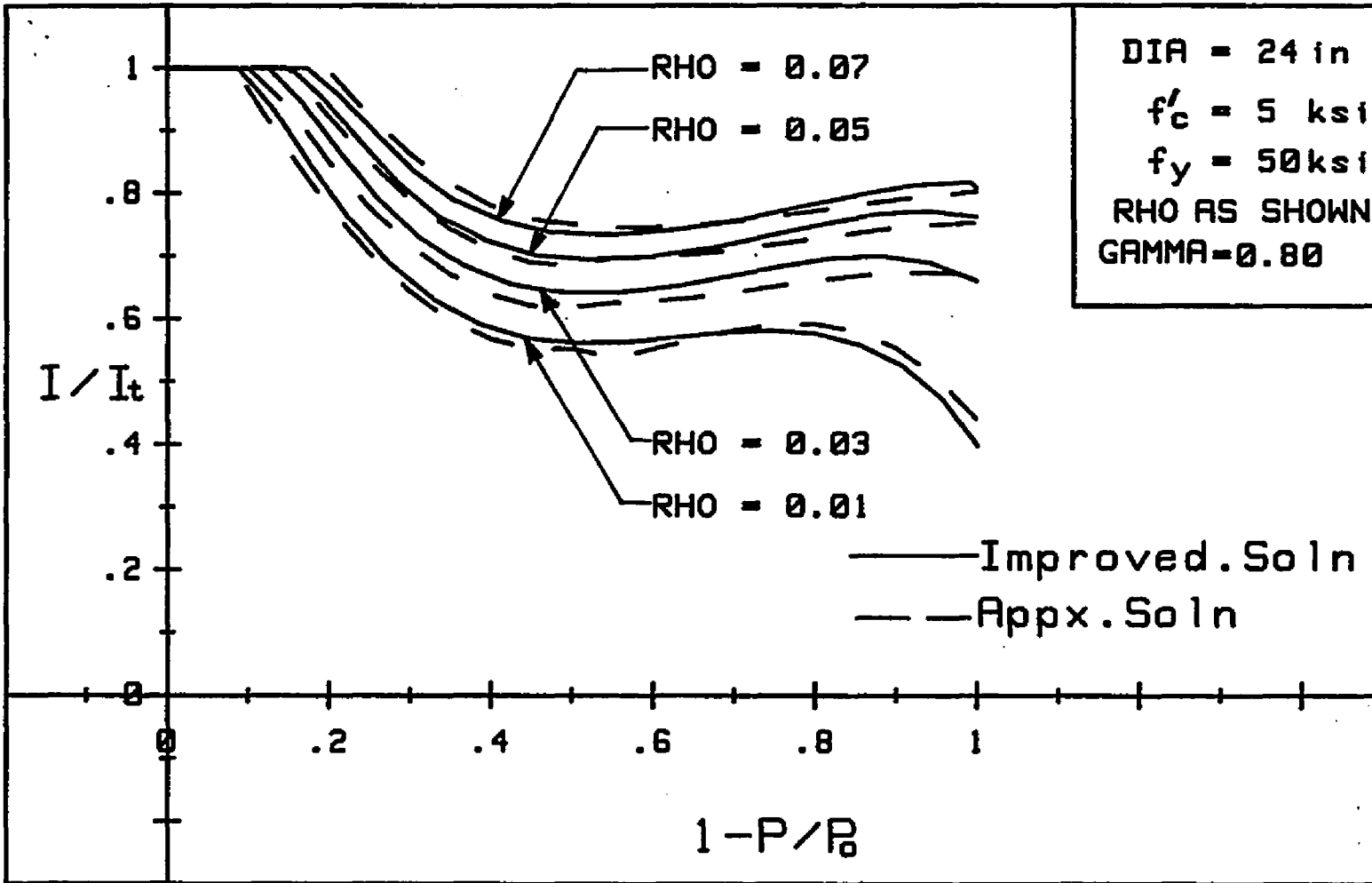


Fig. 5.3. Improved solution vs approximate solution for different steel ratios with  $f'_c = 5$  ksi,  $f_y = 50$  ksi and  $h = 24$  in.

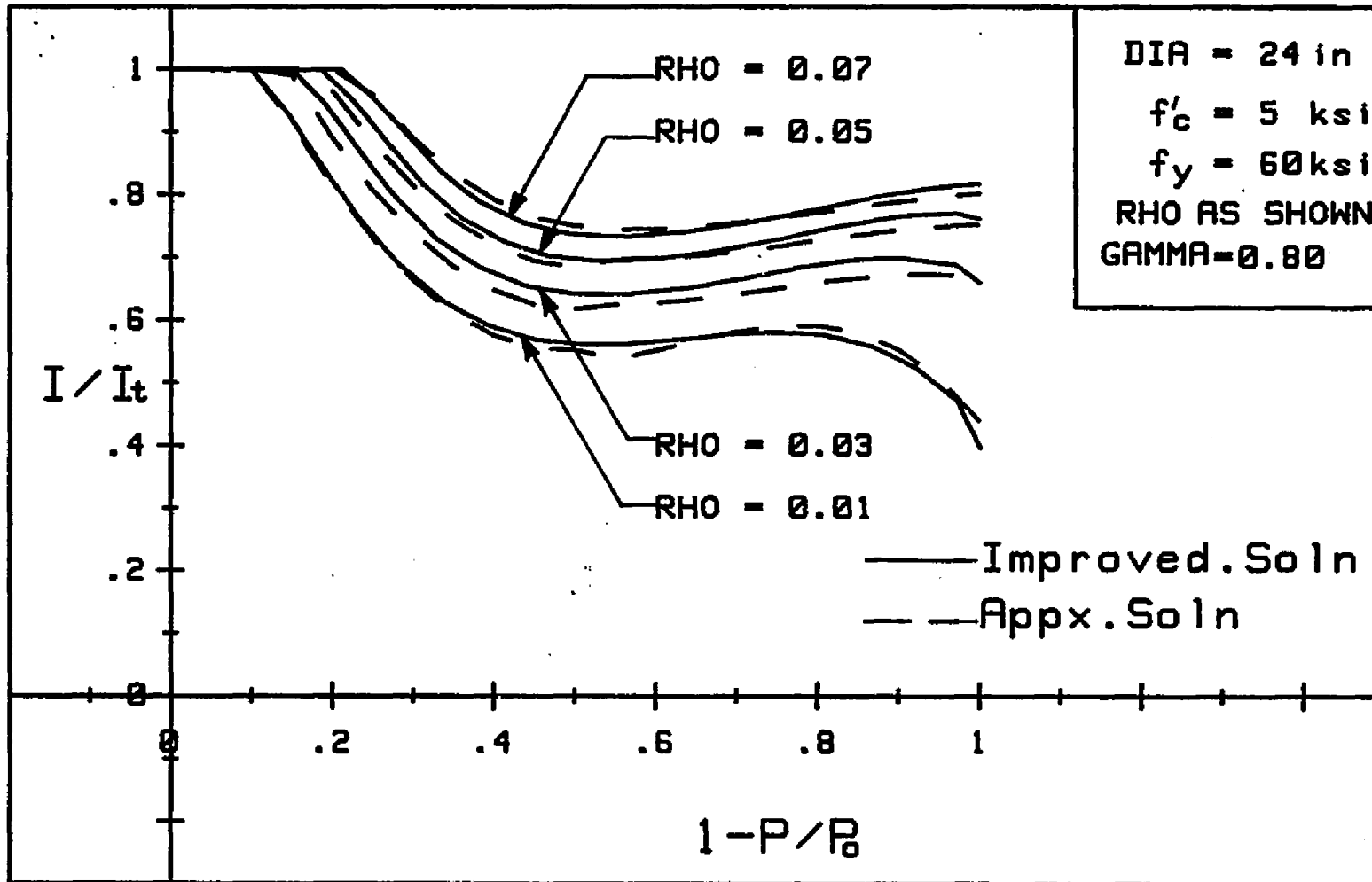


Fig. 5.4. Improved solution vs approximate solution for different steel ratios with  $f'_c = 5$  ksi,  $f_y = 60$  ksi and  $h = 24$  in.

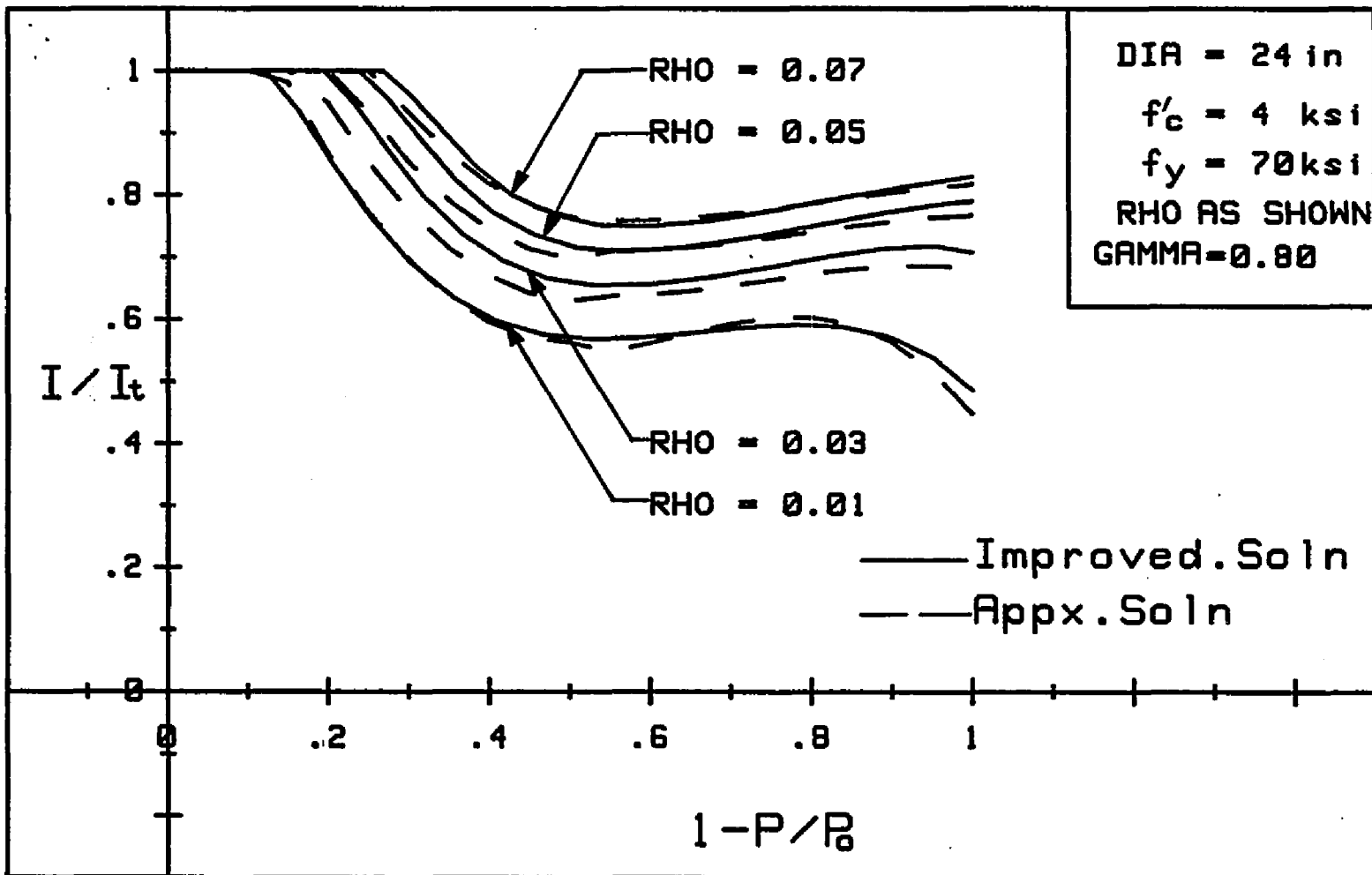


Fig. 5.5. Improved solution vs approximate solution for different steel ratios with  $f'_c = 4$  ksi,  $f_y = 70$  ksi and  $h = 24$  in.

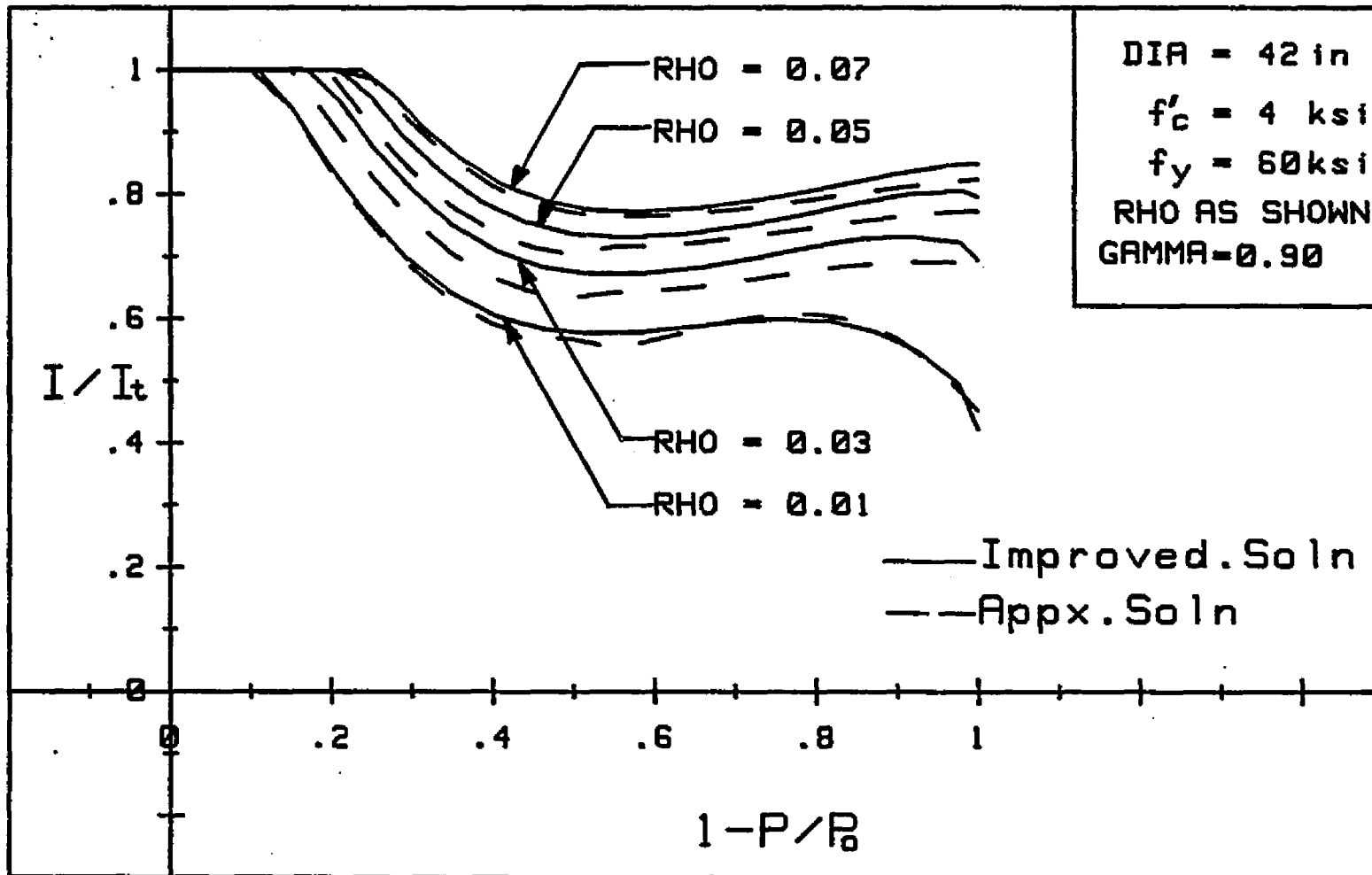


Fig. 5.6. Exact solution vs approximate solution for different steel ratios  $\rho$  with  $f'_c = 4$  ksi,  $f_y = 60$  ksi and  $h = 42$  in.

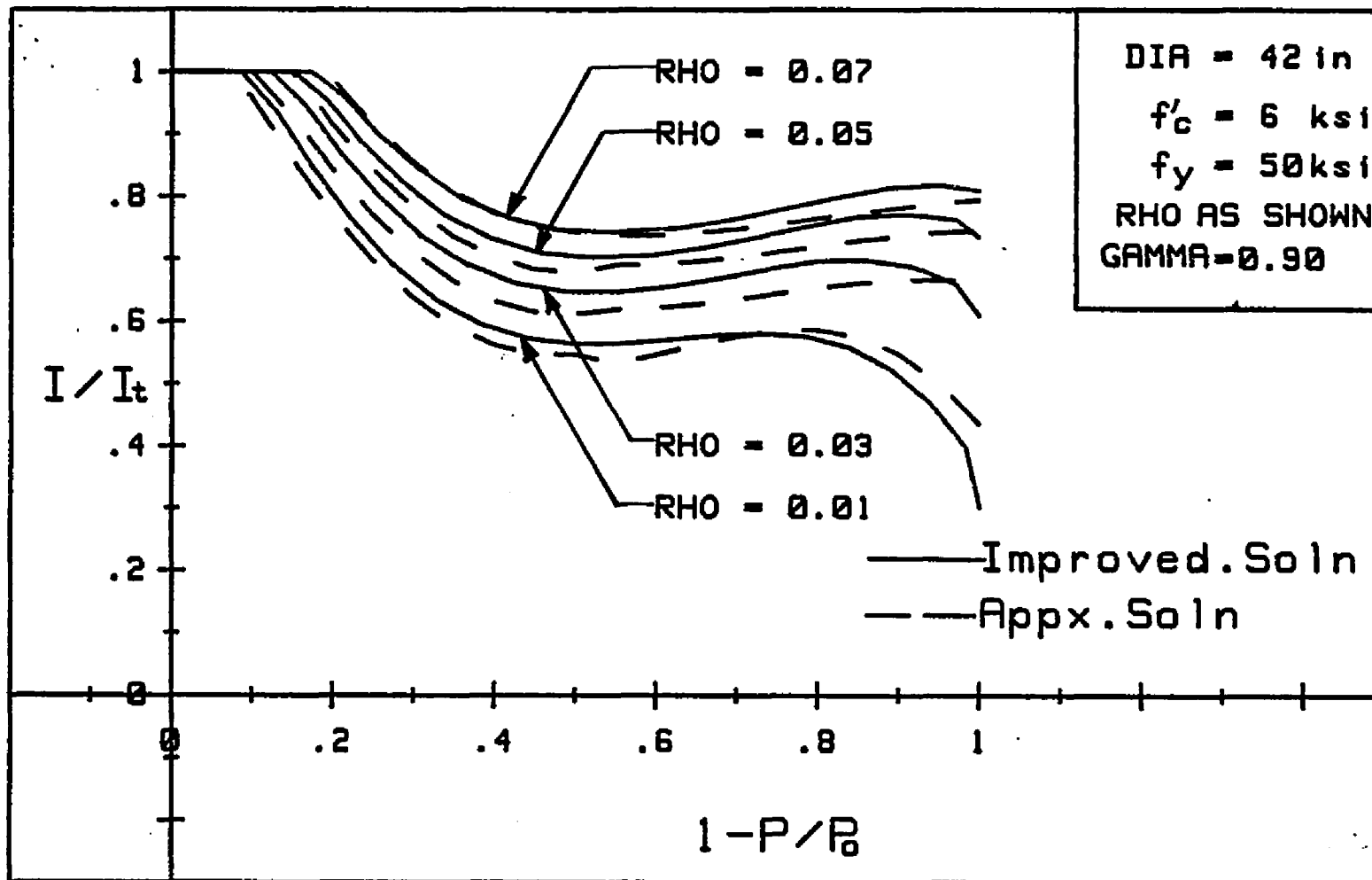


Fig. 5.7. Improved solution vs approximate solution for different steel ratios with  $f'_c = 6$  ksi,  $f_y = 50$  ksi and  $h$  and 42 in.

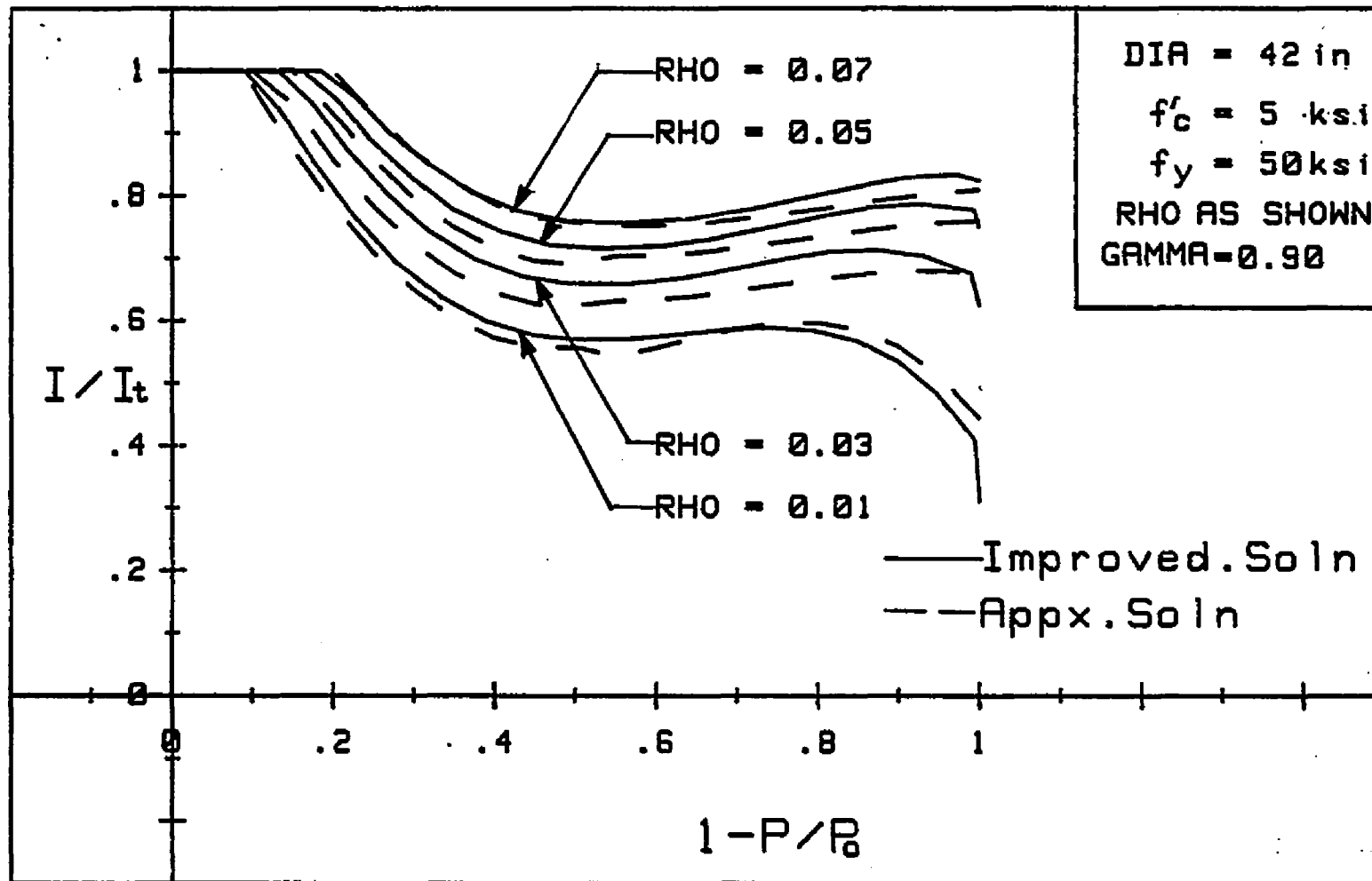


Fig. 5.8. Improved solution vs approximate solution for different steel ratios with  $f'_c = 5 \text{ ksi}$ ,  $f_y = 50 \text{ ksi}$  and  $h = 42 \text{ in.}$

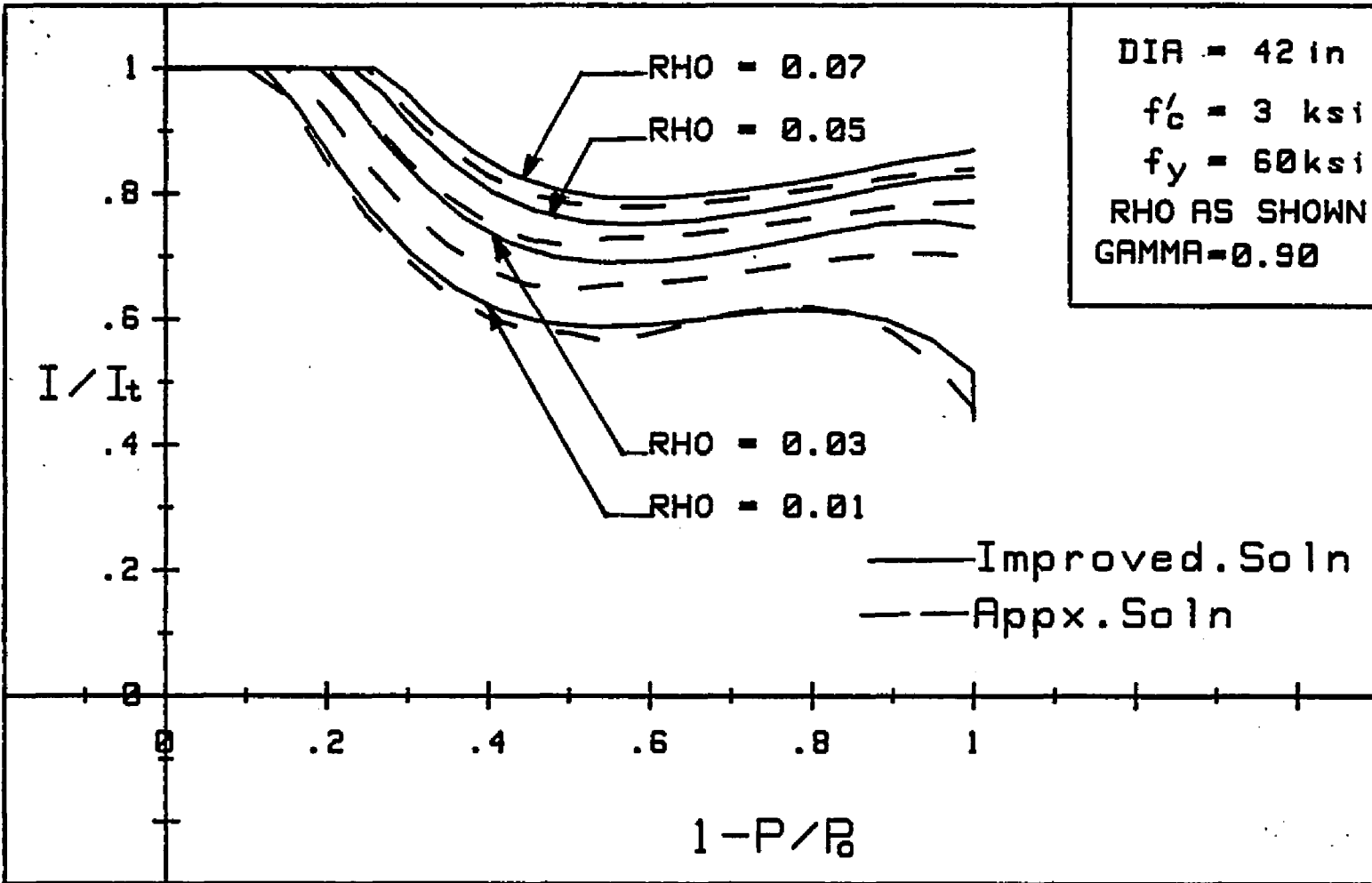


Fig. 5.9. Improved solution vs approximate solution for different steel ratios with  $f'_c = 3$  ksi,  $f_y = 60$  ksi and  $h = 42$  in.

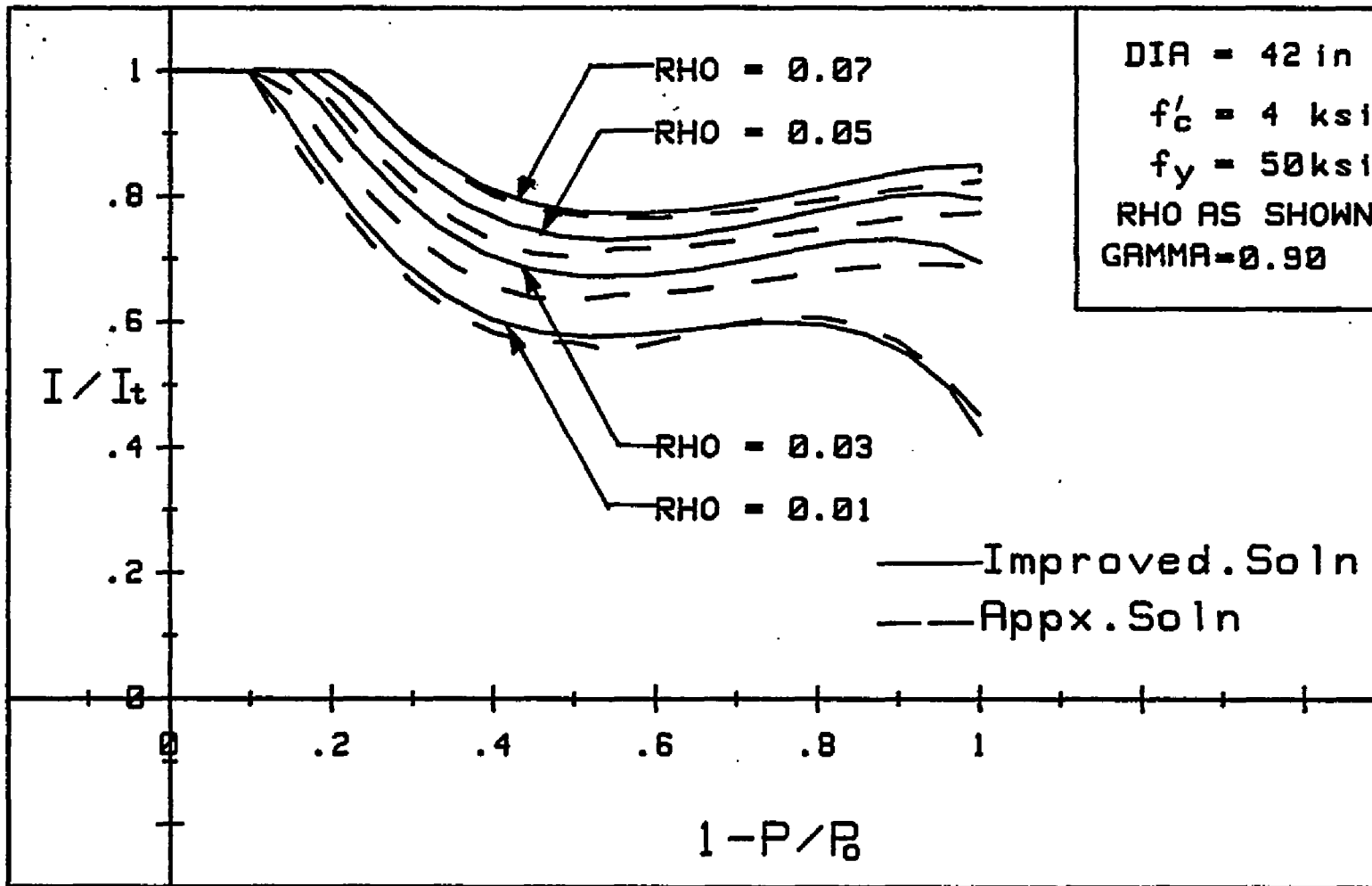


Fig. 5.10. Improved solution vs approximate solution for different steel ratios 84  
 with  $f'_c = 4$  ksi,  $f_y = 50$  ksi and  $h = 42$  in.

model is more complicated to use than the ACI equations, but with the coefficients already tabulated, it becomes an easy task for the designer to evaluate EI values to a significantly higher degree of accuracy.

### 5.2 Development of the Minimum EI Expression

Exact expressions for calculating the stiffness of a circular section were presented in Section 5.1. While these expressions are fairly simple to evaluate, it is possible that some designers may consider them too lengthy for practical use. To address the need of this group, a simpler expression for minimum stiffness is developed in this section.

The simpler expression is derived making conservative assumptions. As shown in Figs. 4.13 and 4.14, the lowest stiffness is obtained by using a lower grade of steel. Thus, the yield stress for the steel is assumed to be 40 ksi, which is the lowest commonly available grade of steel in the United States. This assumption is particularly conservative as the bars, no. 7 and larger, which are commonly used as longitudinal reinforcement in columns are rarely available in grades smaller than 60.

Figure 4.15 demonstrates that higher compressive strength of concrete results in lower stiffness ratio  $I/I_t$ . Therefore, a maximum compressive strength of 6000 psi was assumed. Concrete with a compressive strength greater than

6000 psi is considered high strength. The use of high strength concrete in columns is associated with other problems such as excessive creep and usually requires a more exact analysis.

Figures 4.16 and 4.17 indicate that cross-sections with smaller values of  $\gamma$  have a lower stiffness value. While columns with diameters of 6 feet or larger are not uncommon in bridges, a diameter of 18 inches was taken as a small diameter used in the design of a building. Using a standard clear cover of 1.5 in, the  $\gamma$  for an 18 in diameter column is 0.72. Thus, for any given percentage of longitudinal reinforcement, an 18 in diameter with  $f_y = 40$  ksi,  $f'_c = 6000$  psi, and  $\gamma = 0.72$  will give the lowest stiffness compared to any other cross-section with the same steel percentage and for a particular load.

The above section was analyzed for reinforcement ratios ranging between 0.01 and 0.07. The absolute minimum values derived from the computer solution for the cross-section analyzed above are tabulated for different steel ratios. Table 5.6 shows the minimum EI values as opposed to the governing least conservative EI values obtained from ACI (10-10) and (10-11).

It is important to note that for small reinforcement ratios (1% to 3%), there is a sudden reduction in the stiffness of the section when it is subjected to pure

Table 5.6. Comparison of governing ACI values for EI with values derived from computer solution.

$\rho$	ACI Governing	$\frac{EI}{E_c I_t}$ (ACI)	$\frac{EI}{E_c I_t}$ (Comp. Soln.)
0.01	Eq. (10-11)	0.388	0.283*
0.02	Eq. (10-11)	0.366	0.444*
0.03	Eq. (10-10)	0.388	0.566*
0.04	Eq. (10-10)	0.438	0.644
0.05	Eq. (10-10)	0.488	0.672
0.06	Eq. (10-10)	0.527	0.695
0.07	Eq. (10-10)	0.566	0.705

\* Note that for this case the lowest stiffness is obtained from pure bending of the column with no axial loads.

bending in the presence of zero or little axial load. Therefore, the minimum stiffness for these columns is localized and for all practical purposes corresponds to the pure bending case. Nevertheless, these highly conservative minimum values are used as it is possible for a column to be subjected to zero axial load during a severe earthquake.

The minimum EI expression derived from the computer EI values in Table 5.6 is given by:

$$\frac{EI}{E_c I_t} = 0.118 + 17.8\rho - 135\rho^2$$

It is important to include the creep factor  $\beta_d$  to obtain the reduced flexural stiffness  $EI_R = EI/(1 + \beta_d)$  to be used in the Moment Magnifier Method.

This expression gives less conservative values of EI for values of  $\rho$  greater or equal than 0.02. Figure 5.11 illustrates the minimum EI expression as opposed to MacGregor and ACI governing values. The minimum value for EI obtained from the computer solution corresponding to  $\rho = 0.01$  is smaller than the ACI governing value for EI. This is due to the localized minimum obtained in pure bending case. The minimum EI expression obtained is easier to compute and gives values for EI greater than the ACI values. The benefits of a larger EI value are illustrated in the design example in Appendix B.

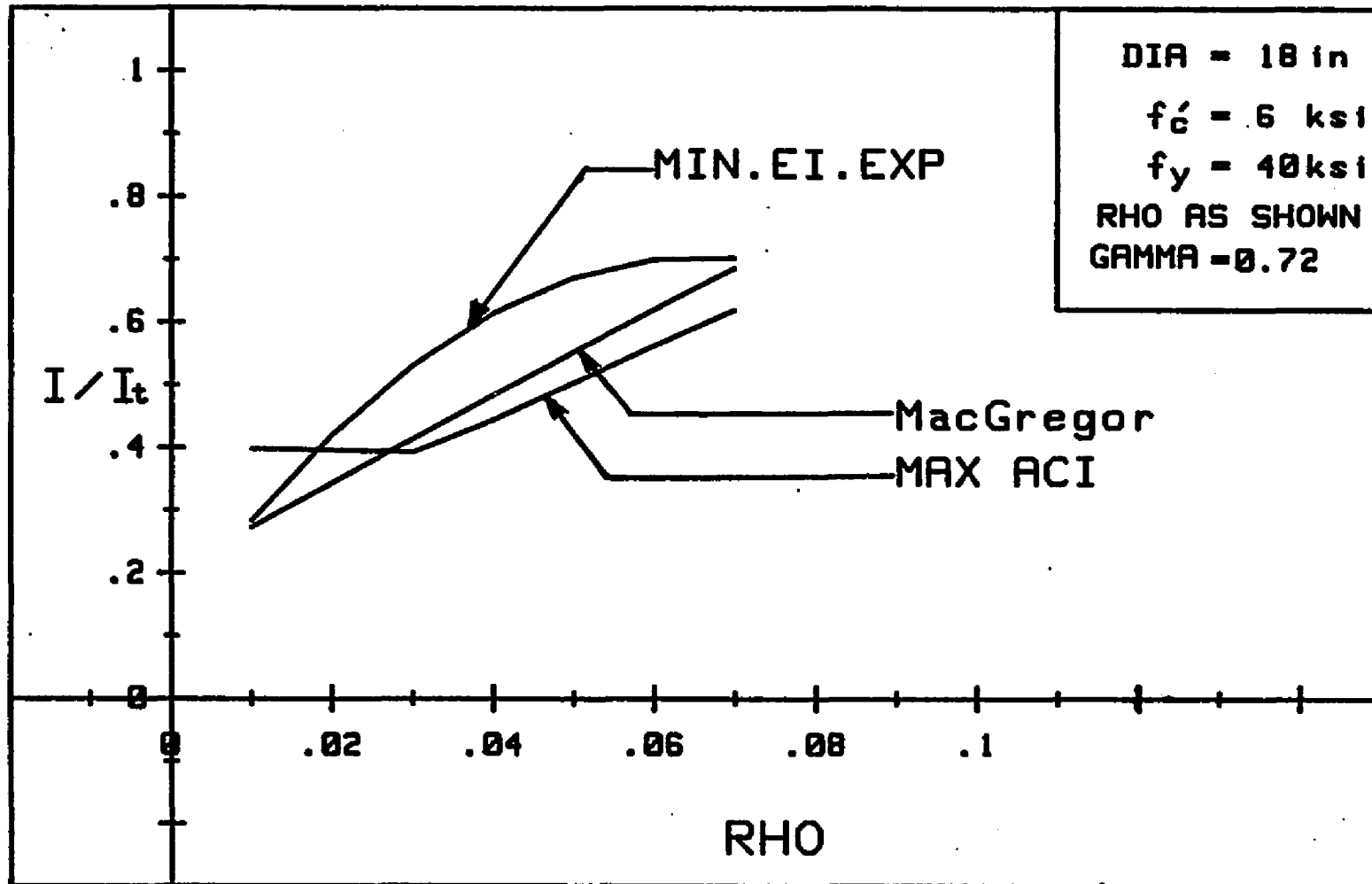


Fig. 5.11. Variation of the ratio  $I/I_t$  with respect to  $\rho$  using the Minimum EI expression as opposed to MacGregor and ACI equations.

## CHAPTER 6

### CONCLUSION AND RECOMMENDATIONS

An examination of the proposed equations and a review of other approximate methods lead to the following general conclusions:

1. The equations proposed by different investigators show that there is considerable scatter in the values obtained for various columns' sections and properties.
2. The value of EI is affected by the amount and location of the reinforcement, the degree of cracking, and materials properties. Other variables such as the inelastic behavior of concrete and the end restraints of the column are to be studied in a second-order analysis.
3. A procedure for calculating EI values for circular columns is proposed in this report using a mathematical model that has been shown to fit the improved computer solution.
4. Modifications must be provided to these calculated EI values in order to extend the basic design

procedures to columns subjected to secondary moments. A second-order analysis is necessary to include slenderness effects of the columns in their true behavior.

5. The minimum EI expression gives values for the stiffness EI that are conservative to use regardless of the load applied and the section properties.
6. Further studies have to be carried out in order to reach a decision for the definition of creep coefficient as the ratio of sustained loads to total loads rather than the ratio of moments as stated in the ACI 318R-83 Code.
7. It is important that more explicit analysis be performed on columns of different cross-sections because the significance of the effect of each variable depends on the cross-section properties and its geometry. To reach a better accuracy in our estimation of EI values, different groupings of different cross-sections such as squares and rectangles have to be studied separately.
8. The moment-magnifier method presented by the ACI Building Code for analyzing the effects of slenderness on the strength of columns is strongly affected by the estimation of the flexural stiffness, EI, used in calculating the critical load. Thus, the

proposed equations which give a more exact approximation of the EI are of great help in obtaining a more realistic solution.

APPENDIX A

FLOWCHART AND COMPUTER LISTING OF  
PROGRAM CIR\_COL

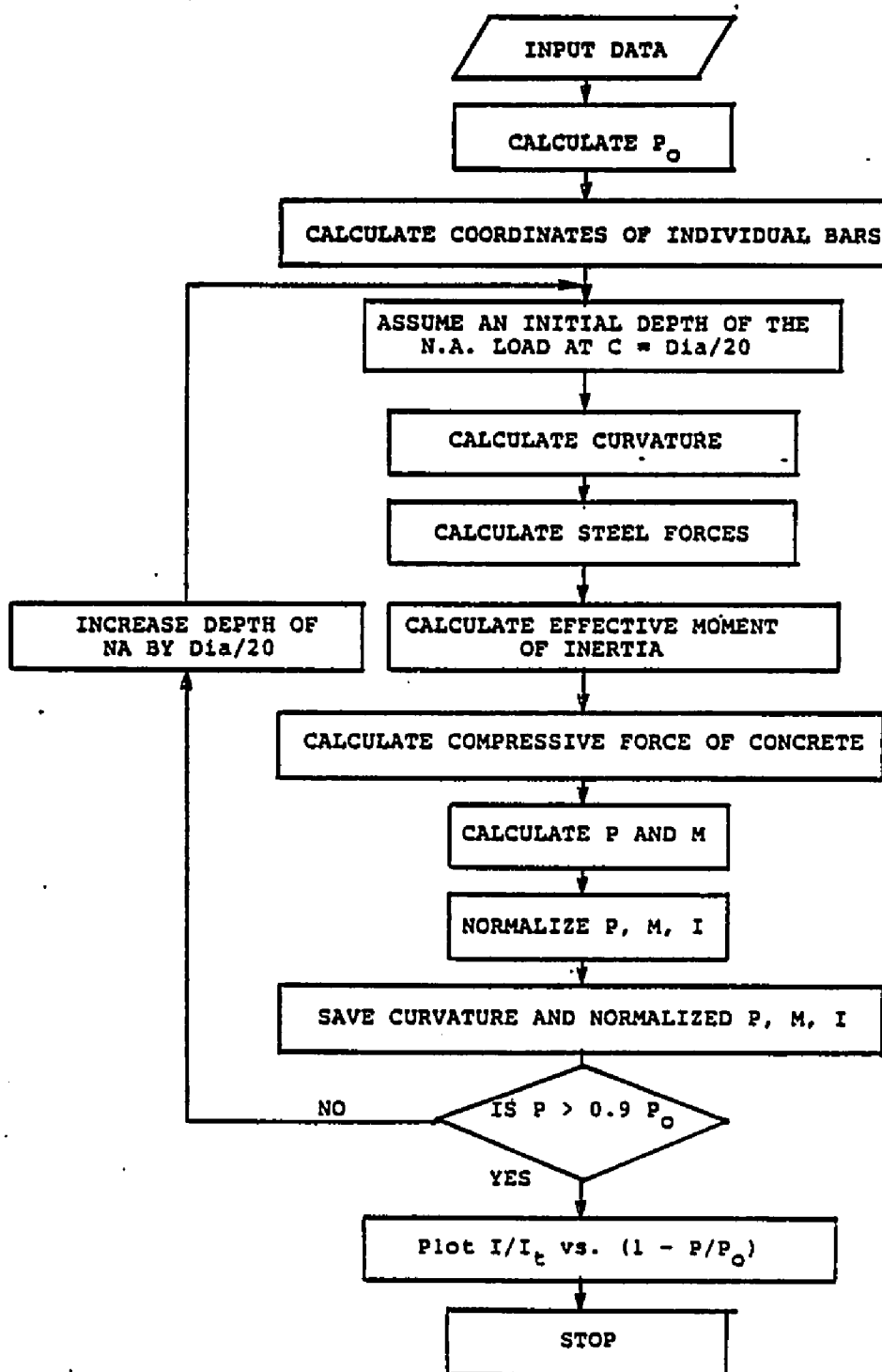


Fig. A.1. Flowchart for CIR\_COL.

```

10 ! PROGRAM CIR_COL
12 ! VERSION JUNE 1986
13 ! THIS PROGRAM GENERATES THE MOMENT CURVATURE RELATIONSHIP AND CALCULATES
14 ! THE EFFECTIVE MOMENT OF INERTIA WITH RESPECT TO AXIAL LOAD.
16 DATA 1,.8 ! DATA FOR ROD AND GAMMA
17 DATA 24.,9.6,15.,.301592894 ! DATA FOR DIA,R,Nb,As
18 DATA 4000.,70.,.003,29000. ! DATA FOR Fc,Fy,Ecu,Es
19 DATA 150.,0.,0. ! DATA FOR Wtc,Shf1,Shfa
20 ! PARAMETER DEFINITIONS:
22 ! DIA COLUMN DIAMETER (INCHES)
24 ! R RADIUS TO LONGITUDINAL REBAR (INCHES)
26 ! Nb NUMBER OF REBARS
28 ! As CROSS SECTIONAL AREA OF REBAR (SQ. INCHES)
30 ! Fc F'c (PSI)
32 ! Fy YIELD STRESS OF STEEL (KSI)
34 ! Ecu ULTIMATE STRAIN OF CONCRETE (IN/IN) -- APPROX. EQUALS TO .003
36 ! Es YOUNG'S MODULUS OF STEEL (KSI)
38 ! Wtc UNIT WEIGHT OF CONCRETE (PCF)
40 ! Shf1 LATERAL SHIFT OF REFERENCE REBAR W.R.T. THE Y AXIS
42 ! Shfa ROTATIONAL SHIFT OF REF. REBAR W.R.T. THE Y AXIS -- +VE CW (DEG.)
44 DIM Soln(180,20),Y(180),Fs(180),X(25),U(25),V(25)
46 COM Titles(24),L1(24),L2(24),L3(24)
48 INTEGER I,L,Nb
50 READ Rod,Gam
52 READ Dia,R,Nb,As
54 READ Fc,Fy,Ecu,Es
56 READ Wtc,Shf1,Shfa
58 ! INPUT "OUTPUT ON SCREEN? (Y/N)",N6
60 ! IF N6="N" THEN
62 ! PRINTER IS 701
64 ! ELSE
66 ! PRINTER IS 1
68 ! END IF
70 ! INITIALIZE Fc=4 TO RUN THE PROGRAM FOR DIFFERENT ROD STARTING
72 ! WITH 1% STEEL RATIO AND INCREMENTING BY 2%.
74 ! CALCULATE COLUMN CAPACITY
76 Ac=PI*Dia^2/4-Nb*As ! NET CROSS SECTIONAL AREA OF CONCRETE
78 Pu=.00085*Ac*Fc+As*Nb*Fy ! COLUMN COMPRESSIVE CAPACITY
80 Cp=.9*Pu
82 ! CALCULATE STEEL-CONCRETE AREA RATIO
84 Roll=Nb*As/Ac
86 ! CALCULATE GAMMA=R/Rc WHERE Rc IS THE RADIUS OF THE COLUMN
88 Gamma=2*R/Dia
90 ! INTERNAL DEFINITIONS
92 H=Dia^2/4
94 Ec=Wtc^1.5*.033*SQRT(Fc) ! YOUNG'S MODULUS OF CONCRETE
96 En=Es/Ec ! MODULAR RATIO
98 Transa=(En-1)*As ! TRANSFORMED AREA OF STEEL
100 Ta=ATN(Shf1/R)+Shfa*PI/180. ! SHIFT REFERENCE AXIS
102 Dela=2*PI/Nb ! SPACE BARS AT EQUAL ANGLES

```

```

379      Ig=PI*Dia^4/64.          ! CALCULATE GROSS MOMENT OF INRTIA
380      Ay=0.                    ! INITIALIZE VARIABLE Ay
397 ! CALCULATE COORDINATE OF INDIVIDUAL REBAR
400     FOR I=0 TO Nb-1
410         Yb=R*COS(Ta+I*Delta) ! REBAR'S COORDINATE
420         Ig=Ig+Transa*Yb^2    ! MOMENT OF INERTIA OF THE UNCRACKED SECTION
430         Ay=Ay+Transa*Yb     ! Yi^2("TRANSFORMED" AREA OF STEEL BAR i)
440         Y(I+1)=Yb
450     NEXT I
460     K=1
470     C=0.
471 ! INCREMENT FOR THE DEPTH OF NEUTRAL AXIS
480     D=Ita=Dia/20.
490     Rc=Dia/2.
500 ! CALCULATE REBAR FORCES AND CURVATURE OF THE SECTION
510     Sue=Fy/Es      ! YIELD STRAIN OF STEEL
520     C=Delta+C
530     Phe=Ecu/C     ! CURVATURE OF THE SECTION
540     Soln(K,3)=Phe ! SAVE THE VALUE
550     Tl=Rc-C
551 ! ESTABLISH IF EACH BAR IS IN COMPRESSION OR TENSION AND
552 ! CALCULATE THE CORRESPONDING STRESS
560     FOR I=1 TO Nb
570         E=(Y(I)-Tl)*Ecu/C
580         IF ABS(E)>Sue THEN
590             F=Fy*ABS(E)/E
600         ELSE
610             F=E*Es
620         END IF
621 ! CALCULATE THE FORCE AT EACH BAR
630         IF F<0. THEN
640             Fs(I)=As*F
650         ELSE
660             Fs(I)=As*(F-.00085*Fc)
670         END IF
680     NEXT I
690 ! CALCULATE EFFECTIVE MOMENT OF INERTIA OF THE SECTION
700     Rr=(Rc-C)/Rc
710     IF C>=Dia THEN
720         Alfa=PI
730     ELSE
740         Alfa=ACS((Rc-C)/Rc)
750     END IF
751 ! CALCULATE EFFECTIVE MOMENT OF INERTIA OF CONCRETE CRACKED SECTION
760     Segi=H^2*(4*Alfa-SIN(4*Alfa))/16.
761 ! CALCULATE THE AREA OF CONCRETE CRACKED SECTION
770     Sega=H*(Alfa-SIN(Alfa)*COS(Alfa))
771 ! CALCULATE THE VERTICAL DISTANCE TO CENTROID CONCRETE CRACKED SECTION
780     Segq=H*Dia/3.*(SIN(Alfa))^3
790 ! DETERMINE NEUTRAL AXIS WITH RESPECT TO ORIGIN

```

```

809     Tay=Ay+Segq
810     Toz=Nb*Transa+Sega
820     Yavg=Tav/Toa
830 ! Ieffective NOT INCLUDING STEEL CONTRIBUTION
840     Segi=Segi+(Segq/Sega-Yavg)^2*Sega
841 ! INCLUDE STEEL CONTRIBUTION FOR COMPUTING FINAL Ieff
850     FOR I=1 TO Nb
860         Segi=Segi+Transa*(Y(I)-Yavg)^2
870     NEXT I
880     ScIn(k,4)=Segi
890 ! CALCULATE COMPRESSIVE FORCE OF CONCRETE
900     IF C>Rc THEN
910         Dum=20
920     ELSE
930         Dum=10
940     END IF
950     IF C>Dia THEN
960         Cr=Dia
970     ELSE
980         Cr=C
990     END IF
1000    Strip=Cr/Dum
1010    Cc=0.
1020    Cm=0.
1030    A=0.
1031 ! CALCULATE AREA OF EACH STRIP
1040    FOR I=1 TO Dum
1050        Alfa=ACS((Rc-Strip*I)/Rc)
1060        Sega=H*(Alfa-SIN(Alfa))*COS(Alfa)
1070        Dsega=Sega-A
1080        A=Sega
1090        IF I=1 THEN
1100            D=Rc-Dia/(3*(Alfa-SIN(Alfa))*COS(Alfa))*(SIN(Alfa))^3
1110        ELSE
1120            D=Strip*(I-.5)
1130        END IF
1131 ! CALCULATE STRAIN AT CENTROID OF EACH STRIP
1140        E=(C-D)*Ecu/C
1141 ! CALCULATE STRESS OF CONCRETE CORRESPONDING TO EACH STRAIN FROM
1142 ! HOGNESTAD'S MODEL
1150        Cf=Fc*(1000+E-(E/.002)^2)*.001
1151 ! CALCULATE FORCE OF THIS STRIP
1160        F=Dsega*Cf
1161 ! SUM FORCES TO COMPUTE AXIAL LOAD ON THE COLUMN FROM EQUILIBRIUM
1170        Cc=Cc+F
1171 ! SUM MOMENTS GENERATED
1180        Cm=Cm+F*(Rc-D)
1190    NEXT I
1200 ! CALCULATE PN AND MOMENT

```

```

1219   Pn=Cc
1220   M=Cm
1230   FOR I=1 TO Nb
1240     Pn=Pn+Fs(I)
1250     M=M+Fs(I)*Y(I)
1260   NEXT I
1261 ! SAVE THE SOLUTIONS FOR Pn AND M
1270   Soln(K,1)=Pn
1280   Soln(K,2)=M
1290   K=K+1
1291 ! CONTINUE INCREMENTING DEPTH OF NA TILL Pn>0.9Pu
1300   IF Pn>Cp THEN
1310     GOTO 1350
1320   ELSE
1330     GOTO 520
1340   END IF
1350   Soln(K,1)=Pu
1360   Soln(K,4)=Ig
1361 ! ESTABLISH THE POINT OF PURE BENDING OF THE COLUMN
1370   FOR I=2 TO K
1380     IF Soln(I,1)*Soln(I-1,1)<0. THEN GOTO 1400
1390   NEXT I
1400   J=I-1
1410   FOR L=2 TO 3
1420     Soln(J,L)=Soln(J,L)-Soln(J,1)*(Soln(I,L)-Soln(J,L))/(Soln(I,1)-Soln(
J,1))
1430   NEXT L
1440   Soln(J,1)=0
1450   Mu=Soln(J,2)
1460   PRINT USING "///,""LOAD-MOMENT INTERACTION TABLE"","/"
1470   PRINT "STEEL-CONCRETE AREA RATIO=";Roll,"      Gamma=";Gamma
1480   PRINT "Pu=";Pu;"kips   Ig=";Ig;"in^4"
1490   PRINT USING "/,7X,""P"";18X,""M"";19X,""CURV"";18X,""I""
1500   PRINT USING "5X,""KIPS"";14X,""IN-KIPS"";16X,""1/IN"";16X,""IN^4"";/"
1510   Curv=0
1520   Mmax=0
1530   K1=4*(K+2-J)
1540   INPUT "STORE DATA ON DISC? (Y/N)",Q$
1550   IF Q$="N" THEN GOTO 1600
1560 ! CREATE FILE_i W/ K1 DATA POINTS @ 8 BYTES IN LENGTH EACH
1570 ! NOTE: TAKES 8 BYTES TO STORE A REAL NUMBER IN BDAT FILE
1573   INPUT "INPUT BDAT FILE NAME",File$
1580   CREATE BDAT File$,K1,8
1590   ASSIGN #File TO File$ ! OPEN I/O PATH TO FILE
1600   FOR I=J TO K
1610     PRINT TAB(1),Soln(I,1);TAB(21),Soln(I,2);TAB(41),Soln(I,3);
1620     PRINT TAB(61),Soln(I,4)
1630     IF Soln(I,3)>Curv THEN Curv=Soln(I,3)
1640     IF Soln(I,2)>Mmax THEN Mmax=Soln(I,2)
1650     Ii=I-J+1

```

```

1669     IF Q$="N" THEN GOTO 1700
1670     OUTPUT @File;Soln(I,1)           ! WRITE P(i) ON FILE
1671     OUTPUT @File;Soln(I,2)           ! WRITE M(i) ON FILE
1680     OUTPUT @File;Soln(I,3)           ! WRITE CURV(i) ON FILE
1690     OUTPUT @File;Soln(I,4)           ! WRITE I(i) ON FILE
1700     NEXT I
1710     Soln(K+1,1)=Pu
1720     Soln(K+1,2)=Mmax
1730     Soln(K+1,3)=Curv
1740     Soln(K+1,4)=Ig
1741     IF Q$="N" THEN GOTO 1800
1750     OUTPUT @File;Pu                   ! WRITE Pu ON FILE
1760     OUTPUT @File;Mmax                 ! WRITE Mmax ON FILE
1770     OUTPUT @File;Curv               ! WRITE Max Curvature ON FILE
1780     OUTPUT @File;Ig                  ! WRITE Ig ON FILE
1790     ASSIGN @File TO *                 ! CLOSE I/O PATH TO FILE
1791     DISP "DATA TRANSFER COMPLETE"
1800 ! PLOT P-M-CURV DIAGRAM
1810     L1$="MOMENT (K-IN.)"
1820     L2$="CURVATURE (1/IN.)X100"
1830     L3$="AXIAL LOAD (KIPS)"
1831     ! PAUSE
1840     ! CALL Plotb(Mmax,Curv,Pu,Soln(I),J,K,Title$,L1$,L2$,L3$,1,2,3,1)
1850     ! PAUSE
1860     L2$="MOMENT OF INERTIA (IN^4)"
1870     ! CALL Plotb(Mmax,Ig,Pu,Soln(I),J,K,Title$,L1$,L2$,L3$,1,2,4,2)
1880     ! PAUSE
1881     V(Fo)=J
1882     U(Fo)=K
1890     FOR I=J TO K
1900     Soln(I,1+Fo)=I-Soln(I,1)/Pu
1910     ! Soln(I,2)=Soln(I,2)/Mu
1920     Soln(I,4+Fo)=Soln(I,4)/Ig
1921     NEXT I
1922     X(1)=0.
1924     P=Roo
1925 ! CALCULATE APPX. SOLUTION
1927     FOR I=1 TO 21
1928     Cc=-.000018*Fc+1.072
1929     Cd=(1+.05*(1-EXP(-.134*(Dia-12))))
1930     IF X(I)>.5 THEN
1934     Cp=1+.01*(67/P-24.94/(P^2)-1.0625)
1935     A1=-3.457*((P+1.6)^(1/4))/P
1936     A2=7.42*((P+1.0)^(1/3))/(P+.14)
1937     A3=-3.84*((P+1.0)^(1/3))/(.67*P+.34)
1938     Sol=(Cc*Cd)*(A1*(X(I)^3)+A2*(X(I)^2)+A3*X(I)+Cp)
1939     ELSE
1940     Cy=(7.5-15*X(I))*(Fy/1000)+.9*X(I)+.55
1942     B1=-P/15+3.21

```

```

1961      B2=-3.09+.03*P
1962      B3=.034*P+1.25
1963      Sol=Cc*Cd*Cy*(B1*(X(I)^2)+B2*X(I)+B3)
1964      END IF
1965      IF Sol>1.0 THEN
1966      Soln(I,11+Fo)=1.0
1967      ELSE
1968      Soln(I,11+Fo)=Sol
1969      END IF
1970      X(I+1)=X(I)+.05
1971      NEXT I
1972 ! INCREMENT STEEL RATIO FROM 1% TO 7% BY 2%
1973      IF Fo=7 THEN
1974      GOTO 1980
1975      ELSE
1976      As=As+.603185789
1977      Fo=Fo+1
1978      Roo=Roo+2
1979      GOTO 230
1980      END IF
1981      L2$="1-P/P"
1982      L3$="I/I"
1983      CALL Plotb(Soln(I),X(I),U(I),V(I),L2$,L3$,b,1,11,Dia,Fc,Fy,Roo,Gam)
2030      END
2031 ! GRAPHICS SUBROUTINE OF THE PROGRAM
2040      SUB Plotb(Soln(I),X(I),U(I),V(I),L2$,L3$,M1,M3,M5,Dia,Fc,Fy,Roo,Gam)
2050      GINIT
2070 ! SET UP PLOTTING SCALE
2082 ! PLOTTER IS 3,"INTERNAL"
2084      PLOTTER IS 705,"HPGL"
2085      OUTPUT 705;"V54"
2090      GRAPHICS ON
2100      PEN 1
2110      VIEWPORT 10,122,16,87
2111 ! SET UP THE FRAME AND LABEL AXES
2120      FRAME
2130      Xmax=1.5
2140      Xmin=.2
2150      Ymax=1.1
2151      Ymin=.3
2160      WINDOW -Xmin,Xmax,-Ymin,Ymax
2170      AXES .1,.1,0,0,2,2,2
2200 ! LABEL AXES
2210      CSIZE 4.7
2260      DEG
2270      LORG 5

```

```
2289 MOVE .5*Xmax,-.75*Ymin
2290 LABEL L2#
2291 ! LDIR 90
2300 MOVE -.5*Xmin,.45*Ymax
2310 LABEL L3#
2360 LDIR 0
2370 CSIZE 3.0,.6
2380 LOR 6
2390 FOR I=0 TO 1 STEP .2 ! LABEL X'S
2400 MOVE I,-.15*Ymin
2410 LABEL I
2420 NEXT I
2430 LOR 8
2440 FOR I=0 TO 1 STEP .2 ! LABEL Y'S
2450 MOVE 0,I
2460 LABEL I
2470 NEXT I
2471 CSIZE 3
2480 MOVE 1.12,1.1
2490 DRAW 1.12,.62
2500 DRAW 1.5,.62
2501 LOR 2
2510 MOVE 1.18,1.025
2520 LABEL "DIA ="
2531 MOVE 1.32,1.025
2532 LABEL Dia
2533 MOVE 1.41,1.025
2534 LABEL "in"
2535 MOVE 1.21,.93
2536 CSIZE 3.6
2540 LABEL "f"
2541 CSIZE 3
2550 MOVE 1.24,.92
2560 LABEL "c"
2561 MOVE 1.32,.93
2562 Fcc=Fc/1000
2564 LABEL Fcc
2565 MOVE 1.41,.93
2566 LABEL "ksi"
2567 CSIZE 3.6
2570 MOVE 1.21,.85
2580 LABEL "f"
2590 CSIZE 3
2600 MOVE 1.24,.84
2610 LABEL "y"
2611 MOVE 1.32,.85
2612 LABEL Fy
2613 MOVE 1.41,.85
2614 LABEL "ksi"
```

```

2633     MOVE 1.29,.93
2634     LABEL "="
2640     MOVE 1.29,.85
2650     LABEL "="
2660     MOVE 1.28,.77
2670     LABEL "AS SHOWN"
2680     MOVE 1.29,.7
2690     LABEL "="
2700     MOVE 1.32,.7
2701     GGA=DRROUND(GAA,3)
2710     LABEL "0.80"
2720     MOVE 1.18,.77
2730     LABEL "RHD"
2740     MOVE 1.15,.705
2750     LABEL "GAMMA"
2760     MOVE -.05,.485
2770     LABEL "t"
2780     MOVE .83,-.24
2781     LABEL "o"
2782     MOVE .6,1.0
2783     LABEL "RHD = 0.07"
2784     MOVE .6,.9
2785     LABEL "RHD = 0.05"
2786     MOVE .6,.4
2787     LABEL "RHD = 0.03"
2788     MOVE .6,.3
2789     LABEL "RHD = 0.01"
2790     CSIZE 4.0
2792     MOVE 1.1,.25
2793     LABEL "Exact.Soln"
2794     MOVE 1.1,.15
2795     LABEL "Appx.Soln"
2796     CSIZE 3.0
2798     ! PLOT
2800     FOR F=4 TO 7
2810     LINE TYPE 1
2840     MOVE Soln(V(F),N3+F),Soln(V(F),N1+F)
2850     FOR I=V(F) TO U(F)
2860     PLOT Soln(I,N3+F),Soln(I,N1+F)
2870     NEXT I
2871     ! PLOT FOR APPX CURVE
2872     LINE TYPE 4.1
2873     MOVE X(I),Soln(I,N5+F)
2874     FOR I=1 TO 21
2875     PLOT X(I),Soln(I,N5+F)
2876     NEXT I
2877     NEXT F
2880     PENUP
2890     SUBEND

```

**APPENDIX B**

**DESIGN EXAMPLE**

The example that follows compares the use of the ACI approximation for EI to the minimum EI expression developed in this report.

The problem is stated as follows: For a 48 in diameter column with bars equally distributed in 20 bundles (Fig. B.1) (i.e., 40 #11 bars), an unsupported length of 36 ft (Fig. B.2) and fixed at one end, check if this column satisfies the design requirements using the minimum EI expression, and if necessary revise the column reinforcement design to satisfy ACI (10-10) or (10-11). Given:

Unfactored Loading:

$$P_{DL} = 572 \text{ kips}; P_{LL} = 705 \text{ kips}$$

$$M_{DL} = 594 \text{ k-ft}, M_{LL} = 994 \text{ k-ft}$$

Materials

Compressive strength of concrete  $f'_c = 4 \text{ ksi}$

Yield strength of reinforcement  $f_y = 60 \text{ ksi}$

Spiral tie #5

Concrete permanently exposed to earth:

Minimum cover = 3 in

Check spacing requirements:

$$\text{Total cover} = 3" + .625 + 1.41/2$$

$$= 4.33"$$

$$\gamma = \frac{48 - 2 \times 4.33}{48} = .82$$

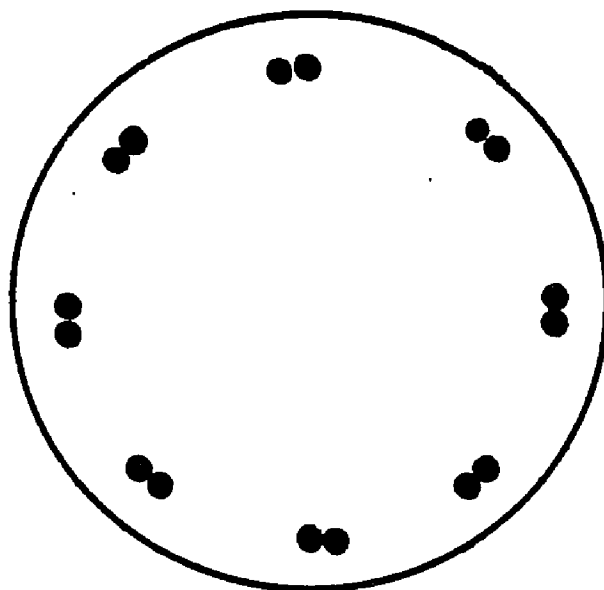


Fig. B.1. Column cross-section with outward bundles arrangement.

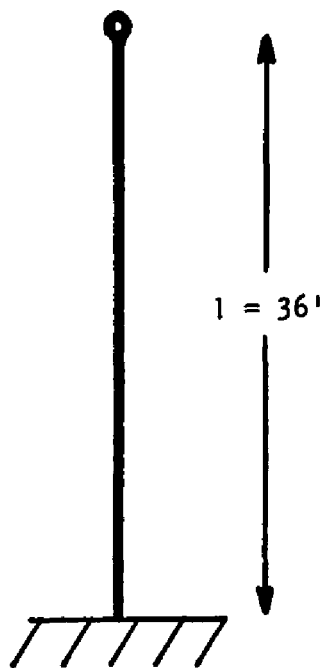


Fig. B.2. Column with 36 ft unsupported length fixed at the bottom and pinned at the top.

Radius to centroid of longitudinal bars:

$$R_c = .82 \times 24" = 19.68"$$

Inside perimeter:

$$2\pi R_c = 2 \times 19.68 = 123.65"$$

Total area of one bundle:

$$2A_b = 2 \times 1.56 = 3.12$$

Equivalent diameter of one bundle:

$$d_e = \sqrt{\frac{4 \times 3.12}{\pi}} = 2 \text{ in}$$

Spacing required between two bundles:

$$1.5 d_e = 1.5 \times 2 = 3 \text{ in.}$$

Spacing found in the problem investigated:

$$s = \frac{123.65 - 40 \times 1.41}{19} = 3.52 \text{ in.}$$

O.K.

- Slender column Moment Magnifier Method using the ACI approximation for EI:

$$U = 1.4 \text{ DL} + 1.7 \text{ LL}$$

$$P_u = 1.4 \times 572 + 1.7 \times 705 = 2000 \text{ kips}$$

$$M_u = 1.4 \times 594 + 1.7 \times 994 = 2521.4 \text{ k-ft}$$

The moment magnification factor is

$$\delta = \frac{C_m}{1 - \frac{P_u}{\phi P_c}}$$

$C_m$  is considered to be equal to 1.  $\phi$  is .75 for members with spiral reinforcement.

The critical load is given by:

$$P_c = \frac{\pi^2 EI}{(kl_u)^2}$$

where EI may be taken as

$$EI = \frac{(E_c I_g / 5) + E_s I_{se}}{1 + \beta_d} \quad \text{ACI (10-10)}$$

or conservatively,

$$EI = \frac{E_c I_g / 2.5}{1 + \beta_d} \quad \text{ACI (10-11)}$$

Calculation for ACI EI values:

$$\begin{aligned} T &= A_s / 2\pi R_c \\ &= \frac{40 \times 1.56}{2\pi \times 19.68} = .51 \end{aligned}$$

$$\begin{aligned} R_1 &= R_c + T/2 \\ &= 19.68 + .51/2 = 19.93 \text{ in} \end{aligned}$$

$$\begin{aligned} R_2 &= R_c - T/2 \\ &= 19.68 - .51/2 = 19.42 \text{ in} \end{aligned}$$

$$\begin{aligned} I_{se} &= \pi (R_1^4 - R_2^4) / 4 \\ &= 12205 \text{ in}^4 \end{aligned}$$

$$I_g = \frac{\pi h^4}{4} = \frac{\pi (48)^4}{4} = 260576 \text{ in}^4$$

$$E_c = 57 \sqrt{f'_c} = 3605 \text{ ksi}$$

$$\beta_d = \frac{1.4 M_{DL}}{1.4 M_{DL} + 1.7 M_{LL}} = .33$$

Therefore

$$EI (10-10) = 407,383,681 \text{ k.in}^2$$

$$EI (10-11) = 282,519,242 \text{ k.in}^2$$

EI (10-10) is less conservative to be used.

Calculation for moment magnification factor  $\delta$ :

$$P_c = \frac{\pi^2 EI (10-10)}{(Kl_u)^2}$$

$$= 4885 \text{ kips}$$

$$\delta = \frac{1}{1 - \frac{P_u}{.75P_c}}$$

$$= 2.2$$

$$\phi M = \delta M_u$$

$$M = \frac{2.2 \times 2521.4}{.75} = 7396 \text{ k-ft}$$

$$\text{or } 88753 \text{ k.in}$$

The point (P,M) = (2000 kips, 88753 k.in) falls outside the P-M interaction diagram for the cross-section investigated (see Fig. B.3). Thus the column cross-section needs to be more reinforced or redesigned.

2. Slender Column Moment Magnifier Method using the minimum EI expression:

$$EI_R = \frac{E_c I_t (0.118 + 17.8\rho - 135\rho^2)}{(1 + \beta_d)}$$

$$\rho = \frac{A_s}{A_g} = \frac{40 \times 1.56}{\pi (24)^2} = 0.0345$$

$$E_c = 57 \sqrt{f'_c} = 3605 \text{ ksi}$$

$$I_t = I_g + (n - 1) \sum_{i=1}^m A_b Y_i^2$$

$$= 339887 \text{ in}^4$$

Therefore

$$EI_R = 525,125,415 \text{ k.in}^2$$

The critical load is:

$$P_c = \frac{\pi^2 \times 525,125,415}{(2.1 \times 36 \times 12)^2} = 6297 \text{ kips}$$

$$= \frac{1}{1 - \frac{2000}{.75 \times 6297}} = 1.73$$

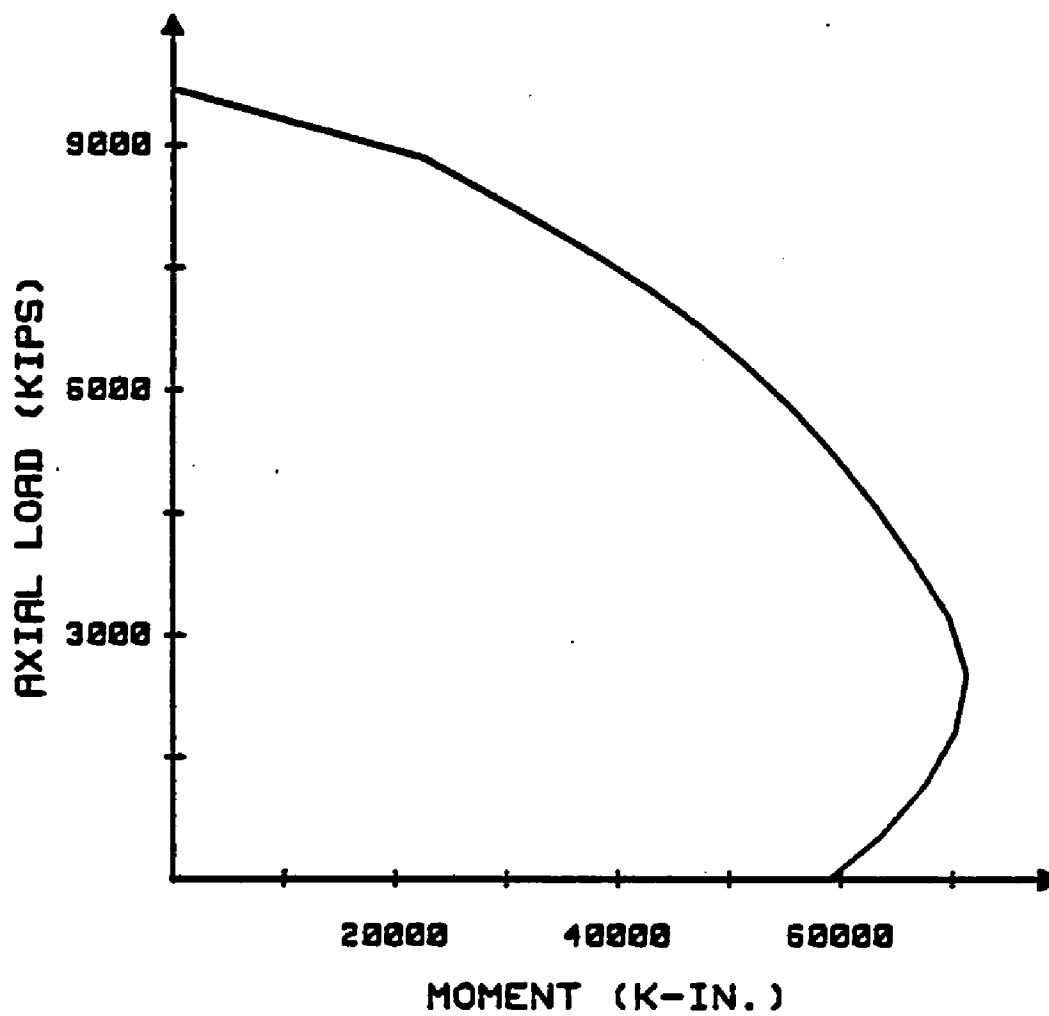


Fig. B.3. Axial load-moment interaction diagram for the column design example.

$$M = \delta M_u$$

$$M = \frac{1.73 \times 2521.4}{0.75} = 5816 \text{ k-ft}$$

$$\text{or } 69792 \text{ k.in}$$

The point (P.M) = (2000 kips, 69792 k.in) falls inside the (P.M) interaction diagram as shown in Fig. B.3. Thus the column design satisfies the strength requirement and does not need to be redesigned.

In order to satisfy the ACI code, EI value has to be increased by adding more longitudinal reinforcement, keeping the diameter dimension unchanged. The number of bars required is: 58 #11, giving an EI (10-10) equal to 252,006,437 k.in<sup>2</sup>, thus  $P_c = 6296$  and  $\delta = 1.73$  equal to the multiplier calculated using the minimum EI expression. The use of 58 #11 in 29 bundles would violate spacing requirements as shown if placed in outward positions, as shown in Fig. B.1.

$$s = \frac{123.65 - 58 \times 1.41}{28} = 1.5"$$

The spacing calculated 1.5" is less than the required 3" spacing calculated previously.

If the bundles are placed inward, as shown in Fig. B.4, the value of  $\gamma$  is lower and the effective moment of inertia decreases. As shown in this example, the minimum EI

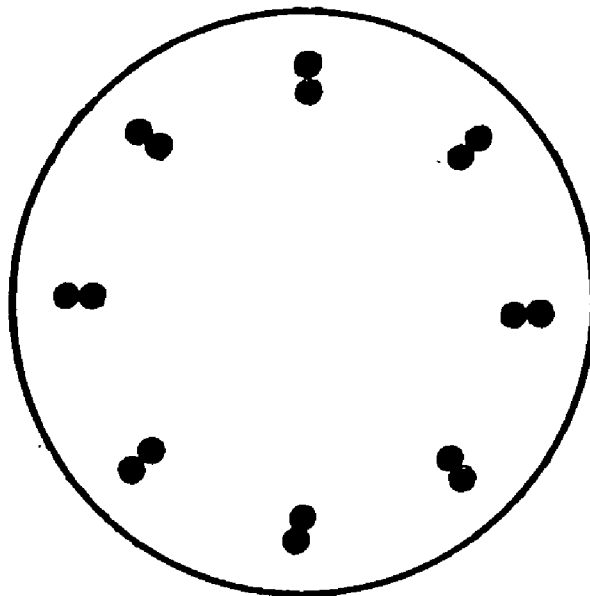


Fig. B.4. Column cross-section with inward bundles arrangement.

expression gives a more economical section to be used. Further refinement can be achieved using the general expression for approximating EI value.

#### LITERATURE CITED

1. ACI Committee 318, "Building Code Requirements for Reinforced Concrete (ACI 318-83)." American Concrete Institute, Detroit, 1983, 40 pp.
2. MacGregor, J. G., Breen, J. E., Pfrang, E. O., "Design of Slender Concrete Columns," ACI Journal Proceedings, Vol. 67, No. 1, January 1970.
3. Park, R., and Paulay, T., "Reinforced Concrete Structures," John Wiley and Sons, Inc., New York, 1975, pp. 172-186.
4. Breen, J. E., and Ferguson, P. M., "The Restrained Long Concrete Column as a Part of a Rectangular Frame," ACI Journal, Proceedings, Vol. 61, No. 5, May 1964, pp. 563-587.
5. Pfrang, E. O., and Siess, C. P., "Behavior of Restrained Reinforced Concrete Columns," Proceedings, ASCE, Vol. 90, ST5, Oct., 1964.
6. Drysdale, R. G., and Huggins, M. W., "Sustained Biaxial Load on Slender Concrete Columns," Journal of the Structural Division, ASCE, Vol. 97, May 1971, pp. 1423-1434.
7. Furlong, R. W., and Ferguson, P. M., "Tests of Frames with Columns in Single Curvature," Symposium on Reinforced Concrete Columns, SP-13, American Concrete Institute, Detroit, 1966, pp. 55-74.
8. Ferguson, Phillip M., "Reinforced Concrete Fundamentals," 4th Edition, John Wiley and Sons, Inc., New York, 1979, pp. 548-553.
9. ACI Committee 318, "Commentary on Building Code Requirements for Reinforced Concrete (ACI 318-83)." American Concrete Institute, Detroit, 1983, 57 pp.
10. MacGregor, J. G., Oelhafen, U. H., and Hage, S. E., "A Re-examination of the EI Value for Slender Columns," Symposium on Reinforced Concrete Columns, SP-50, American Concrete Institute, Detroit, October, 1975, pp. 3-40.

11. Goyal, B. B., and Jackson, N., "Slender Concrete Columns under Sustained Load," *Journal of the Structural Division, ASCE*, Vol. 97, ST11, November 1971, pp. 2729-2750.
12. Winter, George, and Nilson, Arthur H., "Design of Concrete Structures," 9th Edition, McGraw-Hill Book Company, New York, 1979, pp. 323-341.
13. Johnston, B. C. (Ed.), *The Column Research Council Guide to Stability Design Criteria for Metal Compression Members*, Third Edition, John Wiley and Sons, Inc., New York, 1976, 217 pp.
14. "Strength and Servicability Criteria--Reinforced Concrete Bridge Members--Ultimate Design," U.S. Department of Commerce, Bureau of Public Roads, Aug. 1966, 81 pp.
15. Parme, A. L., "Capacity of Restrained Eccentrically Loaded Long Columns," *Symposium on Reinforced Concrete Columns*, SP-13, American Concrete Institute, Detroit, 1966, pp. 354-367.
16. Spang, J. M., "Design Method for Long Reinforced Concrete columns," Department of Civil Engineering, University of Delaware, June 1966, pp. 15-47.
17. Lawrie, R. H., and Heins, C. P., "Design of Modern Concrete Highway Bridges," John Wiley and Sons, Inc., New York, 1984, pp. 493-496.
18. Meyer, S. L., "Data Analysis for Scientists and Engineers," John Wiley and Sons, Inc., New York, 1975, pp. 51-76.
19. Dudewicz, E. J., "Introduction to Statistics and Probability," Rinehart and Winston, New York, 1976, pp. 417-433.